AFCRL-65-766

THE DETERMINATION OF CRUSTAL THICKNESS FROM THE SPECTRUM OF P WAVES

AD624044

CLEARINGHOUSE FOR FEDERAL SCIENTIFIC AND TECHNICAL
Hardcopy $5.00 | Microfiche $1.00
186 pgs
ARCHIVE COPY
Code 1

Luis M. Fernandez, S.J.
SAINT LOUIS UNIVERSITY
St. Louis, Missouri

Contract No. AF 19(604)-7399
Project No. 8652
Task No. 865201

Scientific Report No. 13

DEC 21 1965

September 1965

Prepared for

Air Force Cambridge Research Laboratories
Office of Aerospace Research
United States Air Force
Bedford, Massachusetts

WORK SPONSORED BY ADVANCED RESEARCH PROJECTS AGENCY
PROJECT VELA-UNIFORM

ARPA Order No. 292, Amendment 7
Project Code No. 8100, Task 2

BEST
AVAILABLE COPY

AFCRL-65-766

THE DETERMINATION OF CRUSTAL THICKNESS FROM THE SPECTRUM OF P WAVES

Luis M. Fernandez, S. J.

SAINT LOUIS UNIVERSITY

St. Louis, Missouri

Contract No. AF 19(604)-7[illegible]

Project No. 8652

Task No. 865201

SCIENTIFIC REPORT NO. 13

September 1965

Prepared for

AIR FORCE CAMBRIDGE RESEARCH LABORATORIES

OFFICE OF AEROSPACE RESEARCH

UNITED STATES AIR FORCE

BEDFORD, MASSACHUSETTS

Work sponsored by Advanced Research Projects Agency

Project Vela-Uniform

ARPA Order No. 292 Amendment 7

Project Code No. 8100 Task 2

Requests for additional copies by agencies of the Department of Defense, their contractors, or other government agencies should be directed to:

Defense Documentation Center (DDC)
Cameron Station
Alexandria, Virginia 22314

Department of Defense contractors must be established for DDC services or have their "need-to-know" certified by the cognizant military agency of their project or contract.

All other persons and organizations should apply to the:

Clearinghouse for Federal Scientific
and Technical Information (CFSTI)
Sills Building
5285 Port Royal Road
Springfield, Virginia 22151

TABLE OF CONTENTS

Page

ABSTRACT

The layers of the earth's crust act as a filter with respect to seismic energy arriving at a given station. Consequently the motion recorded at the earth's surface depends not only on the frequency content of the exciting seismic energy and on the response characteristics of the recording instrument, but also on the elastic parameters and thicknesses of the layers. This latter dependence is the basis for a method of investigating the structure of the crust.

In order to obtain information independent of the time history and spatial distribution of the source of energy the spectrum of the vertical component of motion is divided by the spectrum of the horizontal component. This ratio represents the tangent of the apparent angle of emergence as a function of frequency. It depends only on the angle of incidence of the ray and the system of layers below the recording station. The parameters of the crust may be determined by comparison of theoretical and observed spectra of this ratio.

To facilitate this comparison a set of master curves was calculated using the matrix development of Haskell. Calculations of these curves are in terms of a dimensionless frequency. This presentation allows the grouping of the curves corresponding to different crustal models into families of curves. A set of master curves of the apparent angle of emergence for one-layer models and for different angles of incidence and contrasts of velocities between the crust and the mantle is presented. This set is complete in the sense that any one-layer model may be interpolated. A second set for some combinations of two-layer models is also presented.

The characteristics of these curves are discussed from the point of view of their "periodicity" in the frequency domain and of their amplitude in order to investigate the influence of the layer parameters. Considerations either of constructive interference or of Fourier analysis of a pulse multiply reflected within the crust reveal that the amplitude of peaks and troughs in the spectrum depends on the velocity contrast at the interfaces of the system. The "periodicity" or spacing of peaks and troughs depends on the time lags between the first arrival of the direct P wave and the secondary arrivals of the converted waves or of multiply reflected and refracted waves. Closely spaced fluctuations correspond to large time lags, and widely

spaced fluctuations to short time lags.

Observations of the spectrum of the apparent angle of emergence were obtained by dividing the smoothed spectra of the vertical and horizontal component seismograms. In order to avoid the influence of reflections at the crust near the source or of reflections from the core of the earth, the earthquakes selected were of intermediate and large focal depth and were restricted to epicentral distances less than 55°.

Application of the method to the long-period seismograms of the Saint Louis University Network of stations gives an average P velocity in the crust of 6.6 km/sec and a total thickness of the crust of 42 km for the central part of the United States under these stations.

LIST OF SYMBOLS

c = Apparent surface velocity

e_i = Angle of emergence of the P wave in the ith layer.

f_i = Angle of emergence of the S wave in the ith layer.

f = Frequency.

f_n = Folding frequency.

h_i = Thickness of the ith layer.

i_i = Angle of incidence of the P wave in the ith layer.

k = Wave number.

s_i = Angle of incidence of the S wave in the ith layer.

T = Period.

T_m = Total time length of record digitized.

TU = Transfer function of a layer system for the horizontal component of motion.

TW = Transfer function of a layer system for the vertical component of motion.

$\dot{u}_o$ = Horizontal component of particle velocity at the surface.

$\dot{w}_o$ = Vertical component of particle velocity at the surface.

α_i = Compressional velocity in the ith layer.

β_i = Shear velocity in the ith layer.

Δt = Time increment.

ε_{np_i} = Phase angle correspoding to a wave traveling n times as P in the ith layer.

φ = Phase angle of the transfer functions.

γ = Dimensionless parameter to evaluate transfer functions.

LIST OF SYMBOLS (Continuation)

λ_1 = Lame's elastic parameter.

λ = Wave length.

μ_1 = Lame's elastic parameter.

ρ_1 = Density in the ith layer.

σ = Poisson's ratio.

τ_b = Time lag of pulse b respect to first arrival.

ω = Angular frequency.

Ψ_n = Rotational solution of the wave equation.

∇_n = Dilatational solution of the wave equation.

THE DETERMINATION OF CRUSTAL THICKNESS FROM THE SPECTRUM OF P WAVES

1. Introduction

For many purposes the crust of the Earth and the upper mantle may be considered as a system of horizontal layers. When this system is excited by seismic energy its frequency response to the forced vibration is a function of the elastic parameters and thicknesses of the layers. As a result of this behavior the seismograms obtained at the surface contain detailed information pertaining to the crust and upper mantle of the earth immediately below the point of observation. Modern advances in the theory of elastic waves transmitted by layered media and computing facilities by means of electronic computers make it possible today to extract this information and to evaluate to a greater or lesser degree the parameters of the crust from the spectrum of longitudinal seismic waves.

The analysis of the body waves for this purpose is more conveniently performed in the frequency domain. This is the result of recent studies by Haskell (1953, 1962), Phinney (1964), Hannon (1964b), Harkrider (1964) and Fuchs (1965), who have investigated the theoretical calculation of the frequency response of layered systems to the energy of body waves.

In the present investigation the effect of layered media on infinite trains of sinusoidal longitudinal plane waves incident obliquely from below is studied. The response of different stratified models is systematized in such a way that families of curves for different models are obtained. By interpolation the response of intermediate models is made possible. Since the apparent angle of emergence of longitudinal waves is independent of the frequency content of the source, the effect of the layered system on this angle is taken as the basis of the analysis.

1.1 Observations of the effect of local geological parameters on longitudinal seismic waves.

Instrumental observations of the effect of the crustal layer on the periods and amplitudes of seismic body waves were first reported by certain Japanese authors: Imamura (1929), Ishimoto (1931a, 1931b, 1932, 1934), Nasu (1931), Inouye (1934) and Takahasi and Hiramo (1941). These investigators reported differences in the seismograms obtained for the same earthquake, at the same epicentral distance and azimuth, and by similar instruments but located on different geological sites. As a possible explanation of the difference the investigators suggested the reflecting character of the surface layers. At the same time Suzuki (1932) observed changes in the apparent angle of emergence with change in period of the waves. His explanation of the phenomenon was also in terms of the reflections and refrac-

tions taking place within the layers of the crust.

Similar types of observations were made in Europe and America. Gutenberg (1934) noticed the preference of certain stations to detect waves of a given period. The amplitude of the vibrations was also connected with the geological qualities of the site. Neumann (1954) noticed the different response of the "granitic type of rock" and "deep sedimentary rock." Greater amplitudes are always connected with the second type of rock. The amplitude of the seismic waves in relation to the geology of the place where the instruments were located was also studied by Gutenberg (1957). He further noticed that the long-period waves are not so affected by geological variations as are short-period waves. The effect of the ground on the amplitudes of body waves is the main reason why Gutenberg and Richter (1956) introduced the station correction factors when the magnitude of the earthquakes was determined from the amplitude and period of body waves.

The influence of the local near surface geology on the amplitude of short period P waves was observed by Fernandez (1963) using the North American stations of the Long Range Seismic Measurements Program. Similar types of observations for long-period waves by Nuttli (1964) showed that the long periods are not so sensitive to local characteristics of the site. The apparent angle of incidence and its changes with frequency were the object of observations by Nuttli

and Whitmore (1961)and by Nuttli (1964a).

1.2 Theoretical studies of the influence of a layered medium on the spectrum of longitudinal waves.

The series of observations just mentioned were accompanied by theoretical developments of the subject.

The observations of Imamura in 1929 attracted the attention of several Japanese seismologists. The problem of the free vibrations of the layered crust, and especially of the top layer, was not purely academic. In a country like Japan the influence of the ground on the amplitudes and accelerations created by earthquakes was a matter of public safety and of practical interest.

Under certain simplifying assumptions the theoretical problem concerns the solution of the wave equation which satisfies the boundary conditions of a system of horizontal layers. The layers are excited by an incident longitudinal wave which arrives at the base of the system at some angle of incidence. The boundary conditions for the solution of the problem are the continuity of stress and displacement at each internal interface and the vanishing of the stress at the free surface. The numerical calculations required were laborious and the authors simplified the problem to the simple cases of one or two layers and normal angle of incidence.

This is, for example, the approach of Sezawa (1930)who considers a one-layer model over a half-space and a dilatational

pulse propagated vertically. The same method is used by Sezawa and Kanai in a series of studies (1932a, b, 1937) including two-layer models, obliquely incident waves and harmonically oscillating sources. The theoretical seismogram is a function of the product of the frequency of the waves and the thickness of the layers. The same authors, Sezawa and Kanai, in another series of articles (1932c, 1934), studied the results of reflections and refractions in a stratified medium.

Kanai, in a collection of papers (1952, 1953a, b), calculates the resonance curve for the vertical and horizontal components. His results, though limited and partial and obtained by a laborious method, are exact and represent a significant contribution to the transmission problem of seismic waves in layered media.

Finally, Kanai and Yoshizawa (1956) studied the same effect for three-layer models excited not only by infinite trains of harmonic vibrations but also by finite trains of only one or two, or at most a few complete cycles. Kanai, Tanaka and Yoshizawa (1959) extended the number of models and made similar calculations for the motion at the free surface and at the interfaces.

In the meanwhile a new approach to the problem was developed by Thomson (1950), and by Haskell (1953). The method allows the calculation of the solution to the wave equation for any number of layers in terms of a four by four

matrix whose members are a function of the parameters of each layer, the angle of incidence and wave number of the wave. The method is very convenient for digital computer calculations. In his numerical calculations for a standard crustal model of one-layer over a semi-infinite half-space Haskell (1962) gives the ratio of the vertical and horizontal components of ground motion to the components of incident sinusoidal P-wave at the bottom of the layer, as a function of frequency and angle of incidence.

The work of Haskell was extended to different layered models by Hannon (1964a). The effects of the layers on the vertical and on the horizontal component are considered as transfer functions and the influence of changes in the thicknesses and velocities of the layers is carefully examined. Theoretical seismograms have been obtained by Hannon (1964b) by a Fourier synthesis of the transfer functions computed using the Haskell-Thomson matrices.

Similar calculations for different crustal models were the basis for the crustal studies of Phinney (1964) who compared theoretical curves for the ratio of the vertical to the horizontal transfer functions with the ratio of the spectra of vertical and horizontal seismograms. In this way Phinney was able to evaluate the crustal structures at some localities. Nuttli (1964a) used the transfer function to correct the apparent angle of incidence obtained from observations. The transfer functions for the S waves have also

been used by Nuttli (1964b) to correct the angle of polarization of S waves. In the studies of focal mechanisms from the spectrum of body waves Ben-Menahem, Smith and Teng (1964) correct the spectra for the effects of the crust at the station site using the transfer functions.

F ently Phinney (1965), to facilitate the use of theoretical calculation, integrated numerically the solutions for the response to a line source and a point source in elastic media. This method of integration gives a theoretical spectrum of the first seismic arrival, as viewed through an exponentially decaying time window.

Russian seismologists have shown interest in the practical applications of the problem. There are several instances in which they have used the influence of the sedimentary layers on the body waves to calculate the structure of a site for prospecting purposes. Savarensky (1952) studied the changes of the angle of emergency with frequency. Gamburtsev (1954) suggested the "seismic frequency sounding method" to investigate cross sections of interest. This method consists in the comparison of observed apparent angles of incidence at different frequencies with theoretical values calculated using layered models. Ivanova (1959,1960) used the method in a very simple way. Observations are obtained by tuning the seismometer at different frequencies and observing the apparent angle of incidence of the corresponding waves. The waves in question are generated by

explosions in deep wells. The results are compared with theoretical curves obtained using a method developed by Malinovskaya (1959).

Halperin (1962) studied the changes of the angle of incidence with frequency for a wave passing through a low velocity layer. An interesting theoretical study of the effects of thin layers on elastic waves is given by Pod'Yapol'ski (1961) who solves the Zoeppritz equations for complex amplitudes and considers the effect on a sinusoidal wave multiply reflected in a thin layer. The multiple reflection introduces the frequency effect into his calculations.

At the present moment it can be said that our theoretical knowledge of the effect of a layered medium on longitudinal waves is exact and complete. The Haskell method offers a fast technique to calculate the effect of the layers on the vertical and horizontal component of ground motion. Nevertheless the theoretical calculations can be systematized in a better way in order to group together into families of curves models with identical or similar response. For this purpose use may be made of a dimensionless parameter. Such a presentation allows a better application of the theory to observations and consequently a better determination of crustal parameters. Finally, the theory should be applied to more refined observations. This has been done in this study using earthquakes of intermediate and great focal depth.

2. Influence of the Layer Parameters on the Transfer Functions

The Thomson-Haskell matrix formulation of the boundary problem of seismic waves transmitted in a layered medium offers a rapid and exact calculation of the corresponding transfer functions. Only for high frequencies, as indicated by Dunkin (1965) is it possible that the method introduces errors due to numerical calculations. These high frequencies will not be considered here.

A detailed exposition of the method has been given by Haskell (1962) and by several others following Haskell (e.g., Hannon, 1964) and will not be repeated here.

In order to investigate crustal structures using the data of crustal transfer functions determined from the observation of P waves at a given place, it would be desirable to develop an inversion program whereby from the observed transfer functions one might determine a crustal model which best fits, in a least squares sense, the observational data. To this end, and to study the feasibility of such a program, it is necessary to understand the influence that changes of the parameters of the layers may have on the appearance of the transfer function curves. In order to do this two tests have been applied. In the first a crustal model was altered by a small fraction either in the crustal thickness or in the crustal velocity of P waves and

the results compared with the original transfer function. In the second test the first partial derivatives of the transfer functions with respect to the thickness, the elastic parameters and the density of the layers were calculated.

2.1 Results of small changes of the parameters.

The transfer functions for the vertical and horizontal components TW, TU, and the ratio TW/TU are each a function of several parameters here indicated with their respective symbols and corresponding to the ith layer:

h_i = thickness of the layer

α_i = longitudinal P wave velocity

ρ_i = density

β_i = shear wave velocity

i_n = the angle of incidence of the plane wave at the base of the layered system.

ω = frequency of a simple harmonic component of an incident wave.

Each combination of these parameters will give a different value of the transfer functions. For a given crustal model and angle of incidence the values of the transfer functions versus frequency define the transfer function curves.

To study the influence of the changes of the above-mentioned parameters some limitations which are imposed by nature itself may simplify the problem.

A first limitation based on physical properties of the rocks of the crust is the relationship observed between longitudinal and shear waves. It is commonly accepted that for this part of the earth the ratio α_1/β_1 is approximately constant and does not vary greatly from $\sqrt{3}$, corresponding to a value of 0.25 for the Poisson's ratio.

Another useful relationship based on observations exists between the P velocity of crustal layers and the density. According to Birch (1964), for the rocks of the crust, the density increases in almost a linear way with seismic velocities. This convenient relation will be used in our calculations.

Transfer functions, calculated using the FORTRAN II program listed in Appendix I, are presented in the graphs of Figures 1 and 2. In Figure 1 the curves indicated by the asterisks, * , correspond to an angle of incidence at the base of the crust of 35° and to a crustal model A given by the parameters:

	Thickness h (Km)	P Velocity (Km/sec)	S Velocity (Km/sec)	Density (gr/cc)
Crustal Layer	30	6.56	3.7872	2.64
Mantle	∞	8.2	4.7344	3.33

The curves indicated by the triangles, Δ , correspond to model B. This model has exactly the same parameters but with the thickness of the crust increased by 20% to 36 Km.

Examination of these two sets of curves shows that the second set is fore-shortened or "shrunk" in frequency

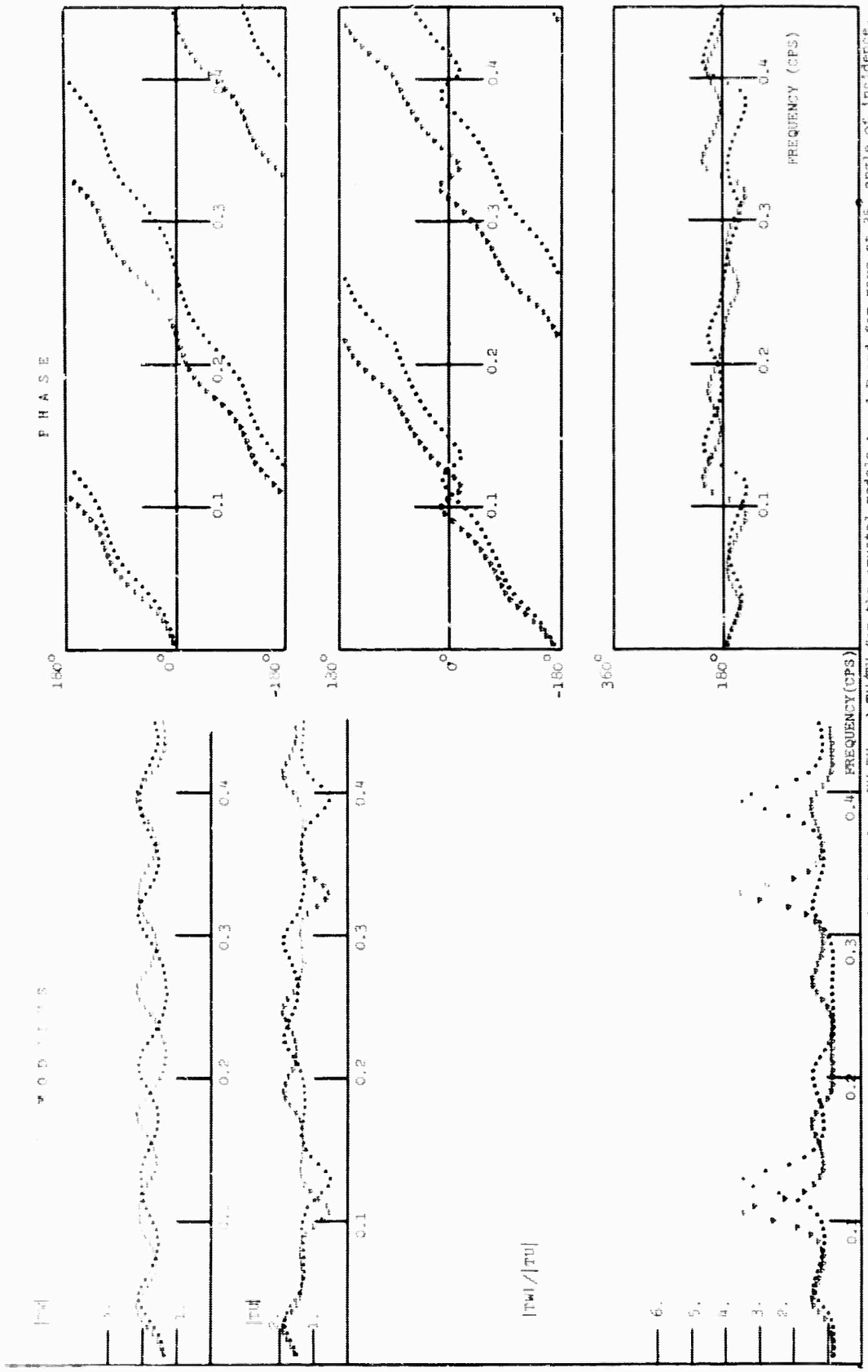

Figure 3 : Modulus and phase of the transfer functions TW,TU and TW/TU for the crustal models A and B and for rays at 35° angle of incidence.

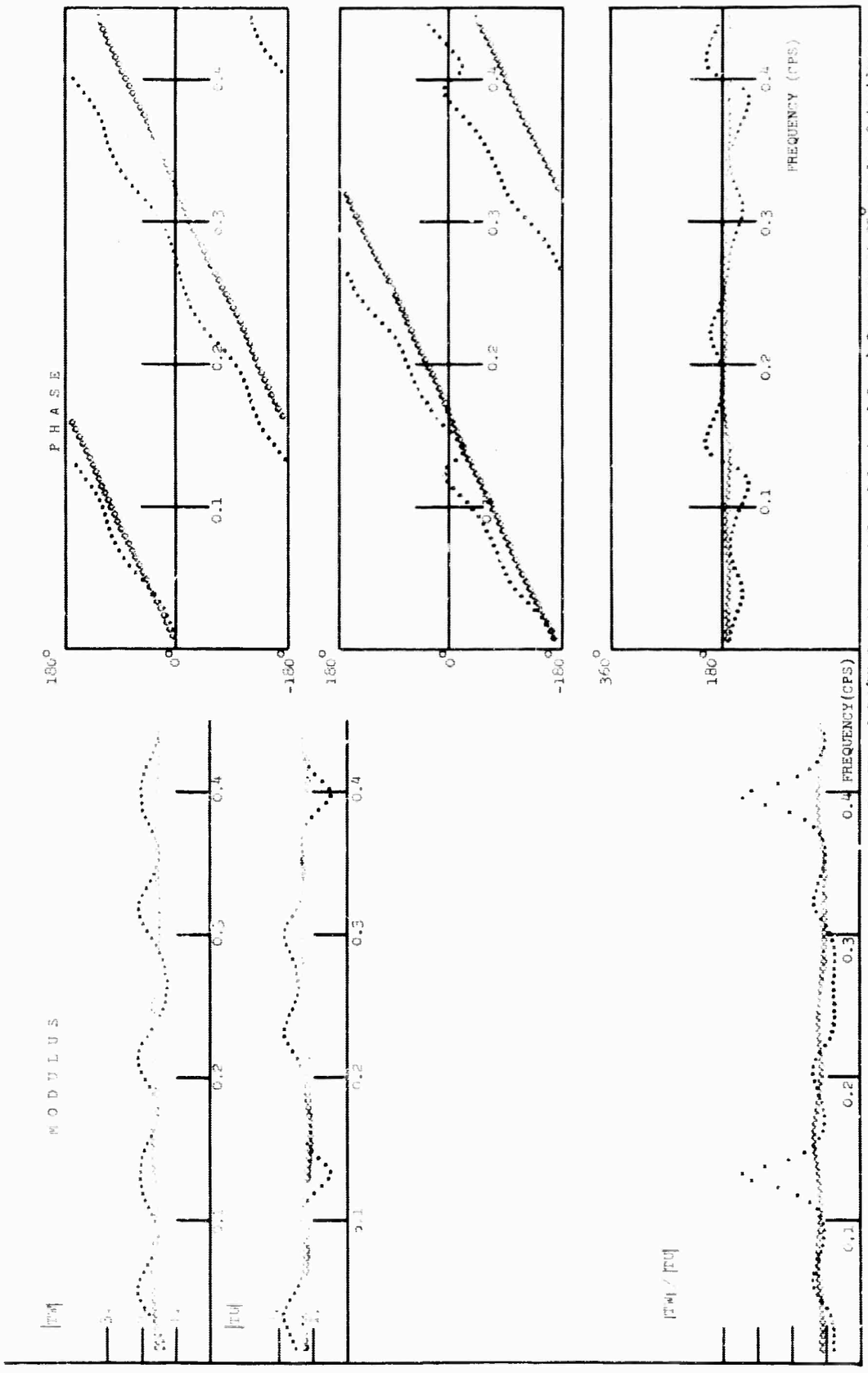

Figure 8 : Modulus and phase of the transfer functions TW, TU and TW/TU for the crustal models A and C and for rays at 35° angle of incidence.

dependence but is otherwise exactly the same in amplitude and shape as the first. This is obvious not only for the absolute values of the three transfer functions TW, TU, and TW/TU, but also for the phase angle presented in the graph at the right side of the figure. As the frequency increases the separation of similar portions of the curves becomes greater. This indicates that both models will show a similar spectrum of body waves at low frequencies but quite different at higher frequencies. The shifting of the features of the curve corresponding to the altered model relative to the original one is exactly 20% on the frequency scale. If the plot were made on logarithmic paper this effect would be shown by a displacement to the left of the second curve; otherwise the appearance of both curves would be exactly the same.

The properties of the matrices used to calculate the transfer functions already suggested this factor, as was indicated by Haskell (1953). Similar effects are observed when multilayered models are considered.

In a similar way the same model A was compared with model C. This model is exactly as model A but the P velocity in the crust was incremented by 20%, to 7.87 km/sec. The results of this change are presented in Figure 2. The shear velocity and the density are also changed according to the relations previously indicated. Examination of the results shows that in this case the change of velocities

affects not only the frequencies but also the amplitudes of the curves.

The effect on the frequencies is obvious, especially in the phase angle curves. In this case the frequency scale is expanded by 20%.

The change of amplitude of the transfer function oscillations was expected, since the contrast of velocities between mantle and crust is smaller; consequently the reflection coefficients for the P and SV reflected within the crust are smaller. The physical interpretation is that for small contrast of velocities the greatest part of secondary energy is transmitted back into the mantle.

This amplitude effect due to the change of velocities influences not only the absolute values of the transfer functions but also the oscillations of the phase angle.

The same two tests were performed for the same models for the angle of incidence of 10^{o}. The results are similar and are presented in Figures 3 and 4.

These results are significant since they show that the transfer functions have a special relationship to frequency such that changes of the parameters displace the peaks and troughs of the curves in the frequency domain. This behavior of the transfer functions presents difficulties when an inversion problem is attempted in terms of frequency.

2.2 First partial derivatives.

The use of surface wave data for the investigation of earth structure has been improved recently by the develop-

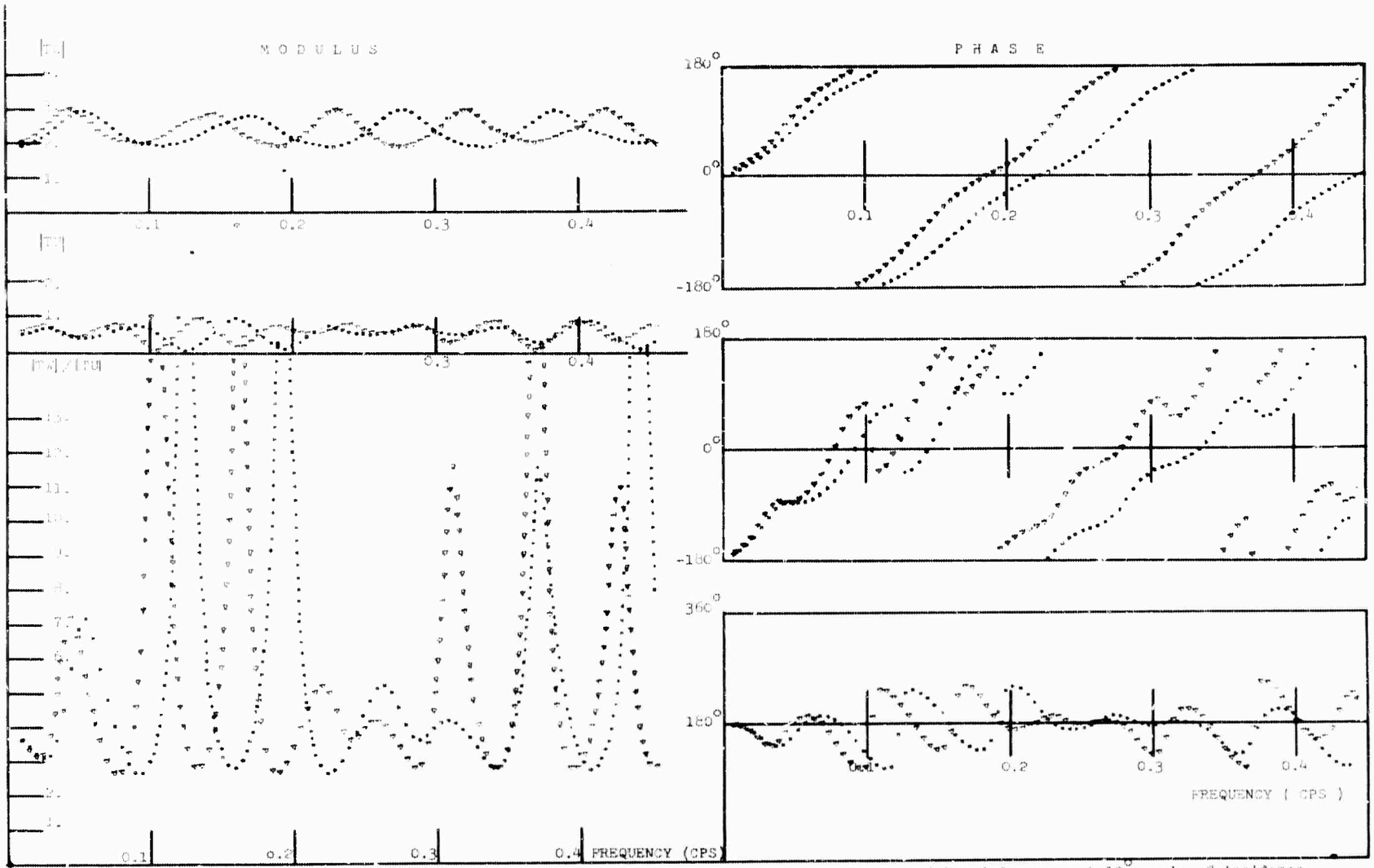

Figure 3 : Modulus and phase of the transfer functions TW, TU and TW/TU for crustal models A and B and for rays at 10° angle of incidence.

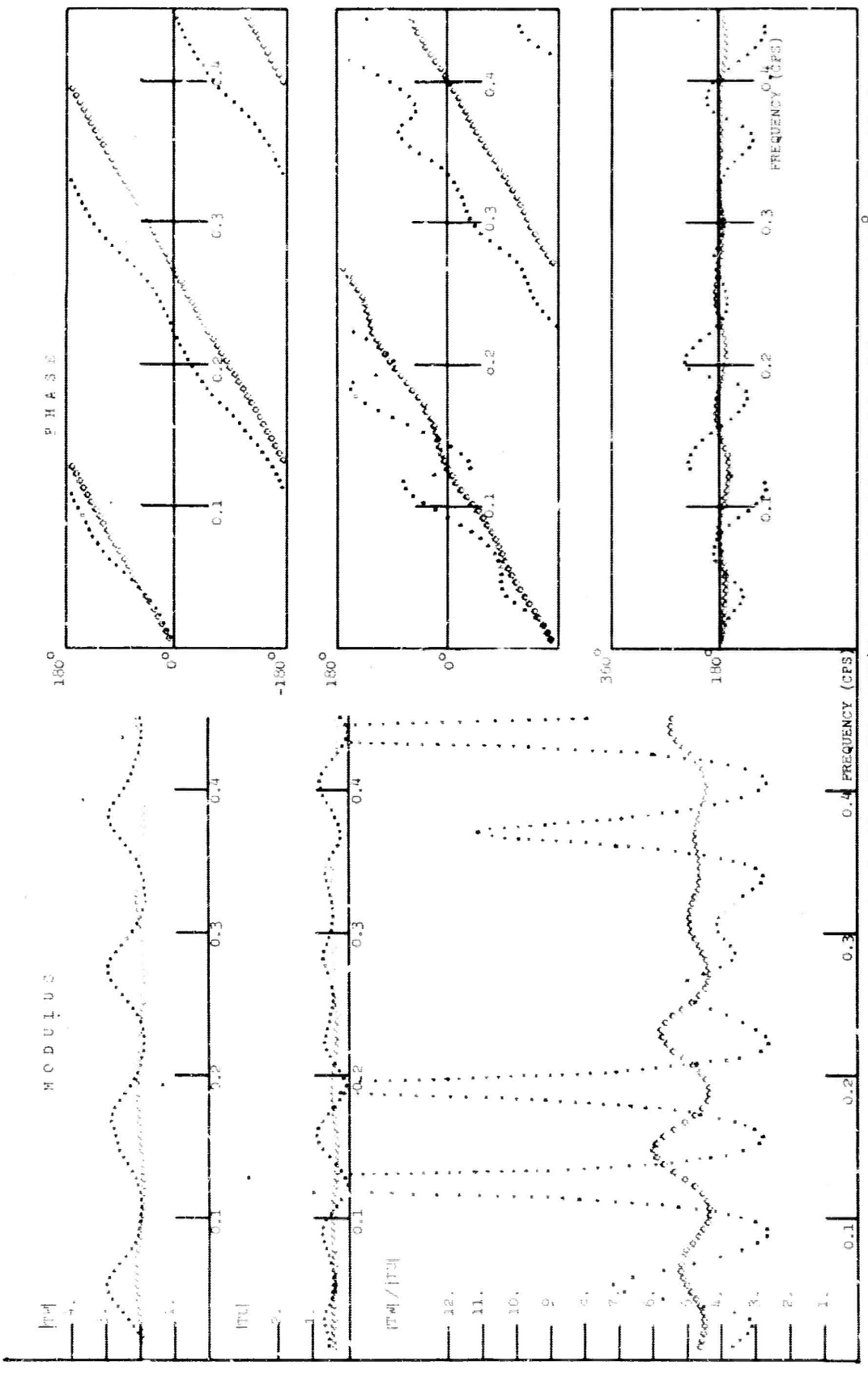

Figure 4 : Modulus and phase of the transfer functions TW, TU and TW/TU for crustal models A and C and for rays at 10° angle of incidence.

ment of an inversion technique based on a least squares curve fitting procedure whereby theoretical group and phase velocity dispersion curves obtained from selected earth models are adjusted so as to best fit observed dispersion curves. Dorman and Ewing (1962) and Brune and Dorman (1963) applied the least squares technique by the repeated calculation of partial derivatives of phase velocity with respect to each of the parameters of the layers. This is done for each iteration of the calculations. Anderson (1964) showed that for reasonable variations in the parameters of the layers, the partial derivatives of the phase velocity may be considered constant. This property reduces the least squares inversion technique calculations and has been used with success, for example, by McEvilly (1964) to evaluate the crust-upper mantle structure in the central region of the United States.

In order to use the body wave spectra to evaluate the structure below the point of observation the same technique could be applied to obtain the best fit in the least squares sense between observations and theoretical curves. As indicated above, a necessary condition to use the simplified technique of Anderson is that the partial derivatives of the transfer functions with respect to the parameters of the layers remain constant for reasonable variations of the parameters. This property was investigated by the direct calculation of the partial derivatives of the transfer functions TW, TU and the ratio TW/TU.

Using the notation and sign conventions of Haskell (1953 and 1962) and Hannon (1964a), the transfer functions for the horizontal and vertical components of ground motions at a given frequency ω are:

$$TV(\omega) = \frac{2c\,(J_{42} - J_{32})}{\alpha_n\, D}$$

$$TW(\omega) = \frac{2c\,(J_{41} - J_{31})}{\alpha_n\, D} \qquad (2\text{-}1)$$

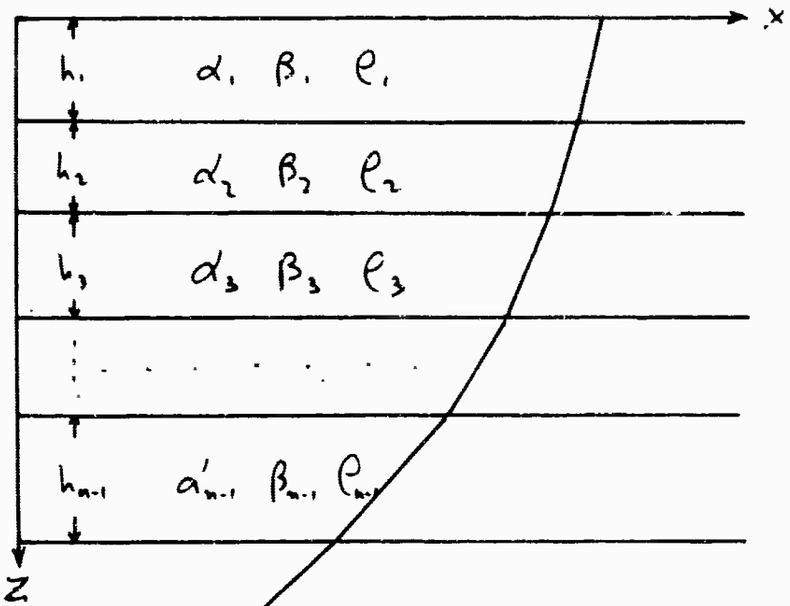

Figure 5. Crustal system of n layers and direction of seismic ray.

where c is the apparent surface velocity,

$$D = (J_{11} - J_{21})(J_{32} - J_{42}) - (J_{12} - J_{22})(J_{31} - J_{41})$$

and the J_{ik} are the elements of the matrix product obtained in solving the boundary value problem of the layer system:

$$J = E_n^{-1}\, a_{n-1}\, a_{n-2} \cdots a_1 \qquad (2\text{-}2)$$

Since each element or sub-matrix a_m of (2-2) depends on the parameters of only one layer it is possible to find the first partial derivatives of J and D with respect to any of the independent parameters in any layer m by finding the partial derivatives of the element matrix a_m and substituting this value in the product J.

For example, the partial derivative of TU(ω) with respect to the thickness of the mth layer will be:

$$\frac{\partial TU(\omega)}{\partial h_m} = \frac{2c}{\alpha_m}\left[\frac{D\,\frac{\partial(J_{42}-J_{32})}{\partial h_m} - (J_{42}-J_{32})\frac{\partial D}{\partial h_m}}{D^2}\right] \qquad (2\text{-}3)$$

and

$$\frac{\partial J}{\partial h_m} = E_n^{-1}\, a_{n-1}\, a_{n-2} \cdots \frac{\partial a_m}{\partial h_m} \cdots a_1 \qquad (2\text{-}4)$$

In order to be able to differentiate a_m with respect to the independent parameters of the layers, each element of a_m should be expressed in terms of the density ρ_m the thickness h_m and the elastic parameter λ_m. For the crust it is assumed that the Lame constants have identical value, that is $\lambda = \mu$

Then, for example, the first element of a_m is:

$$(a_m)_{11} = \frac{2\lambda_m}{\rho_m c^2}\cos\left[k h_m\left(\frac{\rho_m c^2}{3\lambda_m} - 1\right)^{1/2}\right] - \left(2\frac{\lambda_m}{\rho_m c^2} - 1\right)\cos\left[k h_m\left(\frac{\rho_m c^2}{\lambda_m} - 1\right)^{1/2}\right] \qquad (2\text{-}5)$$

and its first partial derivative with respect to the thickness of the mth layer is:

$$\frac{\partial (a_m)_{11}}{\partial h_m} = -\frac{2\lambda_m}{\rho_m c^2} k \left(\frac{\rho_m c^2}{3\lambda_m} \cdot 1\right)^{1/2} \sin\left[k h_m \left(\frac{\rho_m c^2}{3\lambda_m} - 1\right)^{1/2}\right]$$

$$+ \frac{2\lambda_m}{\rho_m c^2} - 1 \; k \left(\frac{c^2 \rho_m}{\lambda_m} - 1\right) \sin\left[k h_m \left(\frac{\rho_m c^2}{\lambda_m} - 1\right)^{1/2}\right] \qquad (2\text{-}6)$$

The same operation may be performed for the 16 elements of the matrix and with respect to the independent parameters h_i, λ_i, ρ_i . These calculations have been combined in a FORTRAN II computer program listed in Appendix (II), and the results of this program were plotted in Figures 6 to 8. The partial derivatives shown in these figures correspond to the same crustal model A studied earlier in this chapter by variation of the parameters.

In general the partial derivatives have large values even for low frequencies. The values of the derivative are greater for the ratio of the vertical and horizontal components TW/TU. By studying the curves of the first partial derivatives it may be noted that the maxima correspond to the maxima of the corresponding transfer functions. This could be expected from the character of the shifting toward higher or lower frequencies of the peaks of the transfer functions, as noted above, when the parameters of the layers

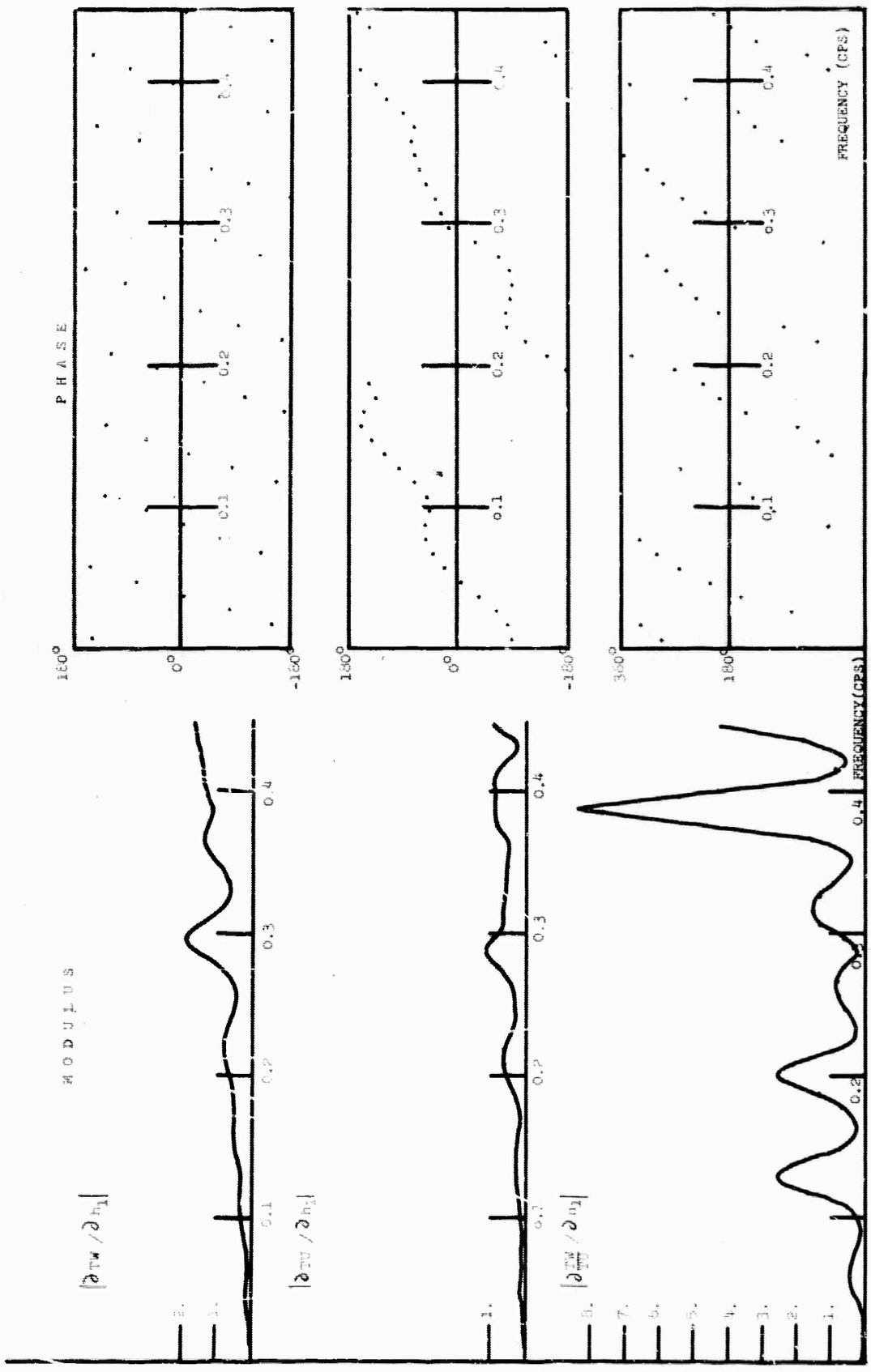

Figure 5 : Modulus and phase of the first partial derivatives of the transfer functions TW, TU and TW/TU with respect to h_1. Model A at 35° angle of incidence.

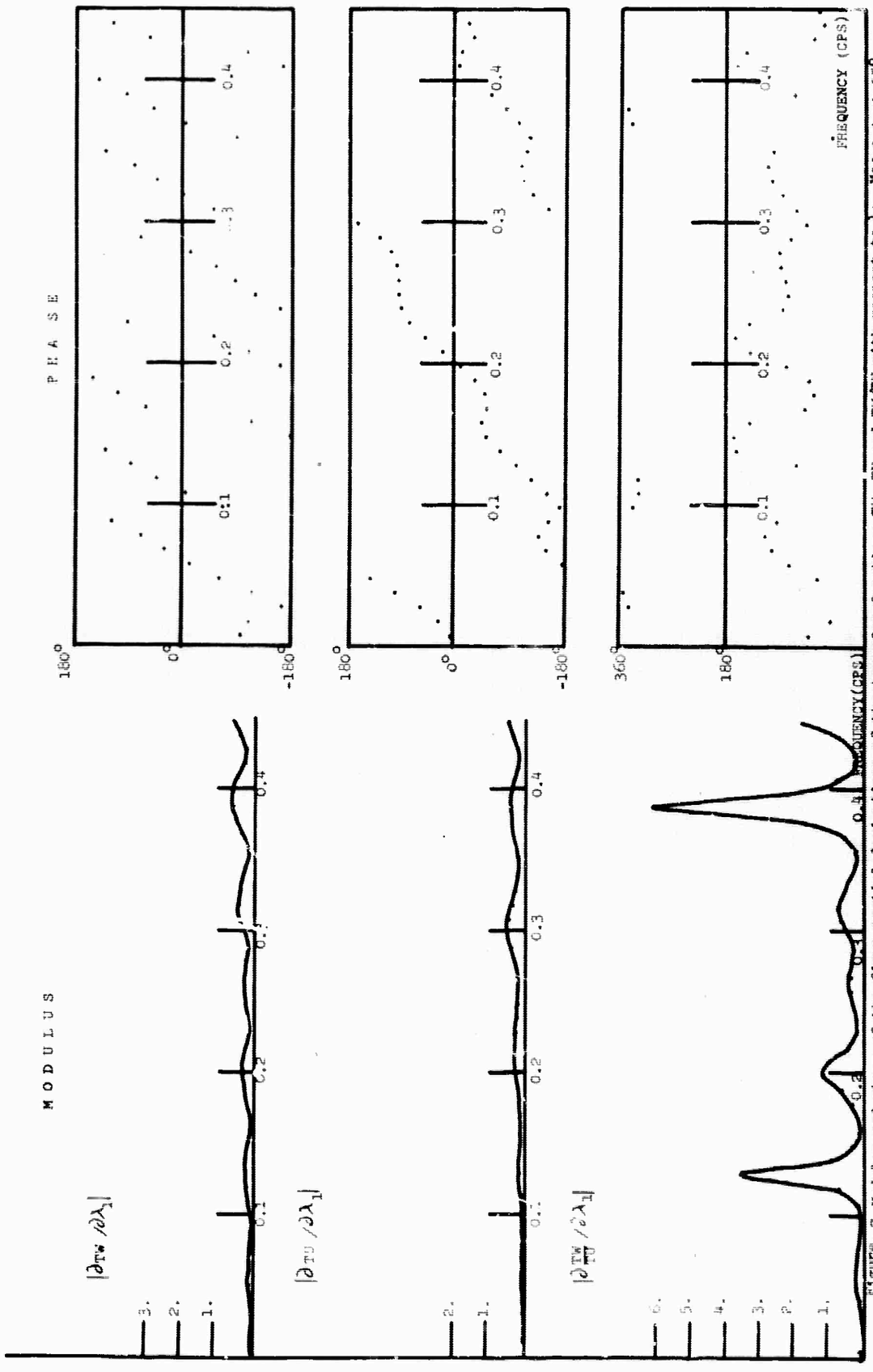

Figure: 7 Modulus and phase of the first partial derivatives of the transfer functions TW, TU and TW/TU with respect to λ_1. Model A at 35° angle of incidence.

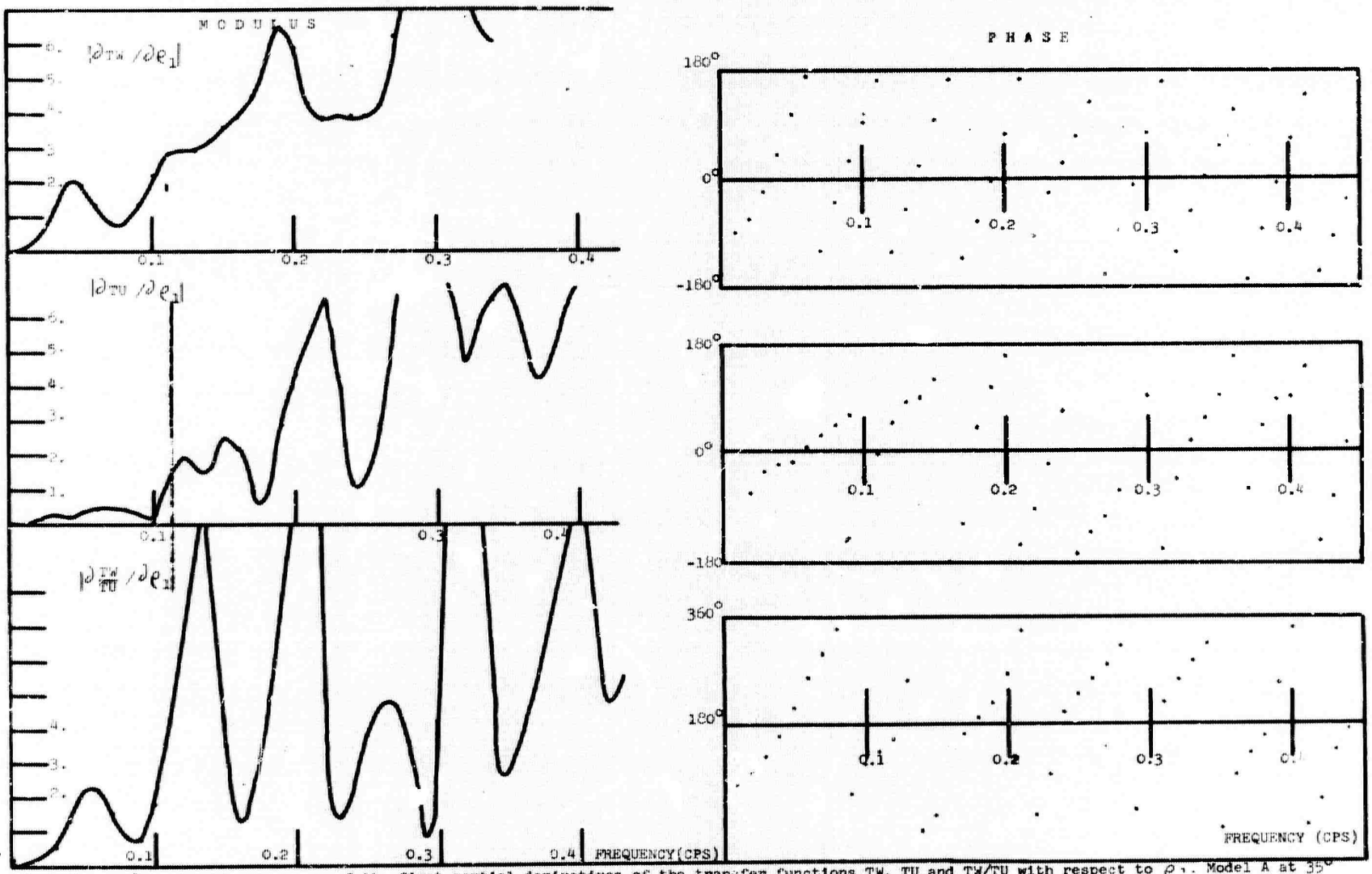

Figure 8 : Modulus and phase of the first partial derivatives of the transfer functions TW, TU and TW/TU with respect to ϱ_1. Model A at 35° angle of incidence.

are changed. This shifting will affect most notably the peaks of the curves. Also, since the shift increases with frequency, the partial derivatives increase also with frequency.

To study the effect of changes in the parameters in a multilayered model the crustal model 1 of Hannon (1964a) was selected. This model is similar to the crustal structure of the central United States and its parameters are:

Layer Number	Thickness (km)	P Velocity (km/sec)	S Velocity (km/sec)	Density (gm/cm^3)
1	1.0	4.40	2.50	2.70
2	19.0	6.20	3.50	2.00
3	18.0	6.40	3.70	2.90
Half-space		8.20	4.00	3.30

The modulus and the phase of the transfer function for the vertical and horizontal component TW and TU and their ratio TW/TU are given in Figure 9. The corresponding first partial derivatives with respect to the thickness, Lame's constant and density of each of the layers are presented in Figure 10 to 18.

These calulations show that thin layers have smaller values of the first partial derivative than do thick layers. This is explained, again, by the shifting of the frequencies since the shifting was proportional to the thickness of the layer in relation to the total thickness of the system. In the case of a thin layer this shifting is small and as such the changes of the transfer functions will be small.

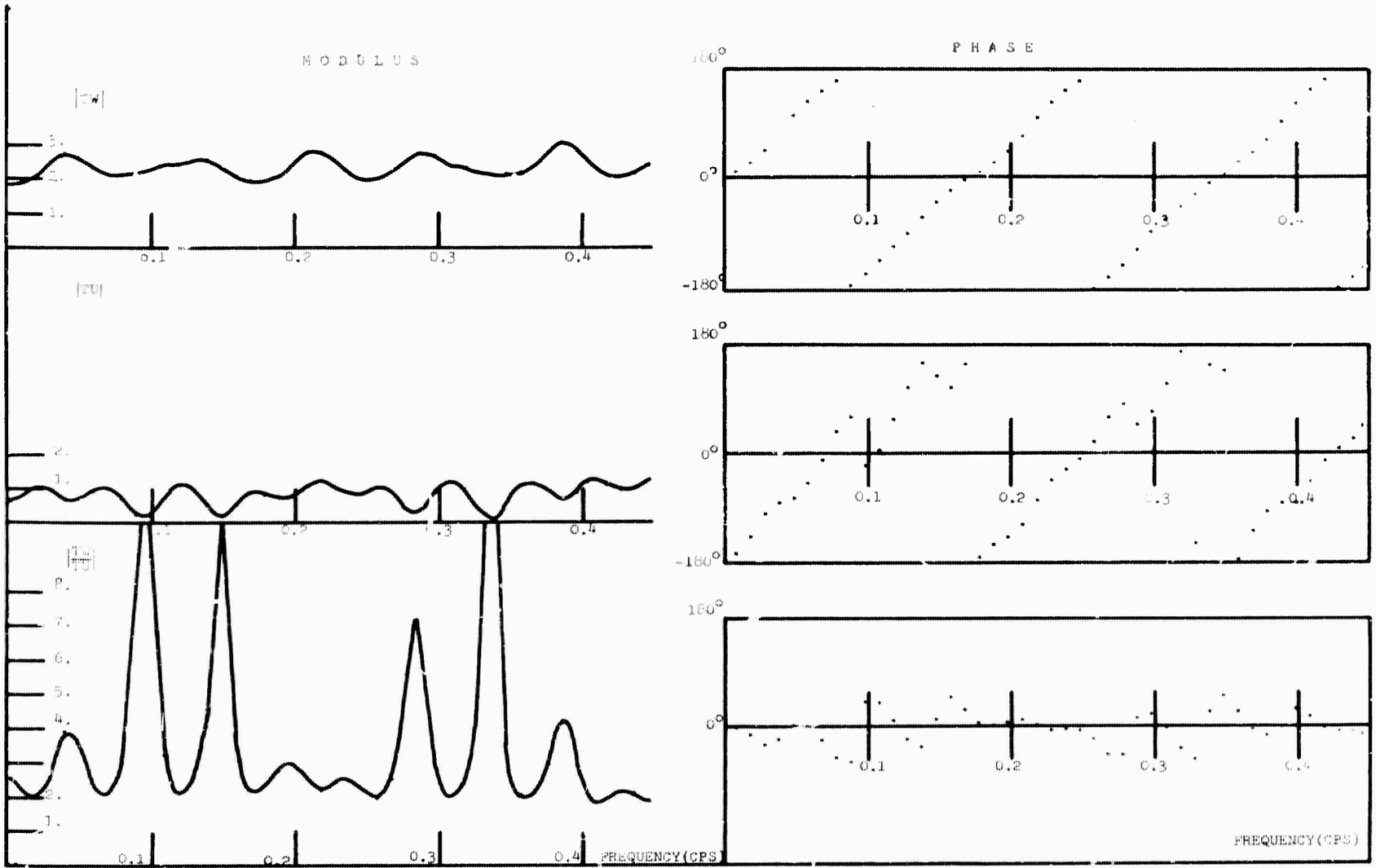

Figure 9: Modulus and phase of the transfer functions TW, TU and TW/TU for the crustal model corresponding to Central United States and for rays at 20° angle of incidence.

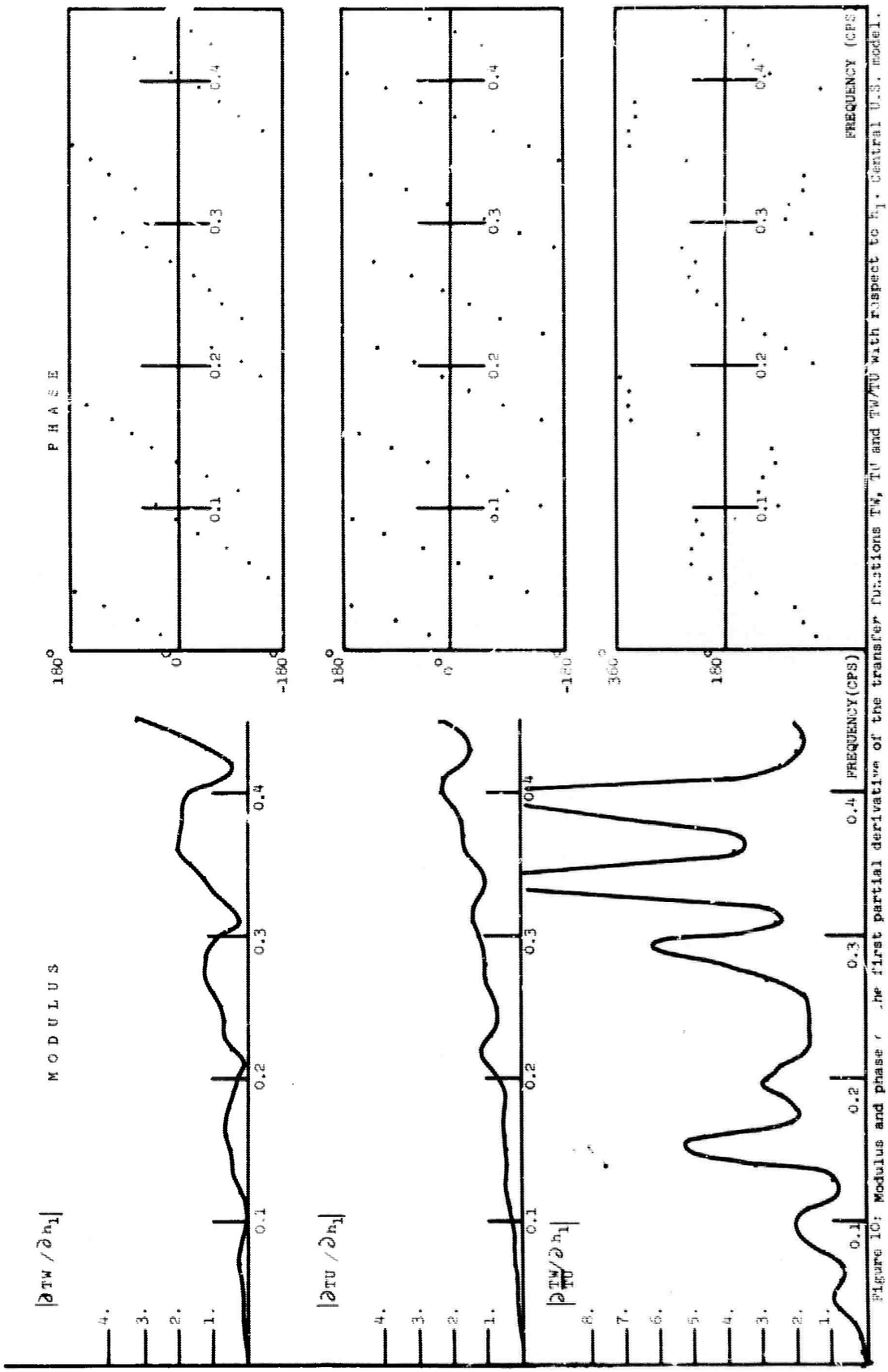

Figure 10: Modulus and phase of the first partial derivative of the transfer functions TW, TU and TW/TU with respect to h_1. Central U.S. model.

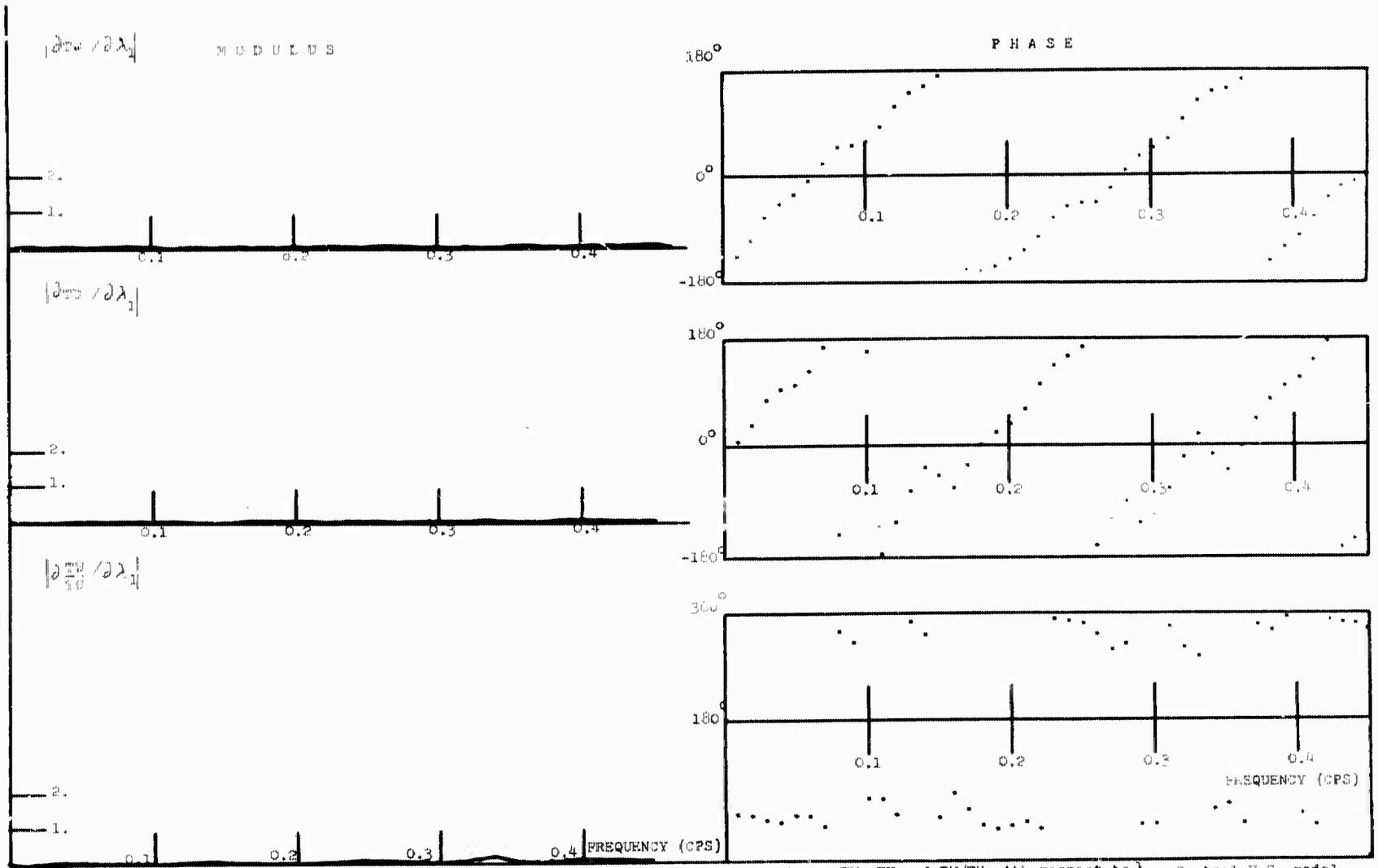

Figure 11 : Modulus and phase of the first partial derivative of the transfer functions TW, TU and TW/TU with respect to λ_1. Central U.S. model.

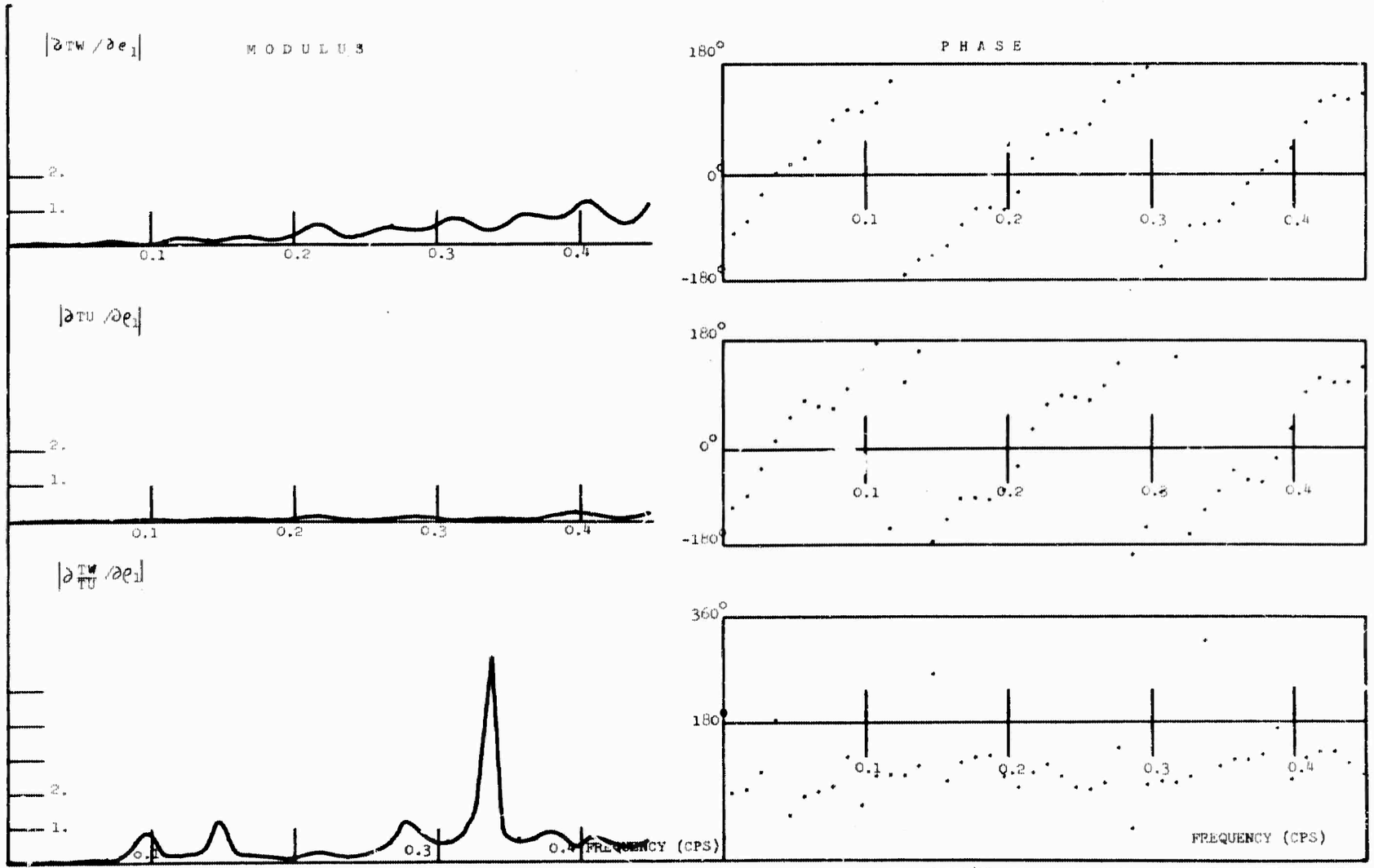

Figure 12 : Modulus and phase of the first partial derivative of the transfer functions TW, TU and TW/TU with respect to e_1. Central U.S. model.

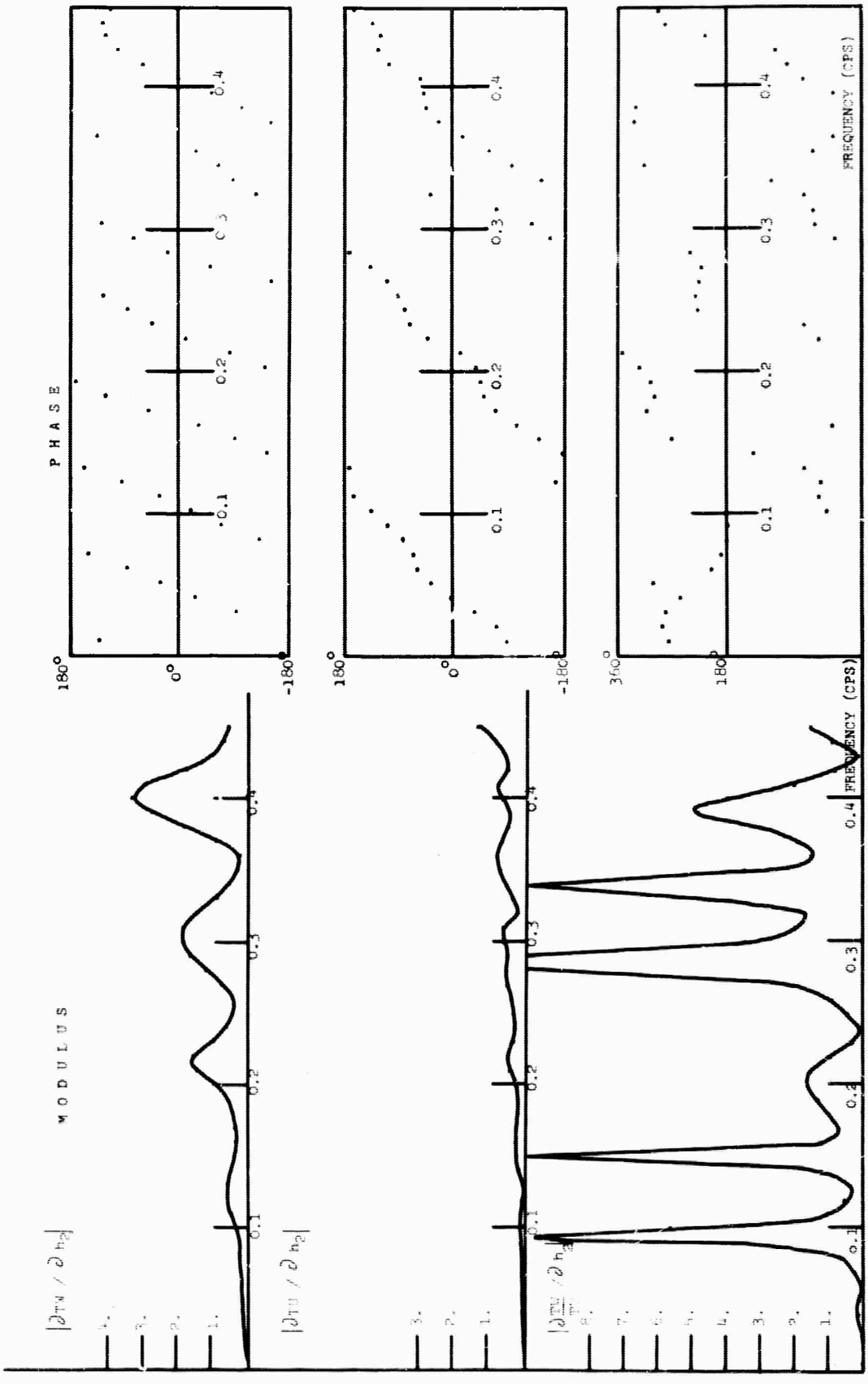

Figure 13 : Modulus and phase of the first partial derivatives of the transfer functions TW,TU and TW/TU with respect to h_2. Central U.S. model.

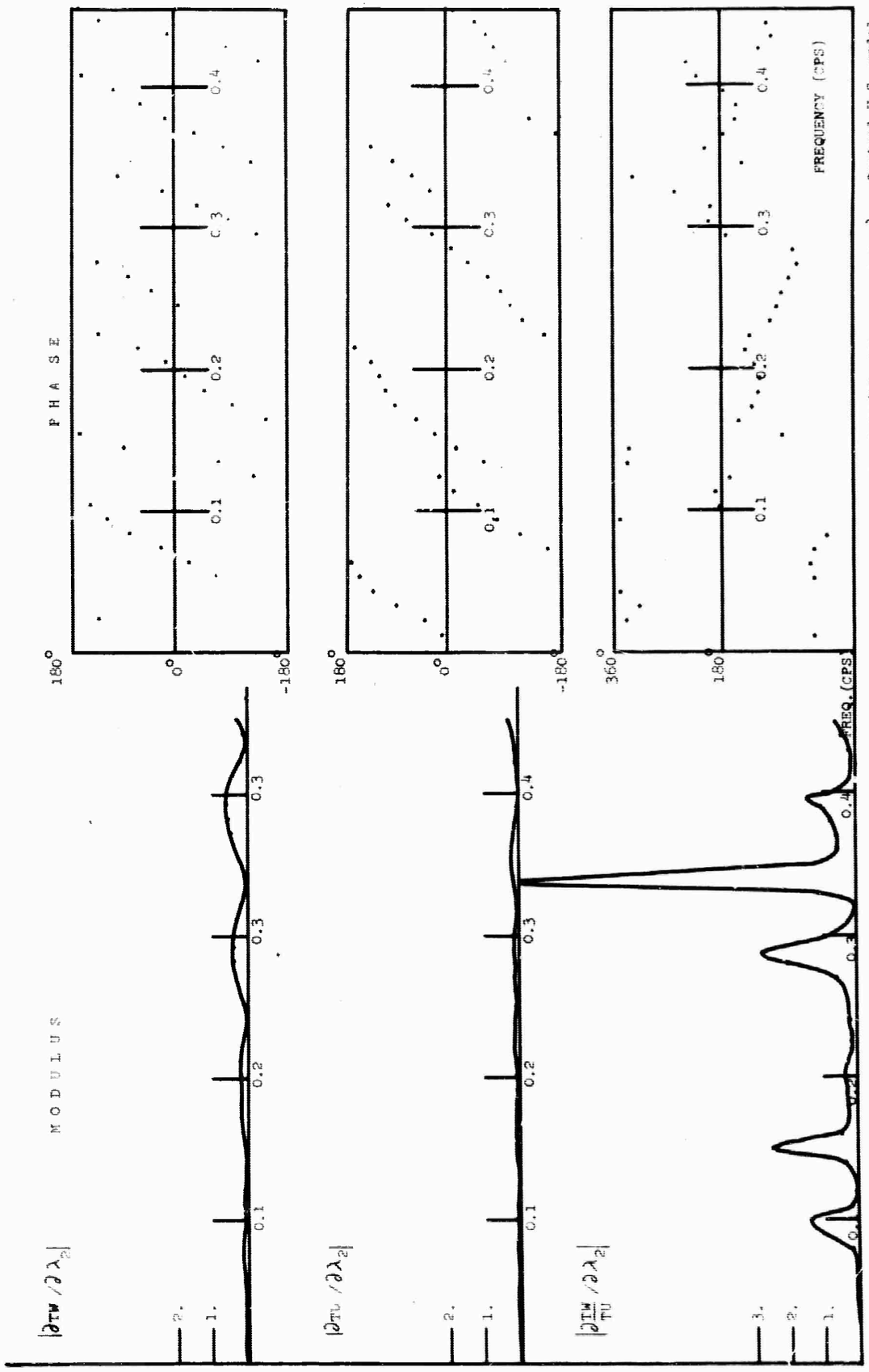

Figure 14 : Modulus and phase of the first partial derivative of the transfer functions TW, TU and TW/TU with respect to λ_2. Central U.S. model

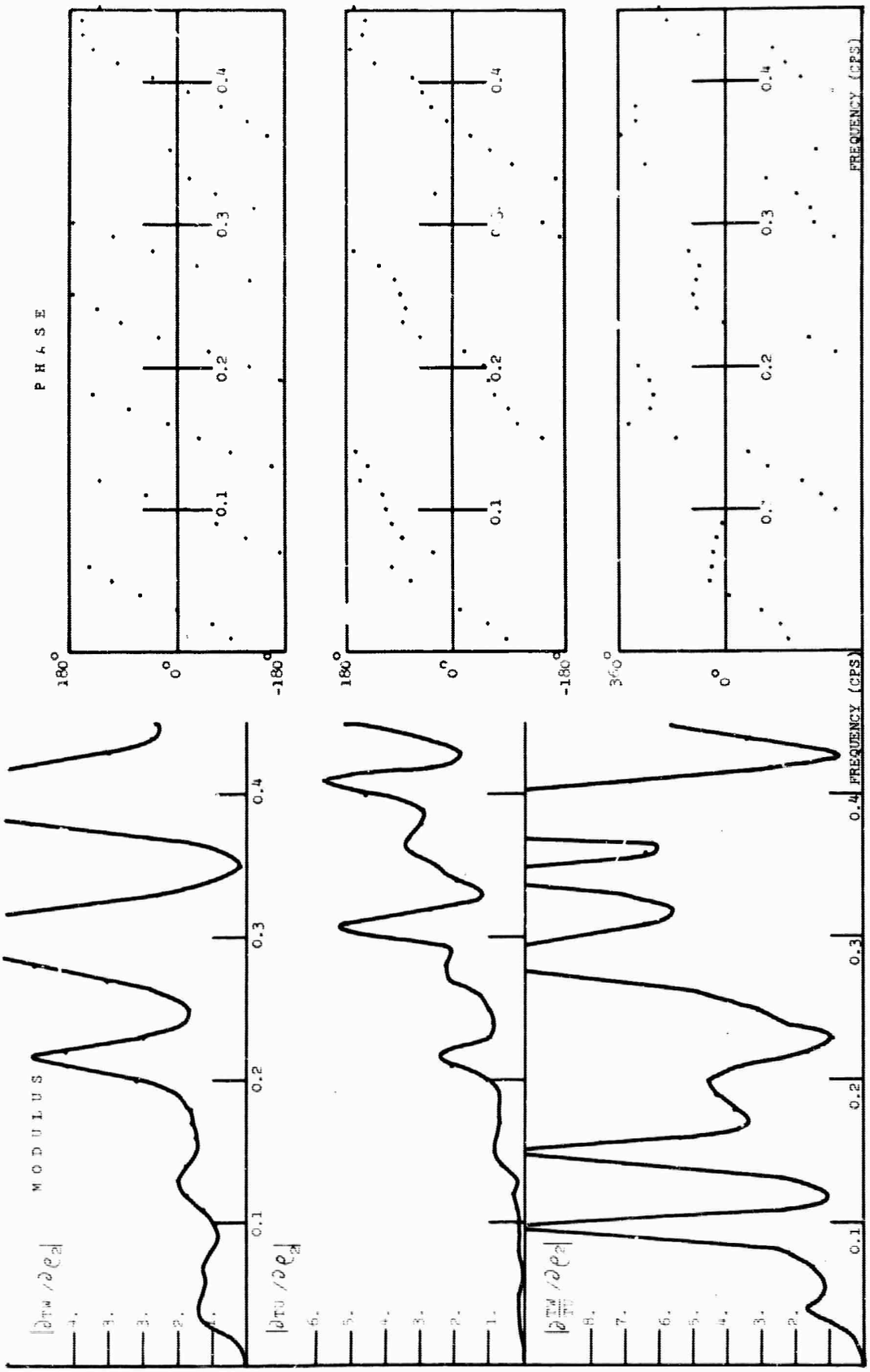

Figure 15 : Modulus and phase of the first partial derivatives of the transfer functions TW, TU and TW/TU with respect to ρ_2. Central U.S. model.

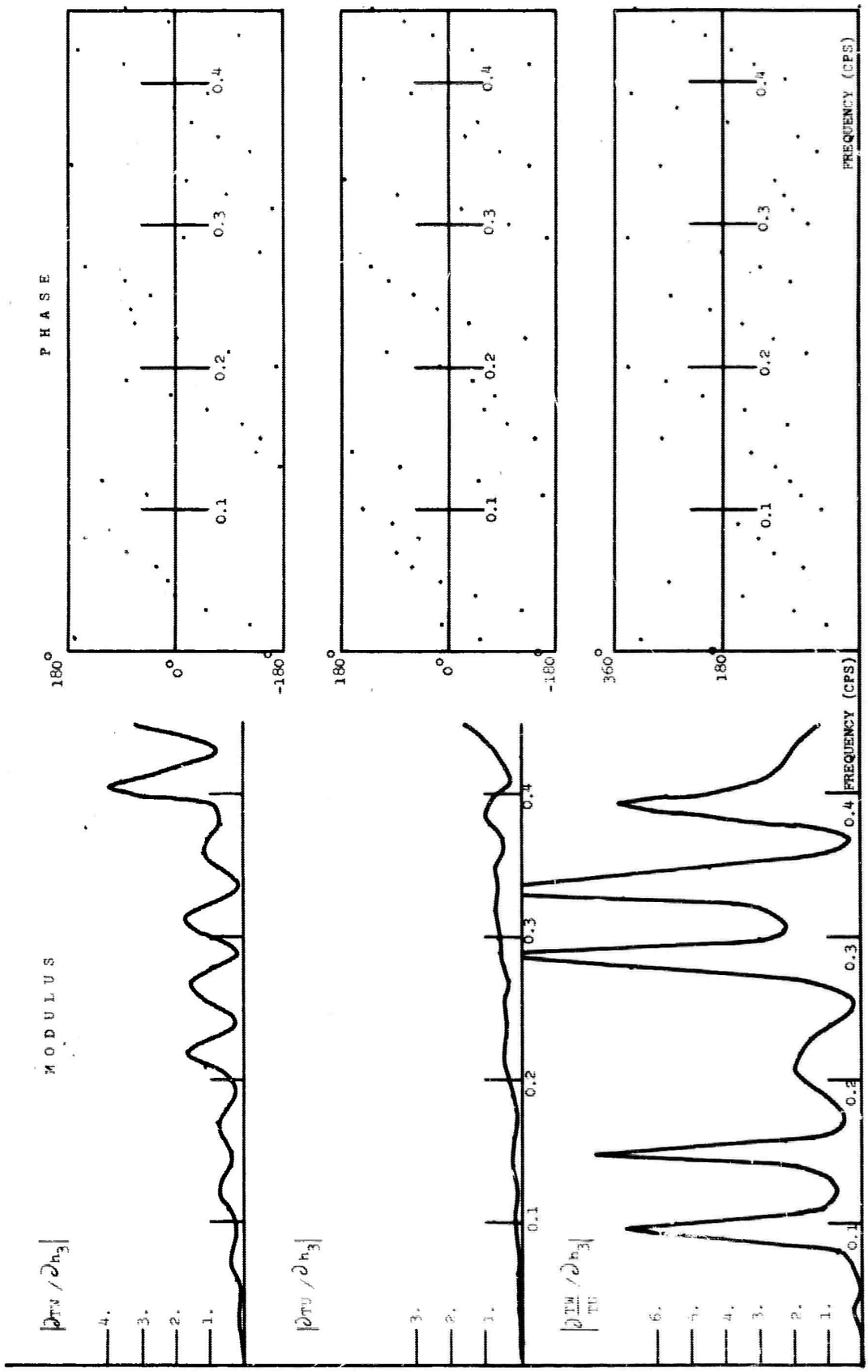

Figure 16 : Modulus and phase of the first partial derivatives of the transfer functions TW, TU and TW/TU with respect to h_3. Central U.S. model.

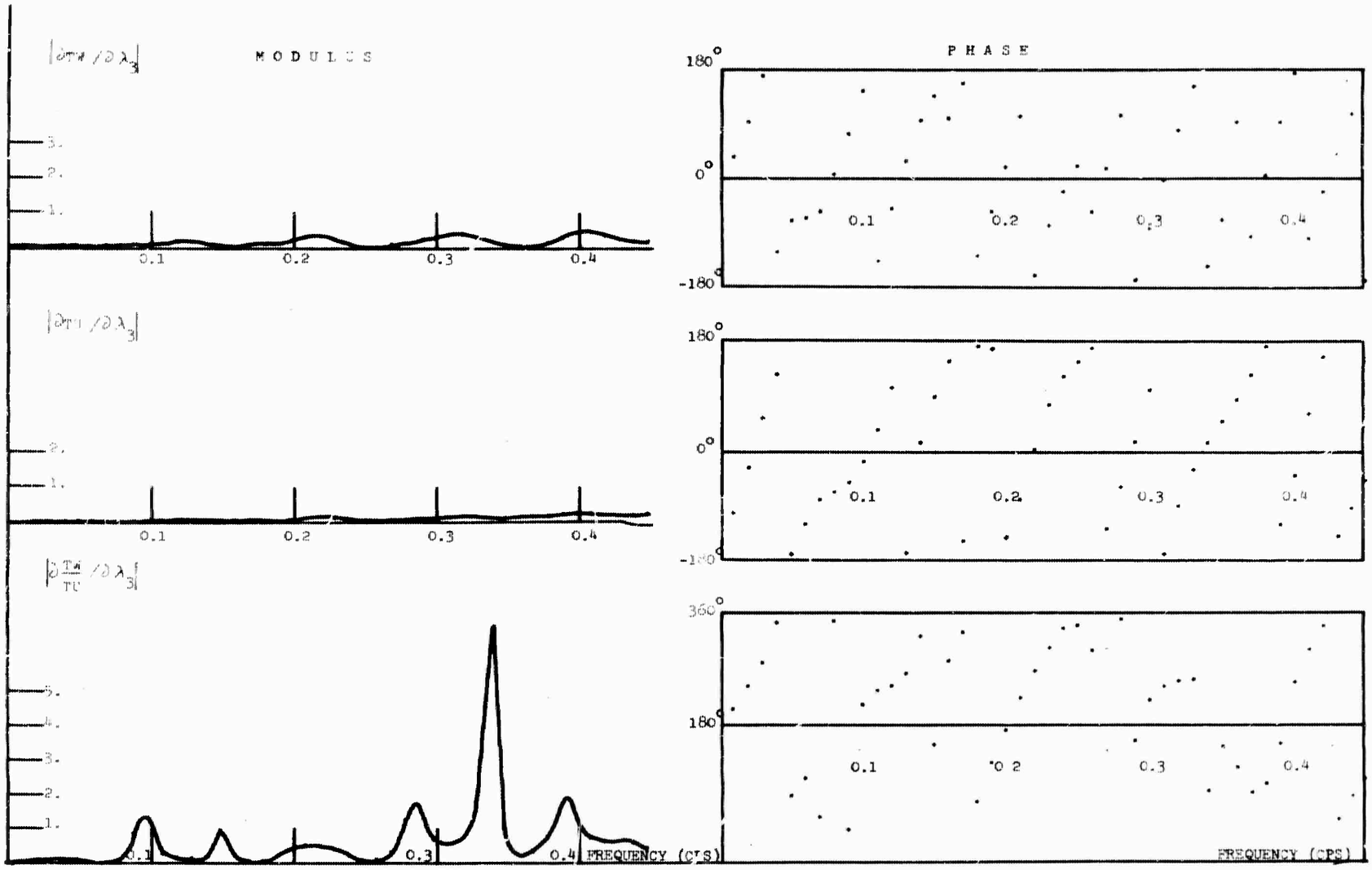

Figure 17 : Modulus and phase of the first partial derivatives of the transfer functions TW, TU and TW/TU with respect to λ_3. Central U.S. model.

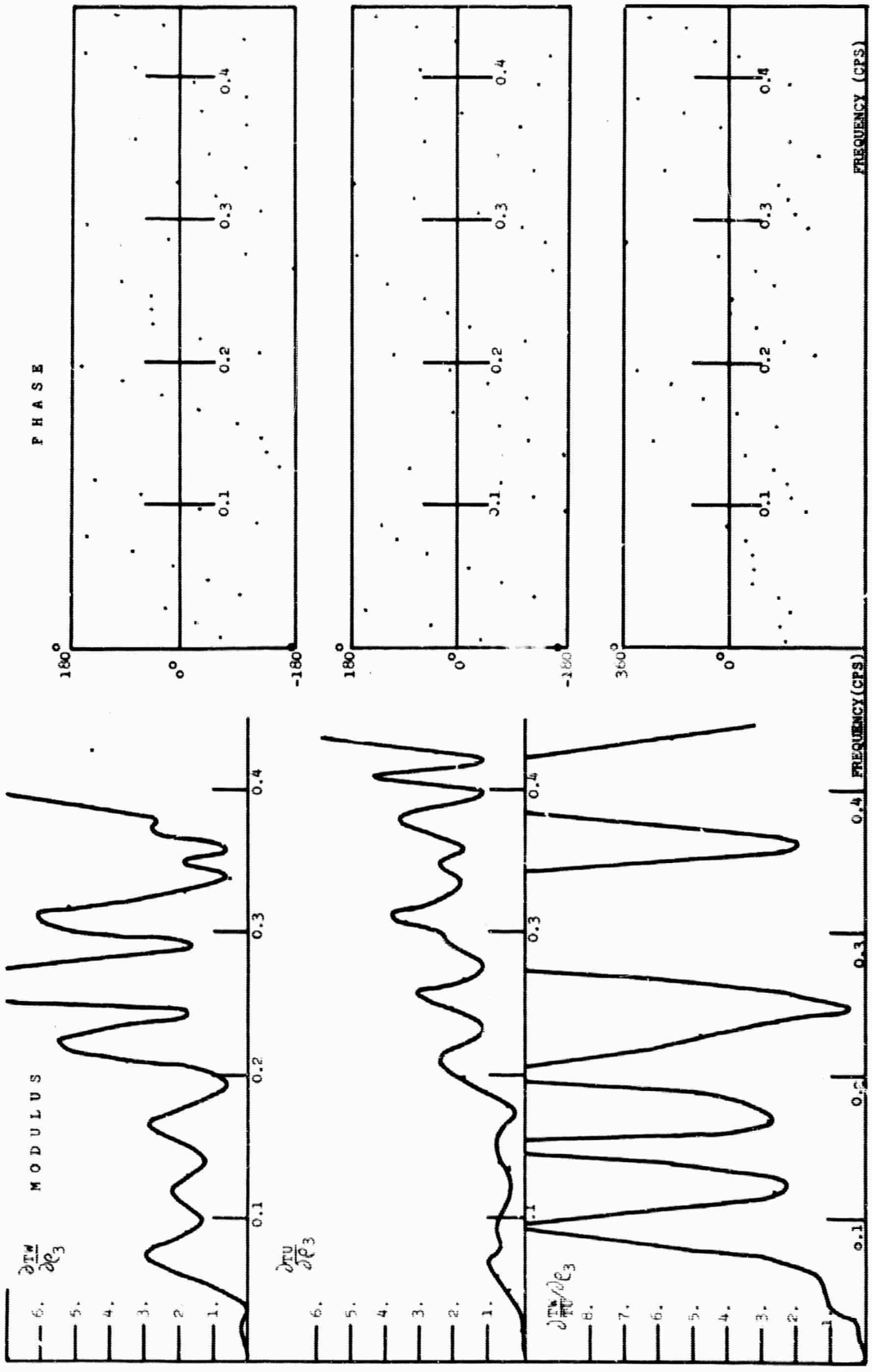

Figure 18: Modulus and phase of the first partial derivatives of the transfer functions TW, TU and TW/TU with respect to ρ_3. Central U.S. model.

The periodical character of the first partial derivatives may be explained by the same shifting of the frequencies. As the frequency increases the peaks are displaced more and more till one peak is displaced to the frequency of the neighboring peak of the original curve. In this event the first partial derivative is not so great. This situation corresponds to the minima of the first partial derivative curves.

Among the different parameters the changes in density affect more the transfer functions. For the angle of incidence of 20° the vertical component transfer function is more sensitive to changes of the parameters than the horizontal component.

To test the stability of the first partial derivatives when small changes of the parameters are introduced in the parameters of the crust, model A and its partial derivatives were compared with the first partial derivatives of model D. This model D is the same as model A with the exception of the thickness of the crust which was incremented by 10% to 33 km.

The numerical results showed that the individual values of the first partial derivatives for a given frequency were quite different for both models. Consequently an inversion process based on the assumption that the first partial derivatives remain constant for reasonable changes of the layer parameters is not possible if the transfer functions are calculated as a function of frequency.

3. Analysis of Factors Affecting the Character of the Transfer Function Curves

Though normal mode theory and the Haskell-Thomson matrix development is the more convenient for numerical calculations of the transfer functions of seismic waves in layered media, nevertheless there are other theoretical approaches to the problem. While these latter are more laborious for numerical calculations, in some respects they give clearer insight into the physical problem and into the phenomena taking place in the stratified medium. This better understanding of the problem helps to evaluate the influence of each of the layer parameters in the transfer function itself.

In this section we present two different approaches to the propagation of seismic energy in layered media in order to understand better the behavior of the transfer functions. The first one is based on considerations of constructive and destructive interference of the primary and reflected waves arriving at a given point of the surface. The second approach considers the Fourier transform of a delta function pulse multiply reflected and refracted in the layered medium.

3.1 Interference patterns of multiply reflected seismic waves.

The effect of layered media on an infinite train of

sinusoidal longitudinal waves of a given angular frequency ω may be investigated from the point of view of constructive interference of the direct arrival of the wave at the surface and the simultaneous arrivals of reflected and refracted waves at the same point of the surface. The result will be a superposition of waves of the same frequency but of different amplitude and phase.

The amplitude of the reflected and refracted rays may be found by solving the Zoeppritz equations (Zoeppritz, 1919) in terms of the angle of incidence of the ray, the type of conversion taking place, and the contrast of velocities between the two media at the interface. For a ray suffering several reflections, refractions, and conversions the final amplitude will be the product of the appropriate coefficients at each interface. Graphical and numerical values for the solutions of Zoeppritz's equations are given by several authors (e.g., Steinhart and Meyer, 1959; McCamy, Meyer, Smith, 1962; Costain, Cook and Algermissen, 1963).

In all these studies the frequency of the wave is neglected since the authors are interested only in the amplitude or transmission coefficients of the interfaces.

However, the resultant amplitude for the displacement at the free surface of a layered media due to the superposition of waves of the same frequency but of varying amplitude and phase is a function of both the amplitudes and the phases of the components.

3.11 The single layer case.

Consider a simple case. Let a plane wave front DE (Figure 19) arrive at the interface of a single layer model.

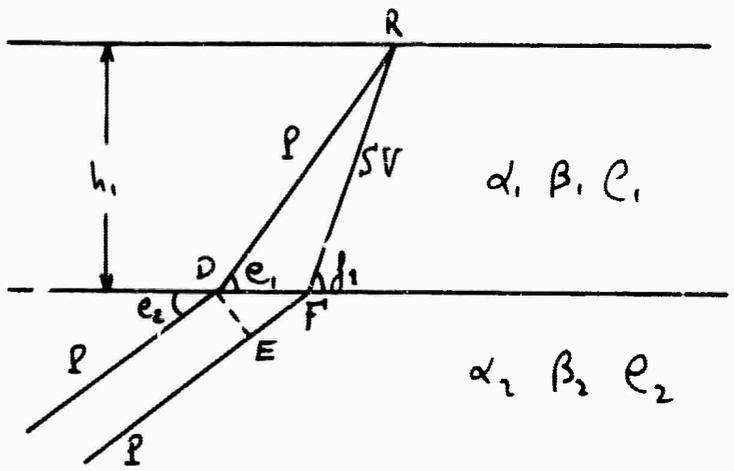

Figure 19. Seismic transmission in a single layer model.

Let R be a point at the surface such that the direct P and the converted SV from the point F meet together. The two rays, PD and PF, were in phase at the wave front DE but they will not be in phase when they arrive at R. The phase difference is a function of the travel time difference Δt of the two paths. If these travel times are T_{EFR} and T_{DR} their difference will be:

$$\Delta t = T_{EFR} - T_{DR} = \left(\frac{h_1}{\sin e_1}\cos e_1 - \frac{h_1}{\sin f_1}\cos f_1\right)\frac{\cos e_2}{\alpha_2}$$

$$+\frac{h_1}{\beta_1 \sin f_1} - \frac{h_1}{\alpha_1 \sin e_1} \qquad (3\text{-}1)$$

where e_2 is the angle of emergence of the ray below the interface

e_1 and f_1 the angles of emergence in the layer for the P and SV waves.

Expression (3-1) can be simplified using the relations

$$\frac{\alpha_1}{\cos e_1} = \frac{\beta_1}{\cos f_1} = \frac{\alpha_2}{\cos e_2} \qquad (3\text{-}2)$$

so that

$$\Delta t = \frac{h_1}{\alpha_1}\left(\frac{\alpha_1}{\beta_1}\sin f_1 - \sin e_1\right)$$

Assuming a Poisson's ratio $\sigma = 0.25$ as an approximate value for the rocks of the crust, the time difference is reduced to

$$\Delta t = \frac{h_1}{\alpha_1}\left(\sqrt{3}\sin f_1 - \sin e_1\right)$$

If T is the period corresponding to the angular velocity ω the phase shift ε_{sv} at R between the P and SV wave will be given by:

$$\varepsilon_{SV} + 2\pi n = \frac{\Delta t}{T} = \Delta t \cdot f = f \cdot \frac{h_1}{\alpha_1}\left(-\sin e_1 + \sqrt{3}\sin f_1\right)$$

$$(n = 0, 1, \ldots) \qquad (3\text{-}3)$$

where f is the natural frequency of the wave.

In a similar way the phase shift ε_{3P} between the direct P arrival and the doubly reflected P wave (Figure 10) may be found.

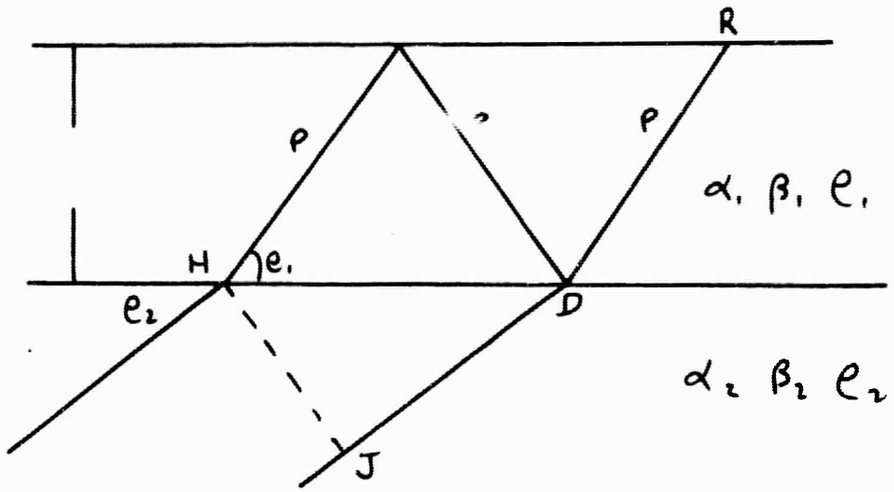

Figure 20. Triple reflection of P wave.

In this case the phase difference ε_{3P} is:

$$\varepsilon_{3P} + 2\pi n = f \cdot \frac{h_1}{\alpha_1} 2 \sin e_1 \qquad (3\text{-}4)$$

$$(n = 0, 1, \ldots)$$

For the simple case of a single layer the only possible combinations of rays arriving to the receiver R, are P and

SV waves that were reflected one or more times at the surface and at the interface.

In general the phase difference between the direct P arrival and a wave that travels in the layer n times as P and m times as SV is given by:

1) Phase shift due to n times as P = $f \cdot \frac{h_1}{\alpha_1} (n-1) \sin e_1$

2) Phase shift due to m times as SV = $f \cdot \frac{h_1}{\alpha_1} m\sqrt{3} \sin f_1$

So if $\varepsilon_{np,\,m_{SV}}$ is the phase shift of the total path:

$$\varepsilon_{np,\,m_{SV}} + 2n'\pi = f \cdot \frac{h_1}{\alpha_1} \left[(n-1) \sin e_1 + m\sqrt{3} \sin f_1 \right] \qquad (3\text{-}5)$$

$$(n' = 0, 1, \ldots)$$

Note that (3-3) and (3-4) are special cases of the general expression (3-5).

The phase difference between any two rays arriving at R one of the traveling N times as P ard M times as SV and the other n times as P and m times as SV is given by:

$$\varepsilon + 2n'\pi = f \cdot \frac{h_1}{\alpha_1} \left[(N-n) \sin e_1 + (M-m)\sqrt{3} \sin f_1 \right] \qquad (3\text{-}6)$$

$$(n' = 0, 1, \ldots)$$

If a continuous train of sinusoidal waves arrives at the interface the amplitude at the surface will be controlled by these phase differences and by the amplitudes of the reflections. If two rays are in phase they will reinforce each

other to give large amplitude; if they are 180° out of phase their resultant will be the difference of the amplitudes. When all the possible reflections are considered and the ground motion is resolved into vertical and horizontal components and the effect of the free surface is considered, the final result is the value of the transfer function for the vertical and for the horizontal component for the given frequency, as found by Haskell (1962). The same consideration for other frequencies will give the transfer function curves in terms of frequency. For the single layer case the problem could be easily solved and prepared for numerical calculations since the amplitude coefficients of the reflected waves become too small after a few reflections and their contribution could be neglected. The problem will be more complex when several layers are considered. This is the reason why for numerical calculations it is more convenient to use the matrix method of Haskell and Thomson. Nevertheless the expression (3-6) for the phase shift is significant since it indicates the influence on the transfer function of the thickness of the layer, and the velocity of the P wave, and the angle of incidence.

The thickness of the layer h_1 is a common factor of all terms in the expressions (3-5) (3-6). This means that the same phase relation could be obtained for a model with a layer of different thickness provided the frequency is changed in such a way that $f \cdot h_1$ remains constant. Since

the thickness of the layer does not have any influence on the transmission coefficients the amplitudes of the transfer functions will be the same and the values will simply be displaced in the frequency domain. This was numerically and graphically shown in the graphs of Figure 1.

The influence of the P velocity on the transfer functions is different. A change of α_1, affects also the frequency in a way similar to the thickness though in the opposite direction. The main influence of the change in velocity, however, is that the transmission coefficients depend on the velocity contrast above and below the interface. The curves, accordingly, will not only be displaced in the frequency domain but the amplitudes will also be affected by a constant multiplier. This effect may be examined in Figure 2 where the transfer functions of two crustal models were compared.

These considerations suggest that the same transfer functions could be obtained if the values $f \cdot h_1/\alpha_1$ and α_1/α_2 were to be held constant, though the transfer functions so obtained would not correspond to the same values of frequency. If only α_1/α_2 changes, the amplitude of the transfer function will change but not the periodical character and general appearance of the curve.

This analysis of the transfer functions suggested the calculations in terms of the dimensionless quantity γ where:

$$\gamma = f \frac{h_1}{\alpha_1} (\sin e_1 + \sqrt{3} \sin f_1) \qquad (3\text{-}7)$$

Since α_1/α_2 can have any value this results in a family of curves with similar periodicity and shape but different amplitude of the oscillations. A family of curves is obtained for each angle of incidence since the transmission coefficients change with angle of incidence. The change with angle of incidence is gradual. This makes it possible to interpolate between the different angles of incidence considered in this study. The set of these curves is presented and discussed in detail in the next section.

3.12 The multi-layered case.

The same considerations that were used for the one layer problem can easily be extended to the two and more layer case.

For the two-layer case Snell's law shows that

$$c = \frac{\alpha_1}{\cos e_1} = \frac{\alpha_2}{\cos e_2} = \frac{\alpha_3}{\cos e_3} = \frac{\beta_1}{\cos f_1} = \frac{\beta_2}{\cos f_2}$$

where c is the apparent surface velocity.

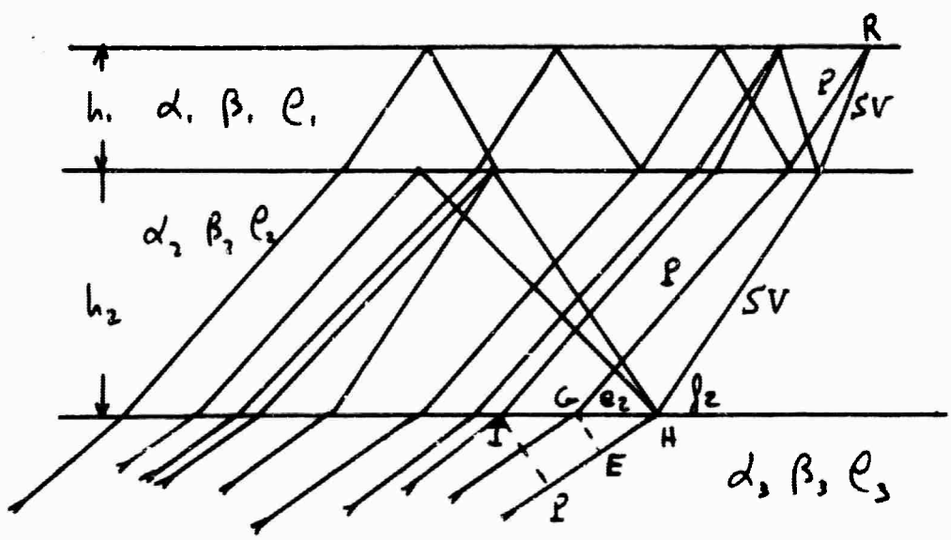

Figure 21. Multiple reflection and conversions of incident P waves.

Referring to Figure 21 from D to R the P wave travels with velocity α_1. Then for a frequency f, the phase change ε_{p1} from D to R is

$$\varepsilon_{p_1} + 2\pi n = \frac{DR}{\lambda_{p_1}} = \frac{f\, h_1}{\alpha_1 \sin e_1} \qquad (n = 0, 1 \ldots)$$

where λ_{p1} is the wave length of P in the first layer. If the wave travels n_1 times as P in this layer, the total phase change in this portion of the path will be

$$\varepsilon_{pn_1} + 2\pi n' = f \cdot \frac{n_1 h_1}{\alpha_1 \sin e_1} \qquad (n' = 0, 1, \ldots)$$

Similarly, for a wave traveling n_2 times as P in the second layer the corresponding phase change ε_{pm2}, will be:

$$\varepsilon_{pn_2} + 2\pi n' = f \cdot \frac{n_2 h_2}{\alpha_2 \sin e_2} \qquad (n' = 0, 1, \ldots)$$

for a wave traveling m_1 times as SV in layer 1, the phase is:

$$\varepsilon_{svm_1} + 2\pi n' = f \cdot \frac{m_1 h_1}{\beta_1 \sin f_1} \qquad (n' = 0, 1, \ldots)$$

and for an SV, m_2 times in layer 2 the phase is:

$$\varepsilon_{svm_2} + 2\pi n' = f \cdot \frac{m_2 h_2}{\beta_2 \sin f_2} \qquad (n' = 0, 1, \ldots) \qquad (3\text{-}8)$$

The phase change for the portion of the path EH depends on the distance GH, that is, on the difference of the projections onto the interface of the crust portions of the two rays. This difference for two rays, one traveling as P, n_1 times in layer 1 and n_2 times in layer 2, and as SV, m_1 and m_2 times respectively, and the other traveling as P, N_1 and N_2 times, and as SV, M_1 and M_2 times, is:

$$\frac{(N_1-n_1)\cos e_1}{\sin e_1} + \frac{(N_2-n_2)\cos e_2}{\sin e_2}$$

$$+\frac{(M_1-m_1)\cos f_1}{\sin e_1} + \frac{(M_2-m_2)\cos f_2}{\sin e_2}$$

and the phase ε_{EH} corresponding to EH is

$$\varepsilon_{EH} + 2\pi n' = f\cdot\frac{h_1(N_1-n_1)\cos^2 e_1}{\alpha_1} + \frac{h_2(N_2-n_2)\cos^2 e_2}{\alpha_2}$$

$$+\frac{h_2(M_2-m_2)\cos^2 f_2}{\alpha_2} + \frac{h_1(M_1-m_1)\cos^2 f_1}{\alpha_1} \qquad (3\text{-}9)$$

$$(n' = 0, 1\ldots)$$

The total phase difference ε for the two rays, from (3-8) and (3-9) is:

$$\varepsilon + 2\pi n' = f\cdot\left\{\frac{h_1}{\alpha_1}\left[(N_1-n_1)\sin e_1 + \sqrt{3}(M_1-m_1)\sin f_1\right]\right.$$

$$\left.+\frac{h_2}{\alpha_2}\left[(N_2-n_2)\sin e_2 + \sqrt{3}(M_2-m_2)\sin f_2\right]\right\}$$

$$(n' = 0, 1, \ldots)$$

This expression for the phase difference of all the rays arriving at the point R suggests, as in the single layer case, that it may be advantageous to use a dimensionless quantity γ in the calculation of the transfer functions for two-layer models. This time the definition of γ is:

$$\gamma = f \cdot \left[\frac{h_1}{\alpha_1} (\sin e_1 + \sqrt{3} \sin f_1) + \frac{h_2}{\alpha_2} (\sin e_2 + \sqrt{3} \sin f_2) \right] \tag{3-10}$$

or $\gamma = \gamma_1 + \gamma_2$

if $$\gamma_i = f \cdot \frac{h_i}{\alpha_i} (\sin e_i + \sqrt{3} \sin f_i) \qquad (i = 1, 2, \ldots)$$

When calculations are performed with models of exactly the same values for the h_1/h_2 and α_1/α_2 ratios, the transfer functions have similar form provided the angles of emergence are the same through the layers of the crust. The amplitude of the oscillations depends on the velocity contrast of the two layers with the mantle. If this contrast is kept constant the same numerical values, for a given γ, are obtained no matter what the individual values of the thicknesses and velocities.

The same considerations apply in obtaining a dimensionless parameter, γ, for the case of an n-layered model. In this case

$$\gamma = f \cdot \sum_{i=1}^{n} \frac{h_i}{a_i} \left(\sin e_i + \sqrt{3} \sin f_i \right)$$

$$= \sum_{i=1}^{n} \gamma_i \qquad (3\text{-}11)$$

Consequently, if all layer thicknesses are multiplied by a constant, R, the same results will be obtained for equal values of γ. In terms of frequency the change will be inversely proportional to R. If all the velocities including the velocity of the semi-infinite medium are multiplied by a constant, the same transfer function is obtained for the values of γ since the angles of emergence, e_i and f_i, through the layers remain constant. If the velocity contrast with the mantle is changed while the velocity contrasts within the layers remain constant, families of curves are obtained with similar form but different amplitude. The more layers are present the more combinations are possible and the number of families increases greatly.

3.2 The Fourier transform of a pulse and its reflections.

The problem of the transfer function of layered media for seismic waves could be considered as the ratio of the Fourier transforms of the incident pulse at the bottom of the system and the Fourier transform of the record obtained at the surface of the layers.

For simplicity sake it is convenient to choose a unit delta function for the incident pulse since the Fourier transform of this function has unity as modulus and zero phase for all the frequencies (see Figure 22a,b).

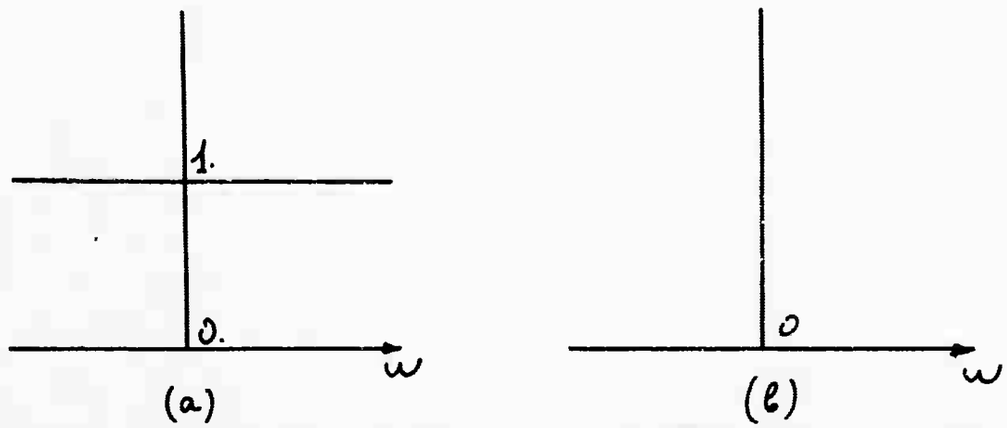

Figure 22. a) Modulus of the delta function Fourier transform
b) Phase

At the surface the record will consist of a first arrival followed by several reflections and conversions of energy arriving with certain time delays with respect to the initial P. Let us assume that no critical values of the angle of incidence are reached in any of the layers; consequently no total reflection takes place, with the appropriate phase shift, depending on the angle of incidence. Then the only possible phase shifts are 0 or π, which on the record will be shown as pulses of the same sign as that of the direct or initial P or pulses of the opposite sign. The vertical component record, neglecting small absorptions

that could take place in the crust, will look like Figure 23, and its time domain function will be of the type:

$$f(t) = a\,\delta(t) + b\,\delta(t-\tau_b) + c\,\delta(t-\tau_c) + \dots \qquad (3\text{-}12)$$

where the τ are the time lags, and a, b, ... are Zoeppritz coefficients.

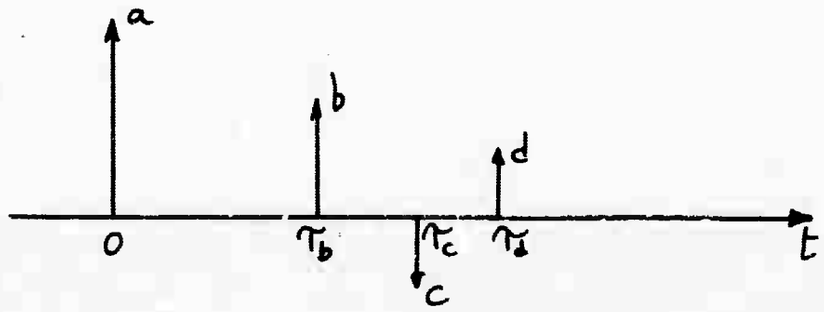

Figure 23. Typical record of pulse multiply reflected.

Considering only the first arrival and the first secondary wave let us find the corresponding Fourier transform in the frequency domain. Let

$$f_1(t) = a\,\delta(t) + b\,\delta(t-\tau_b)$$

Then

$$F_1(\omega) = a + \frac{b}{\sqrt{2\pi}} \int_{-\infty}^{+\infty} \delta(t-\tau_b)\, e^{-i\omega t}\, dt$$

Let us change the variable:

$$t' = t - \tilde{\tau}_b$$

Then:

$$F_1(\omega) = a + \frac{b}{\sqrt{2\pi}} \int_{-\infty}^{\infty} \delta(t')\, e^{-i\omega(t'+\tilde{\tau}_b)}\, dt'$$

$$= a + b\, e^{-i\omega\tilde{\tau}_b} = a + b\left[\cos(\omega\tilde{\tau}_b) - i\sin(\omega\tilde{\tau}_b)\right]$$

This is a complex quantity. Its modulus is:

$$\left|F_1(\omega)\right| = \left\{\left[a + b\cos(\omega\tilde{\tau}_b)\right]^2 + b^2\sin^2(\omega\tilde{\tau}_b)\right\}^{1/2}$$

$$= \left[a^2 + b^2\cos^2(\omega\tilde{\tau}_b) + 2ab\cos(\omega\tilde{\tau}_b) + \right.$$

$$\left. + b^2\sin^2(\omega\tilde{\tau}_b)\right]^{1/2} = \left[a^2 + b^2 + 2ab\cos(\omega\tilde{\tau}_b)\right]^{1/2} \quad (3\text{-}13)$$

and the phase is

$$\varphi = \tan^{-1} - \frac{b\sin(\omega\tilde{\tau}_b)}{a + b\cos(\omega\tilde{\tau}_b)} \quad (3\text{-}14)$$

The transfer functions presented by Hannon (1964a) are the ratio of the vertical and horizontal component at the surface, to the total amplitude at the bottom of the layers. Our expression for $F_1(\omega)$ represents this same ratio of the surface components to the total amplitude at the bottom

since the spectrum of the amplitude for the delta function has unity as modulus and zero as phase.

For the simple case just considered of a single reflection the modulus of the transfer function consists of the square root of a function that oscillates sinusoidally about the line $a^2 + b^2$, with amplitude 2_{ab} and with period determinable from the quantity $\omega\tau_b$. For large values of the coefficient b the amplitude of the oscillation will be large. This would correspond to the converted SV wave or to the first reflected P wave since the amplitude of the reflections and refractions decays rapidly after a few partitions of energy at interfaces or the free surface. In general, the larger the contrast between the interfaces the larger is the coefficient for the reflections, and the larger the oscillations of the transfer functions. Furthermore, the frequency of the oscillations will be more rapid with larger τ_b. This corresponds to long time lags between first arrival and reflections, and shows that in general very fast oscillations of the transfer function will have small amplitude and long-period components will have larger amplitude.

The same argument is easily extended to the consideration of several reflections. For a record of the type of Figure 23 on which multiple reflections of the primary pulse are shown, the time function of the record will be as in equation (3-12) and its Fourier transform in the

frequency domain has as modulus

$$F(\omega) = \Big\{ \Big| a + b\cos(\omega\tau_b) + c\cos(\omega\tau_c) + \dots \Big|^2 + \Big| b\sin(\omega\tau_b) + c\sin(\omega\tau_c) + \dots \Big|^2 \Big\}^{1/2}$$

$$= \Big\{ a^2 + b^2 + c^2 + \dots + 2\big[ab\cos(\omega\tau_b) + ac\cos(\omega\tau_c) + \dots \big] + 2\big[bc\cos\omega(\tau_b - \tau_c) + \dots \big] \Big\}^{1/2} \qquad (3\text{-}15)$$

This modulus is the square root of a function composed of the constant value $(a^2 + b^2 + c^2 + \dots.)$ plus a series of sinusoidal components of different period and amplitude. In practical calculations only a few of these sinusoidal components should be considered since they become very small after a few reflections and refractions.

The phase angle for the same transfer function is:

$$\varphi = \tan^{-1} \frac{b\sin(\omega\tau_b) + c\sin(\omega\tau_c) + \dots}{a + b\cos(\omega\tau_b) + c\cos(\omega\tau_c) + \dots} \qquad (3\text{-}16)$$

This phase angle is zero for zero frequency and indicates that long wave lengths are not affected by the layers. As

the frequency increases the numerator of the expression increases and the denominator decreases, so the phase angle increases. But again the value of the phase angle is controlled by the sinusoidal components with the larger amplitude terms. This can be observed in the graphs of the transfer functions presented in the next chapter.

Since the periodicity of the modulus and phase of the transfer functions depends on the time lags between first arrival and later reflections and refractions, it is convenient to calculate these time lags as a function of the layer parameters.

3.21 Time lags between primary arrival and multiple reflections.

The first arrival of energy after the direct P will be, in the case of the one-layer model, the converted SV. From Figure 19 and equation (3-3) this time interval Δt is (assuming $\sigma = 0.25$)

$$\tau_{SV} = \frac{h_1}{\alpha_1}\left(\sqrt{3}\sin f_1 - \sin e_1\right) \qquad (3\text{-}17)$$

The time interval for the wave reflected as P at the free surface and as P again at the bottom of the layer (see Figure 20 and equation (3-4)) is given by

$$\tau_{3P} = \frac{h_1}{\alpha_1} 2 \sin e_1 \qquad (3\text{-}18)$$

In general the time interval between the first direct P and a ray reflected n times as P and m times as SV, where n+m = 2r, r = 0, 1, 2, .. is:

$$\tau_{nP,mSV} = \frac{h_1}{\alpha_1}\left[(n-1)\sin e_1 + \sqrt{3}\, m \sin f_1\right] \qquad (3\text{-}19)$$

and the period of the transfer function component will be, from (3-13), a function of

$$\omega\tau_{nP,mSV} = 2\pi f \cdot \frac{h_1}{\alpha_1}\left[(n-1)\sin e_1 + \sqrt{3}\, m \sin f_1\right]$$

This expression indicates, again, that if for different one-layer crustal models the quantities sin e_1 and sin f_1 remain constant the same periodicity or character of the transfer function will be obtained when the results are calculated in terms of the dimensionless parameter

$$\gamma = f \cdot \frac{h_1}{\alpha_1}\left(\sin e_1 + \sqrt{3}\sin f_1\right)$$

The amplitude of the oscillations will depend on the velocity contrast between the layer and the semi-infinite half-space.

3.22 The multi-layered case.

The problem could be extended to consider multi-layered models. For the two-layer case let us consider the time lag between the first direct P arrival and a ray reflected, respectively:

n_1 and m_1 times as P and as SV in the first layer,

n_2 and m_2 times as P and as SV in the second layer,

then the time lag of the reflected wave is:

$$\tau_{n_1 P,\, n_2 P,\, m_1 SV,\, m_2 SV} = \frac{h_1}{\alpha_1}\left[(n_1 - 1)\sin e_1 + \sqrt{3}\, m_1 \sin f_1\right] + \frac{h_2}{\alpha_2}\left[(n_2 - 1)\sin e_2 + \sqrt{3}\, m_2 \sin f_2\right] \quad (3\text{-}20)$$

and the sinusoidal component of the transfer function introduced by this reflection for a constant time lag will oscillate in the ω dimension with a period

$$T(\omega) = \frac{2\pi}{\tau} \quad (3\text{-}21)$$

Since the transfer functions are plotted against the parameter γ it is convenient to express this period in terms of γ units. Then using (3-11), (3-13) and (3-21) the period of the sinusoidal component will be

$$T(\gamma) = T(\omega)\,\frac{1}{2\pi}\sum_{i=1}^{n}\frac{h_i}{\alpha_i}\left(\sin e_i + \sqrt{3}\sin f_i\right) = \frac{1}{\tau}\sum_{i=1}^{n}\frac{h_i}{\alpha_i}\left(\sin e_i + \sqrt{3}\sin f_i\right) \quad (3\text{-}22)$$

For example, for the first SV arrival in a single layer crust the time lag τ_{SV} given by (3-17) was:

$$\tau_{SV} = \frac{h_1}{\alpha_1}\left(\sqrt{3}\sin f_1 - \sin e_1\right)$$

The period of the transfer function component introduced by the first SV reflection measured in γ units will be:

$$T(\gamma) = \frac{(\sin e_1 + \sqrt{3} \sin f_1)}{\sqrt{3} \sin f_1 - \sin e_1} \qquad (3\text{-}23)$$

Similarly the period of the transfer function components for the case of multilayered models is given by:

$$T(\gamma) = \frac{\sum_{i=1}^{n} \frac{h_i}{\alpha_i} (\sin e_i + \sqrt{3} \sin f_i)}{\tau} \qquad (3\text{-}24)$$

where τ is given by (3-20) in terms of the thicknesses of the layers, h_i, and the P velocities in these layers, α_i .

This analysis of the sinusoidal components of the transfer function is used to classify the multilayered models in groups with identical or similar transfer function curves.

Since the thickness of the layers does not affect the amplitude of the components but only their periodicity according to (3-24), identical transfer curves will be obtained when all the thicknesses of the layers are multiplied by the same factor. Thus the significant effect of the thicknesses of the layers of the models is not their absolute value but their ratio.

Change in the velocities of longitudinal waves in the layers may change the amplitude of the components of the

transfer functions. Nevertheless if their ratio is kept constant, the amplitudes will remain constant and also the periodicity of the components, according to (3-24). Thus the significant effect of the velocities is also their ratio. Nevertheless it is possible to keep constant the periodicity of the components and at the same time to change their amplitude. Since in (3-24) the period does not depend on the velocity of longitudinal waves in the mantle it is possible to change this velocity without affecting the periodicity. But changing the contrasts of velocity between the mantle and the crust layers will affect the amplitude of the sinusoidal components of the transfer function (3-15) (3-16).

These observations are the basis for the evaluation of the transfer functions for two and more layer models. By changing the contrast of velocities between the mantle and the layers but keeping constant the relationship between the velocities of the layers of the crust, families of curves of identical shape but of different amplitude are obtained. As before, these allow interpolation for intermediate models.

4. Master Curves for the Transmission of Seismic Longitudinal Waves in Layered Media

The theoretical considerations of the preceding section prepare the way for a presentation of the transfer functions for different crustal models in a methodical way.

In the present section we shall first present and discuss the complete set of single-layer crustal models. Then we will discuss the case of two-layer models, and several families of this type will be presented.

Unless otherwise indicated the following general assumptions will be presumed to hold:

1) The layers are horizontally stratified.
2) Poisson's ratio in the crust is equal to 0.25.
3) The density changes linearly with the P velocity.
4) The apparent surface velocity must be greater than the P velocity in the top layer and greater than the S velocity in any layer.

The second assumption is based on numerous measurements made on the rocks of the crust and upper mantle. The third assumption, as noted in section 3, is based on experimental studies of the changes of density in the crust with seismic velocities by Birch (1964) and Nafe and Drake as cited by Talwani et al. (1959). Small departures from these two assumptions such as may be present in nature do not alter the values of the transfer function in an appreciable way.

Assumption 4 is placed in order to avoid the total reflection which will take place, even for the SV converted ray, if the assumption is violated.

In order to study the transfer functions the FORTRAN II Computer Program of Hannon (1964a) was modified to calculate these functions in terms of the dimensionless parameter γ as defined in section 3 (see Appendix I). The program can also be used to calculate the functions in terms of frequency with the use of an optional control. The results are plotted on logarithmic scale.

In discussing the transfer function curves we shall make use of the terms, periodicity and amplitude. Periodicity refers to the oscillatory character of the curves with their peaks and troughs. The term amplitude refers to the maximum values of the transfer functions over these oscillations.

4.1 One-layer models.

The simplest crustal model is a single layer over a half-space. In this layer the velocity for the P and S waves may be considered to correspond to the average velocity of the P and S waves in the crust of the real earth, whether the crust may actually consist of several layers or whether there may exist velocity gradients in the crust. The thickness of the layer is equal to the total thickness of the real crust. Though this is a simple model, nevertheless from the theory of transfer functions given in the

last chapter it may be expected that the small velocity contrasts which may be present within the crust would introduce only small amplitude components into the transfer function which will not alter substantially the general appearance of the transfer function. The largest contrast of velocity which might be expected within the crust would be found near the top of the crust between the sedimentary layers and the basement rock, but these layers are thin in comparison to the total thickness of the crust and consequently their influence, though important in terms of amplitude, will be spread over a long-period component which not affect to any great extent the appearance of the low frequency region. These theoretical suggestions are confirmed by actual calculation when the transfer functions of the two-layered models are compared with the corresponding ones of the one-layer models. The main features of both are common and correspond to the large velocity contrast existing between the mantle and the crust.

The set of one layer models (Figures 24 to 36) is complete in the sense that for each angle of incidence a single family of curves exists with identical periodicity which represents all possible crustal thicknesses and all possible crust-mantle velocity contrasts. For example, in Figure 30, corresponding to an angle of incidence of 30° at the bottom of the crust, all possible models of different thickness will give the same type of curve; only the amplitude will

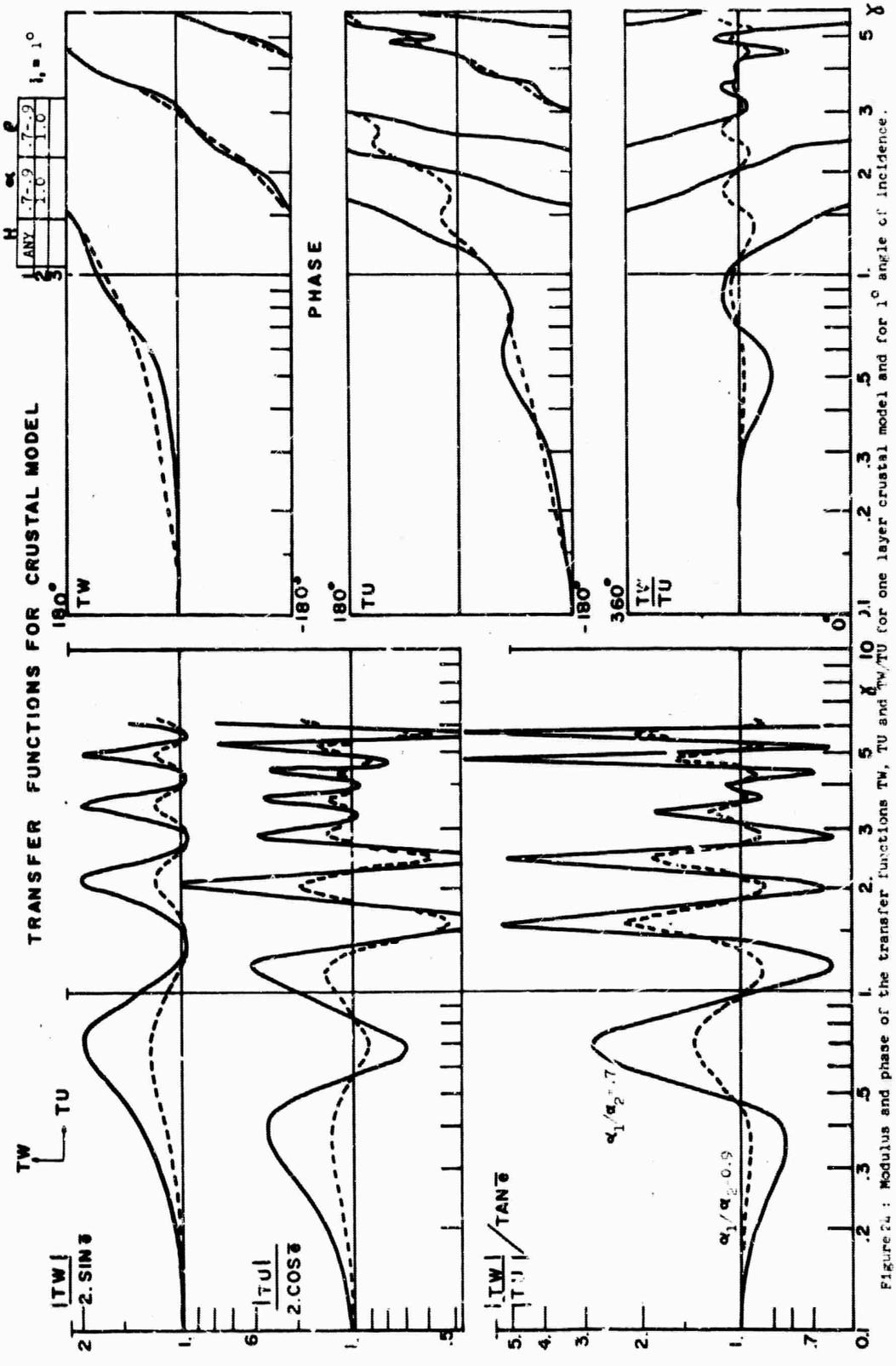

Figure 24 : Modulus and phase of the transfer functions TW, TU and TW/TU for one layer crustal model and for 1° angle of incidence.

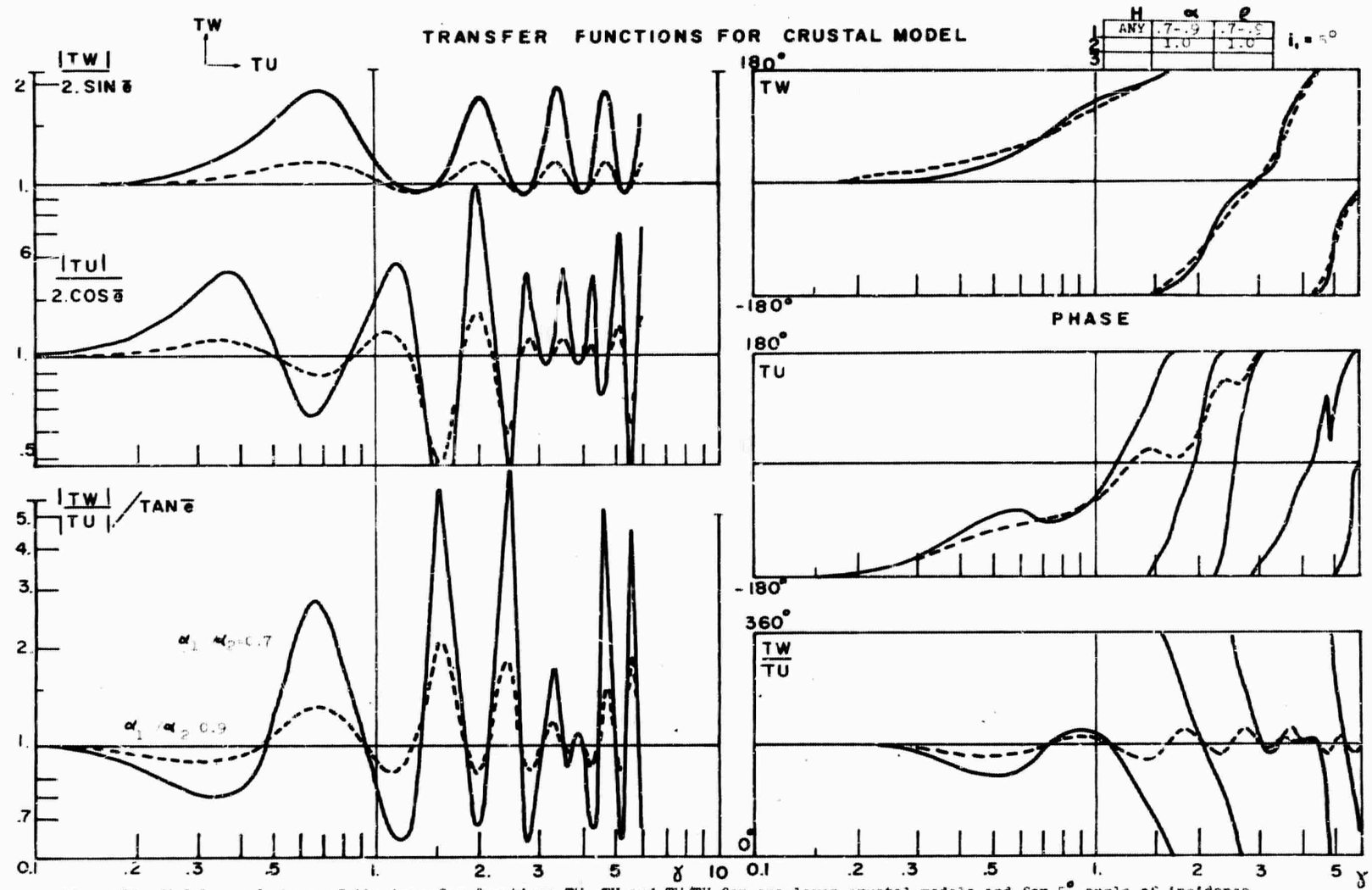

Figure 25 : Modulus and phase of the transfer functions TW, TU and TW/TU for one layer crustal models and for 5° angle of incidence.

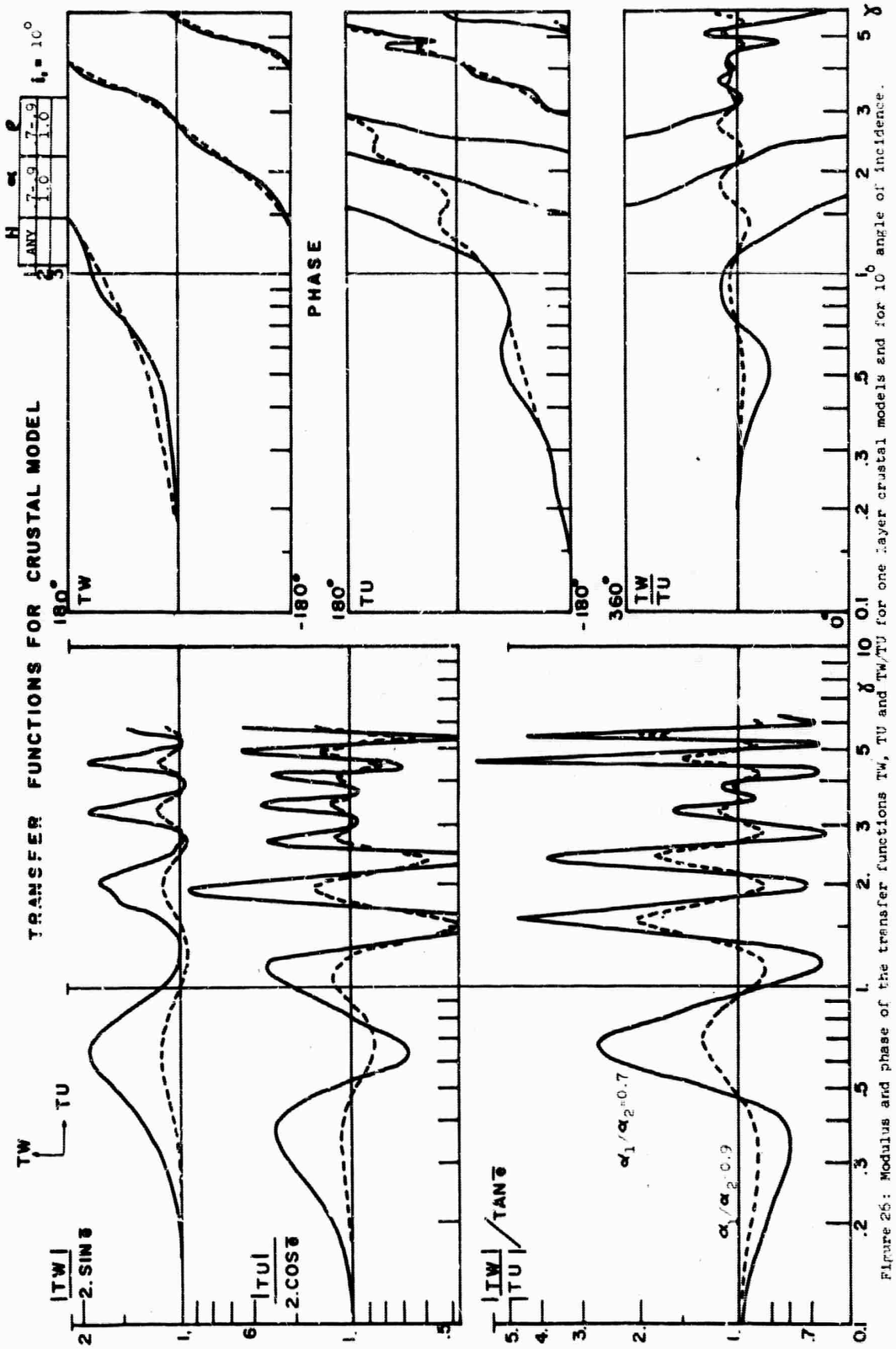

Figure 25: Modulus and phase of the transfer functions TW, TU and TW/TU for one layer crustal models and for 10° angle of incidence.

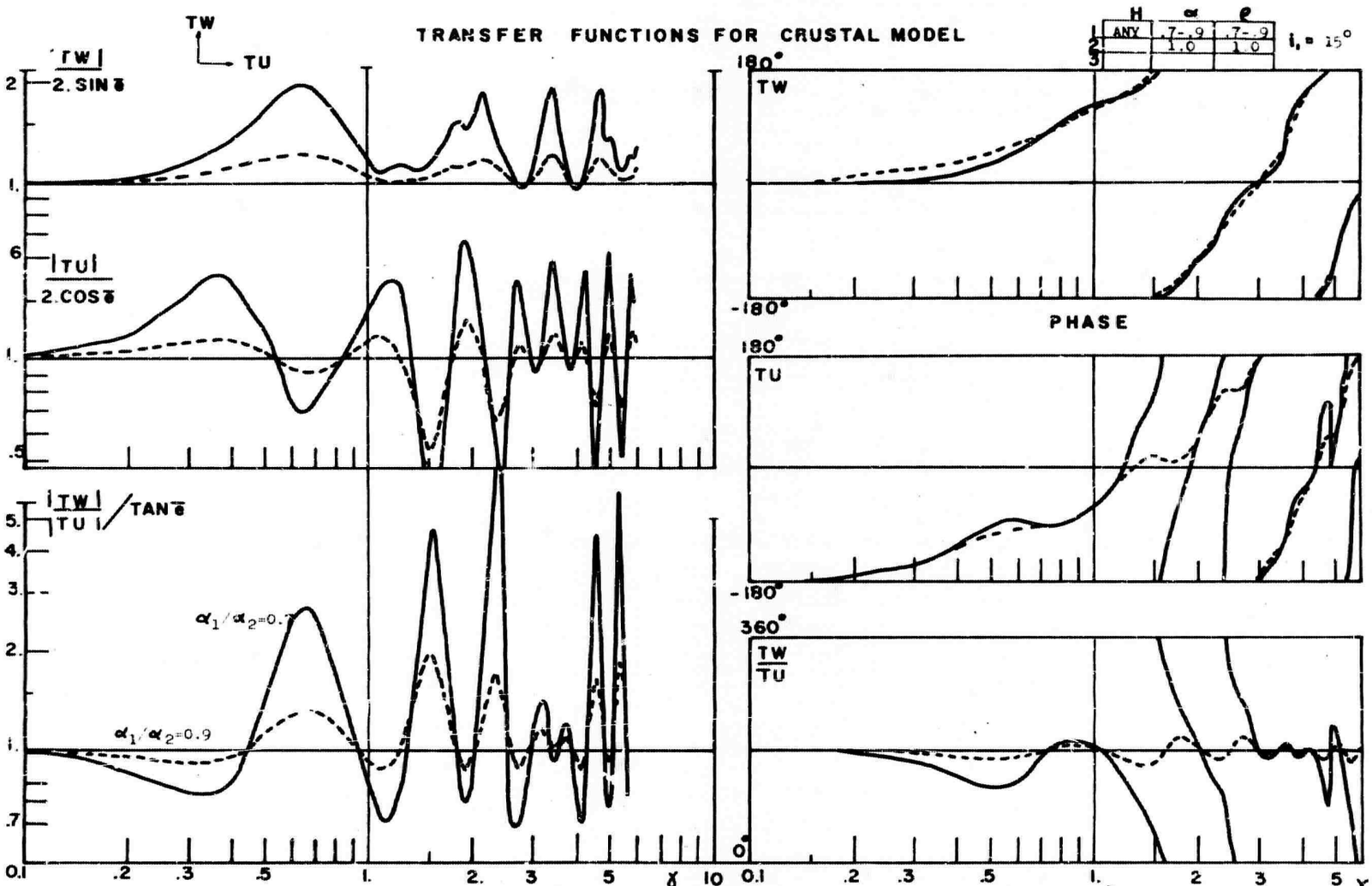

Figure 27 : Modulus and phase of the transfer functions TW, TU and TW/TU for one layer crustal models and for 15° angle of incidence.

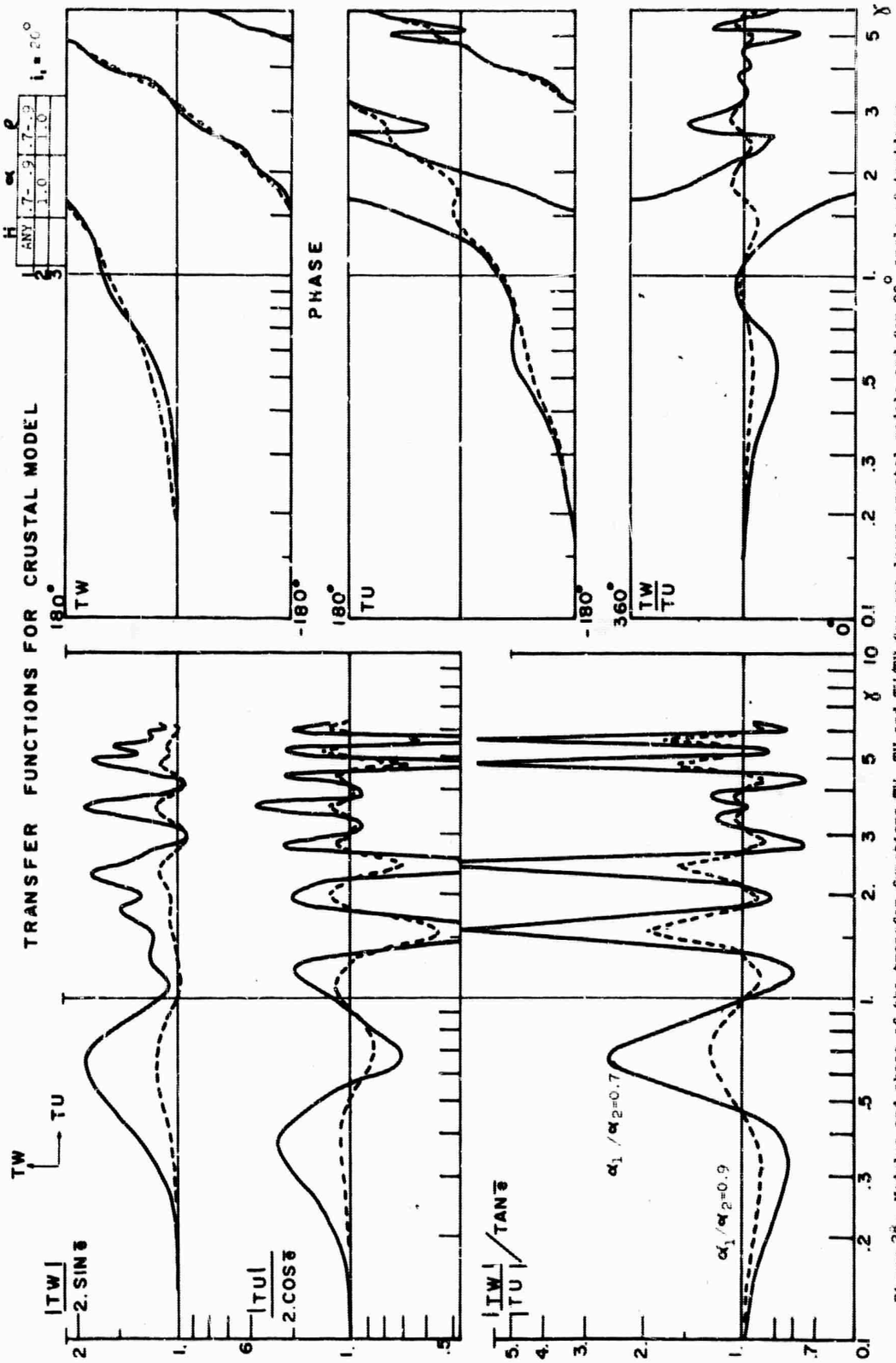

Figure 28: Modulus and phase of the transfer functions TW, TU and TW/TU for one layer crustal models and for 20° angle of incidence.

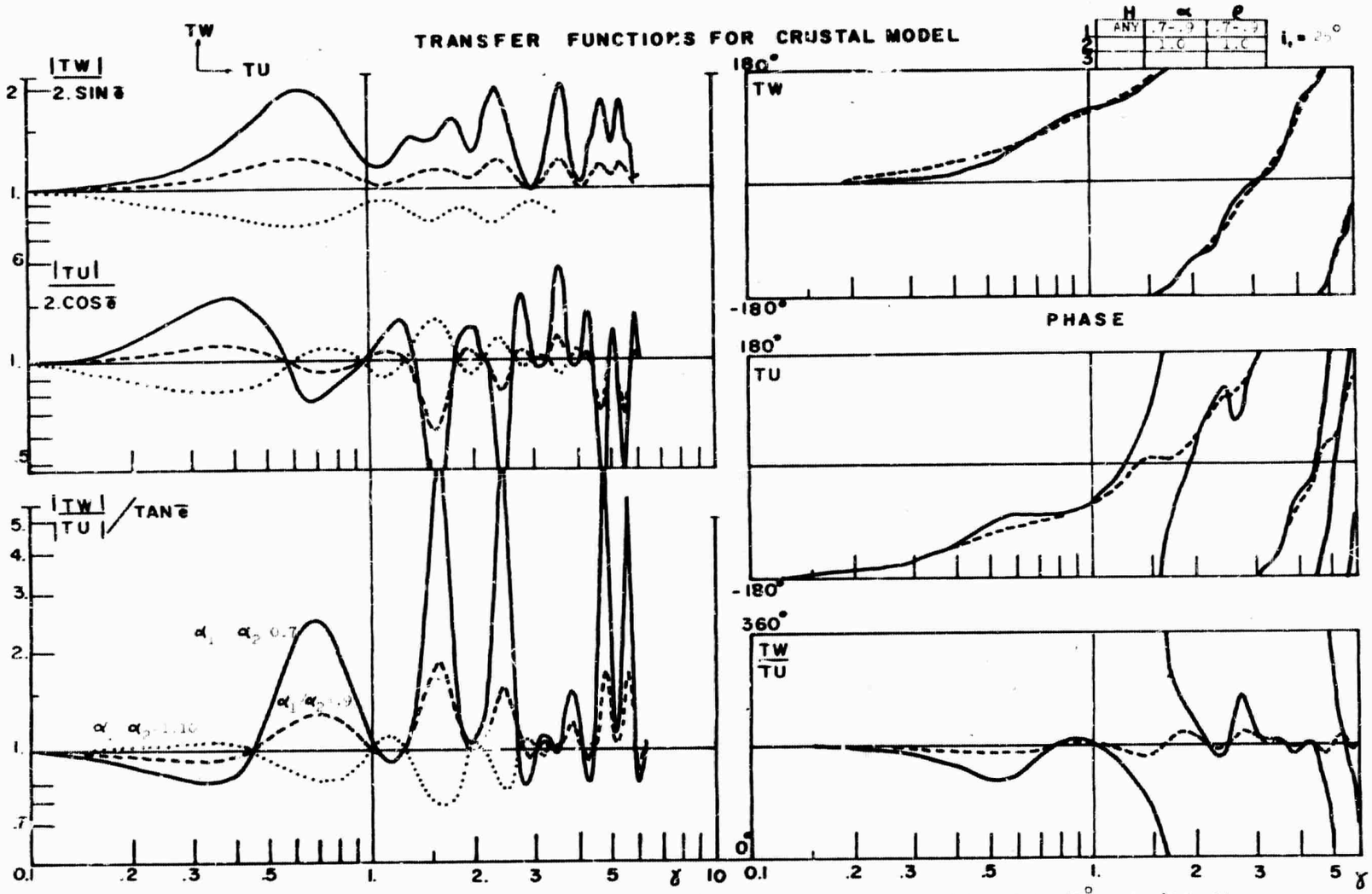

Figure 12: Modulus and phase of the transfer functions TW, TU and TW/TU for one layer crustal models and for 25° angle of incidence.

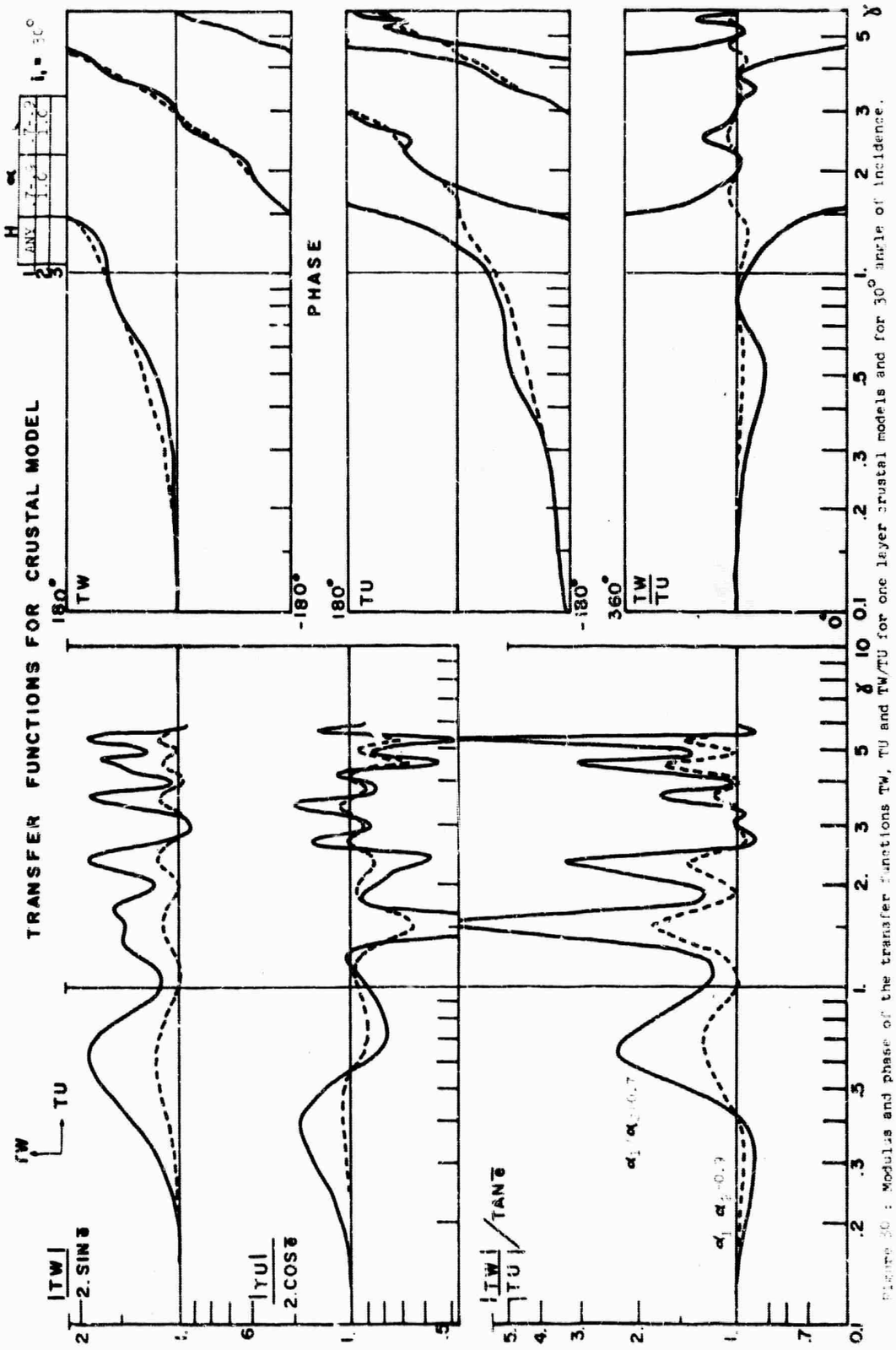

Figure 30 : Modulus and phase of the transfer functions TW, TU and TW/TU for one layer crustal models and for 30° angle of incidence.

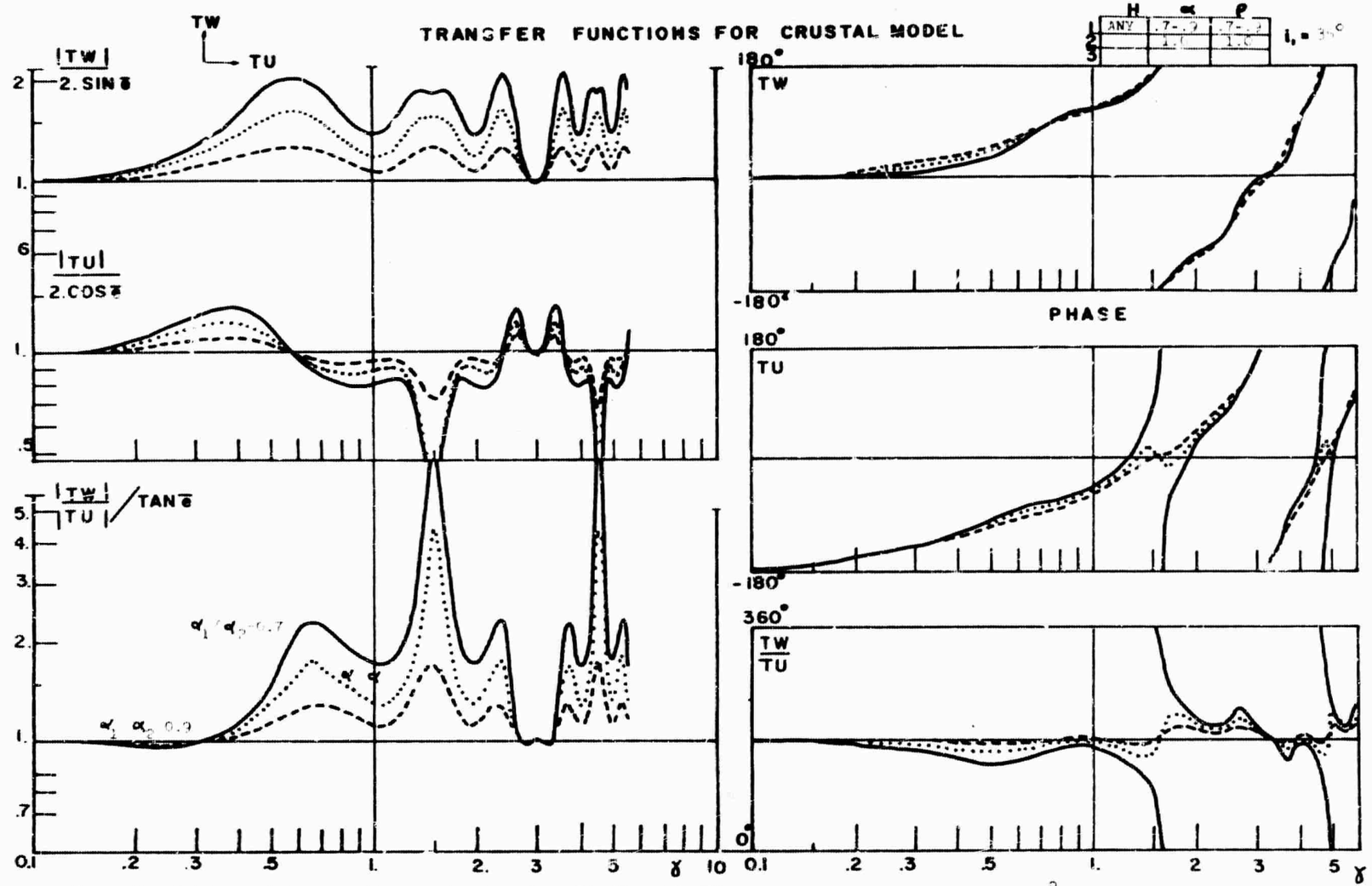

Figure 3 : Modulus and phase of the transfer functions TW, TU and TW/TU for one layer crustal models and 30° angle of incidence.

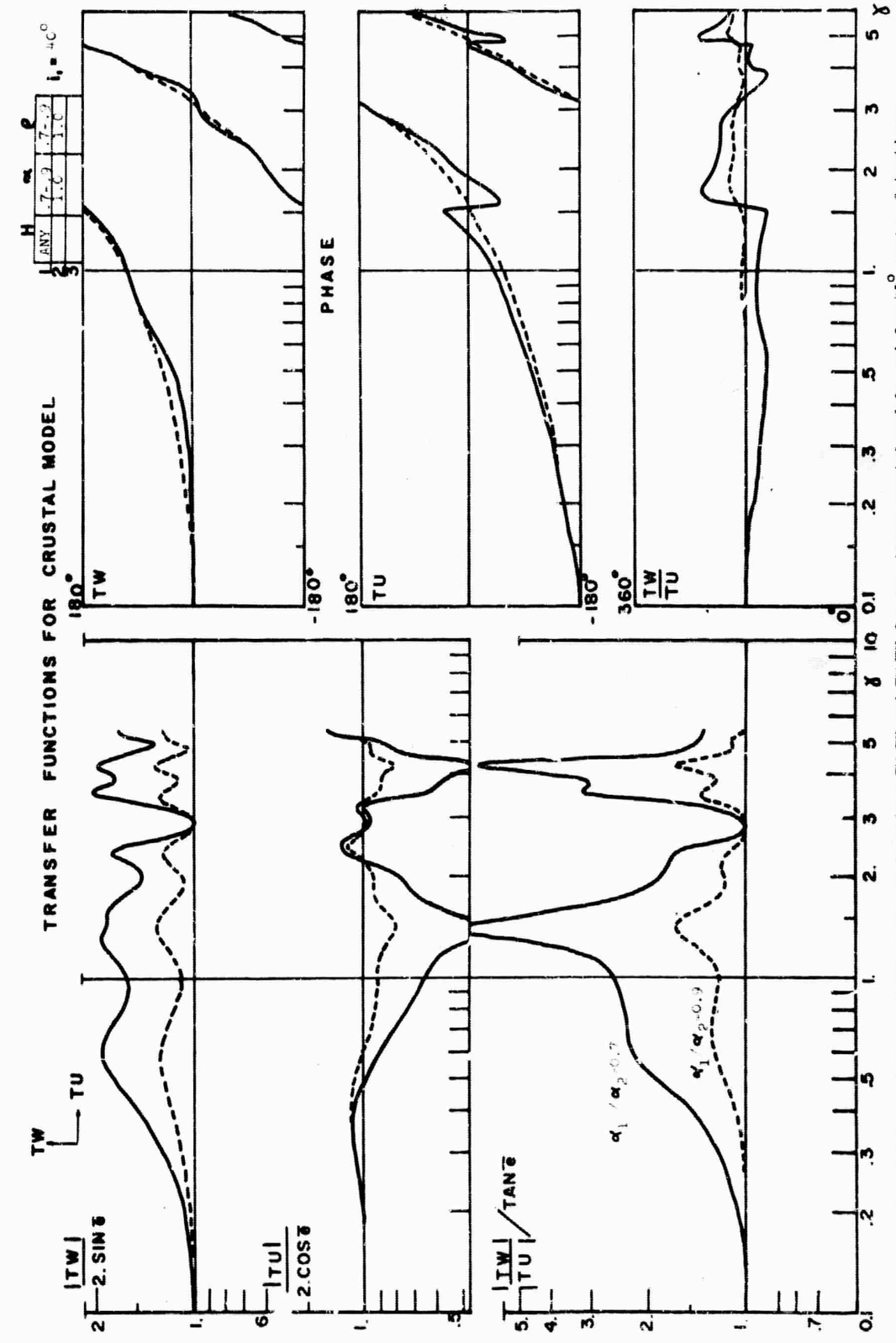

Figure 2 : Modulus and phase of the transfer functions TW,TU and TW/TU for one layer crustal models and for 40° angle of incidence.

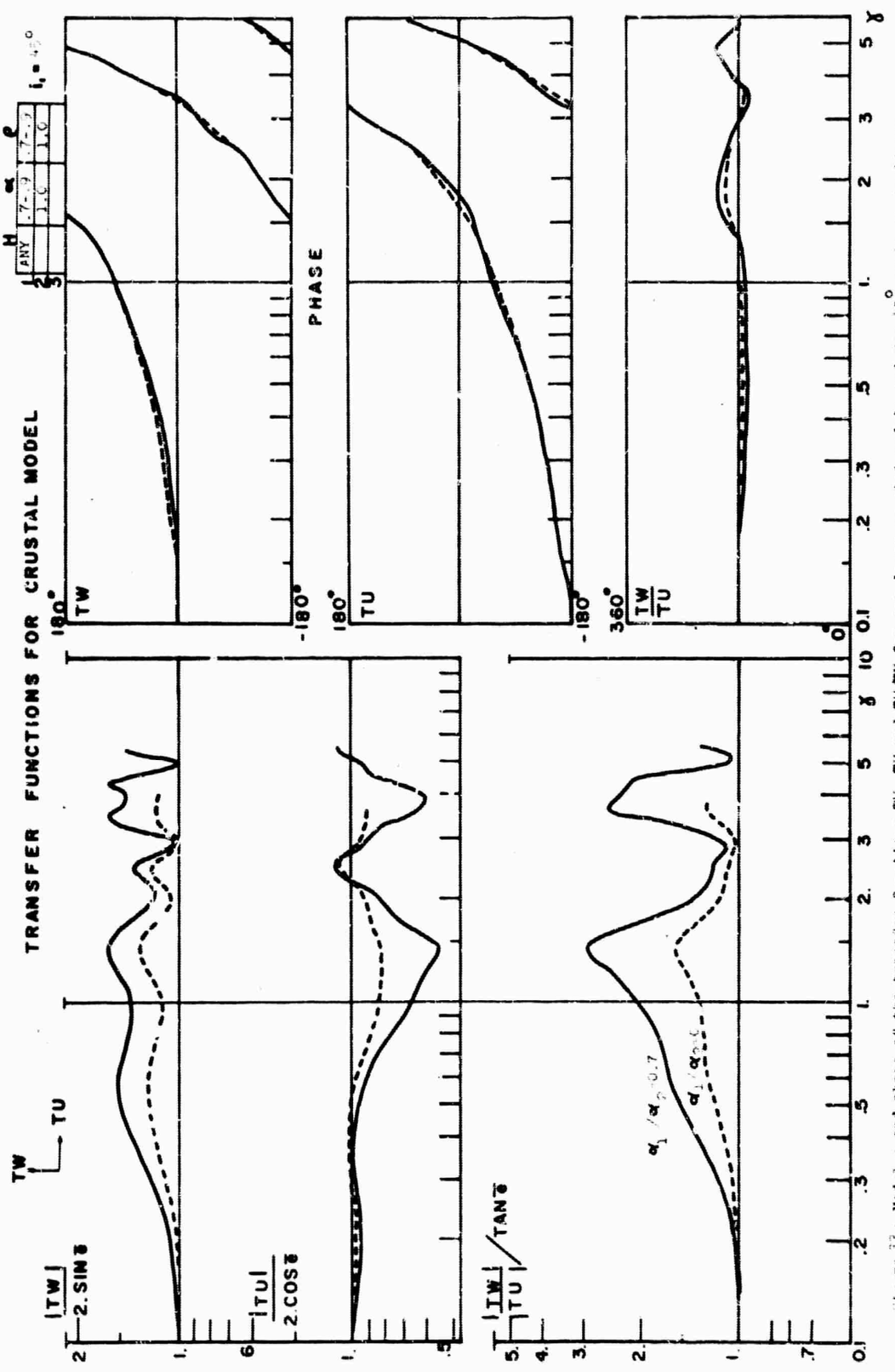

Figure 33: Modulus and phase of the transfer functions TW, TU and TW/TU for one layer crustal models and for 45° angle of incidence.

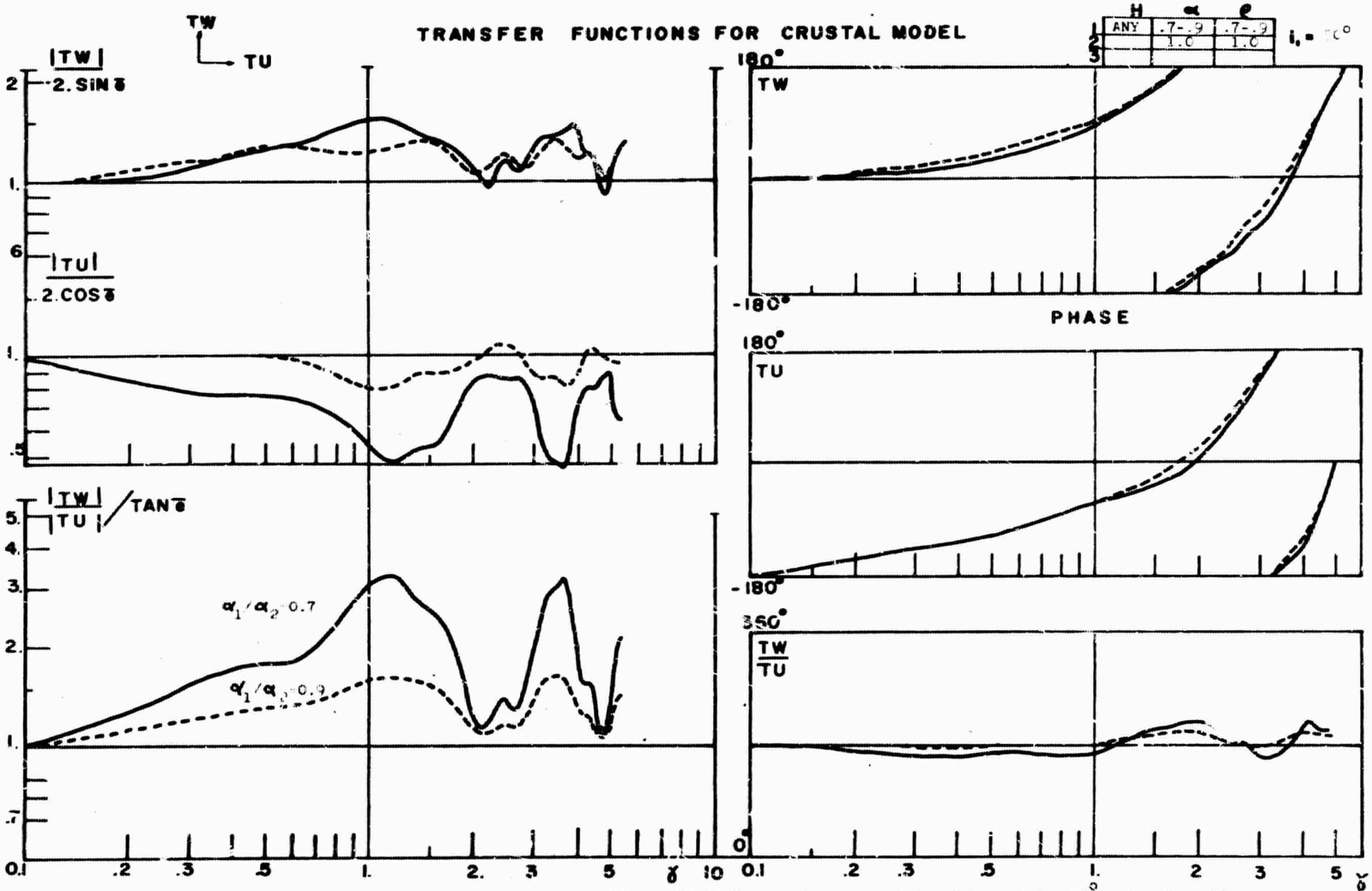

Figure 34 : Modulus and phase of the transfer functions TW, TU and TW/TU for one layer crustal models and for 0° angle of incidence.

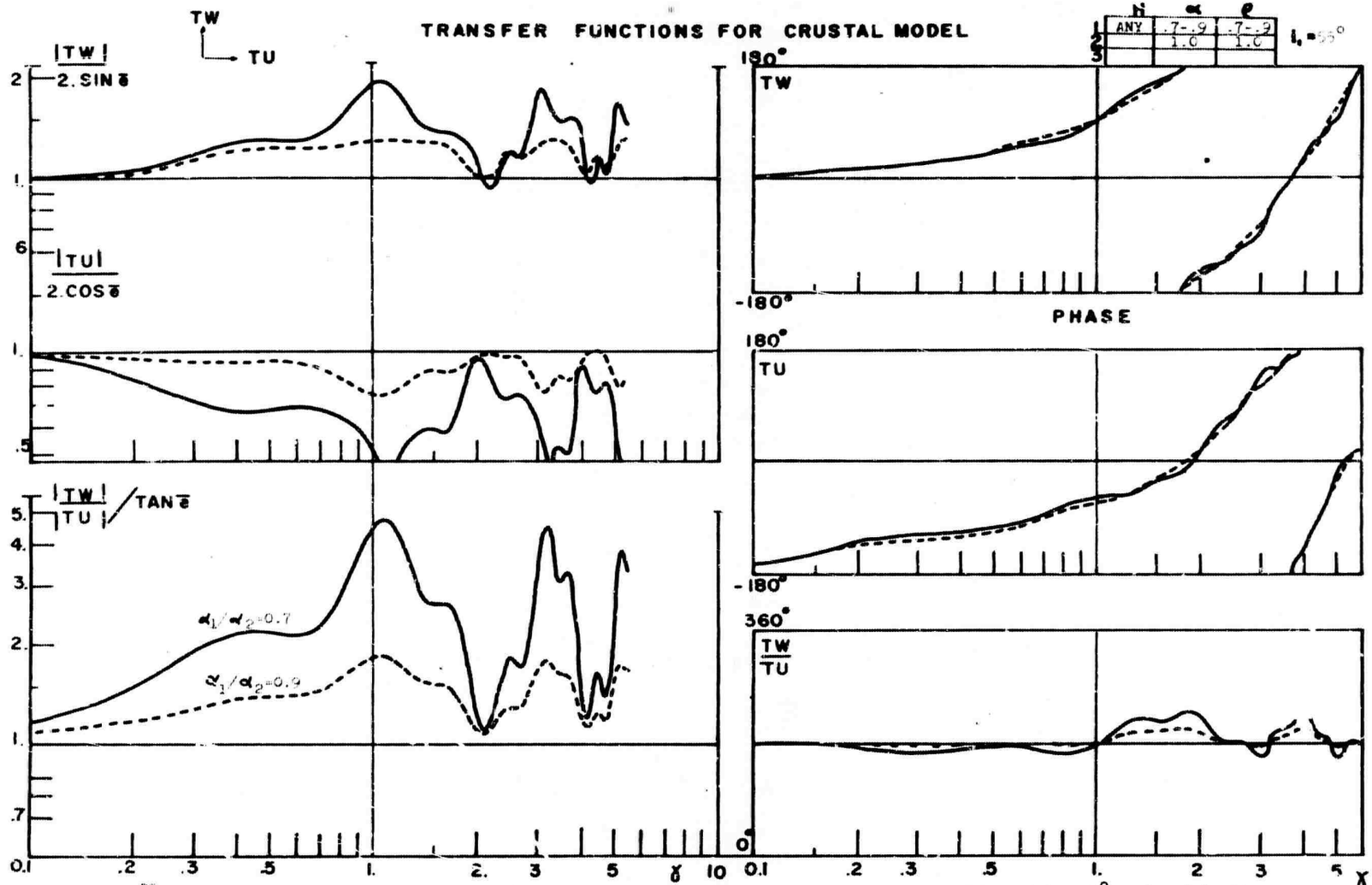

Figure 35 : Modulus and phase of the transfer functions TW, TU and TW/TU for one layer crustal models anf for 55° angle of incidence.

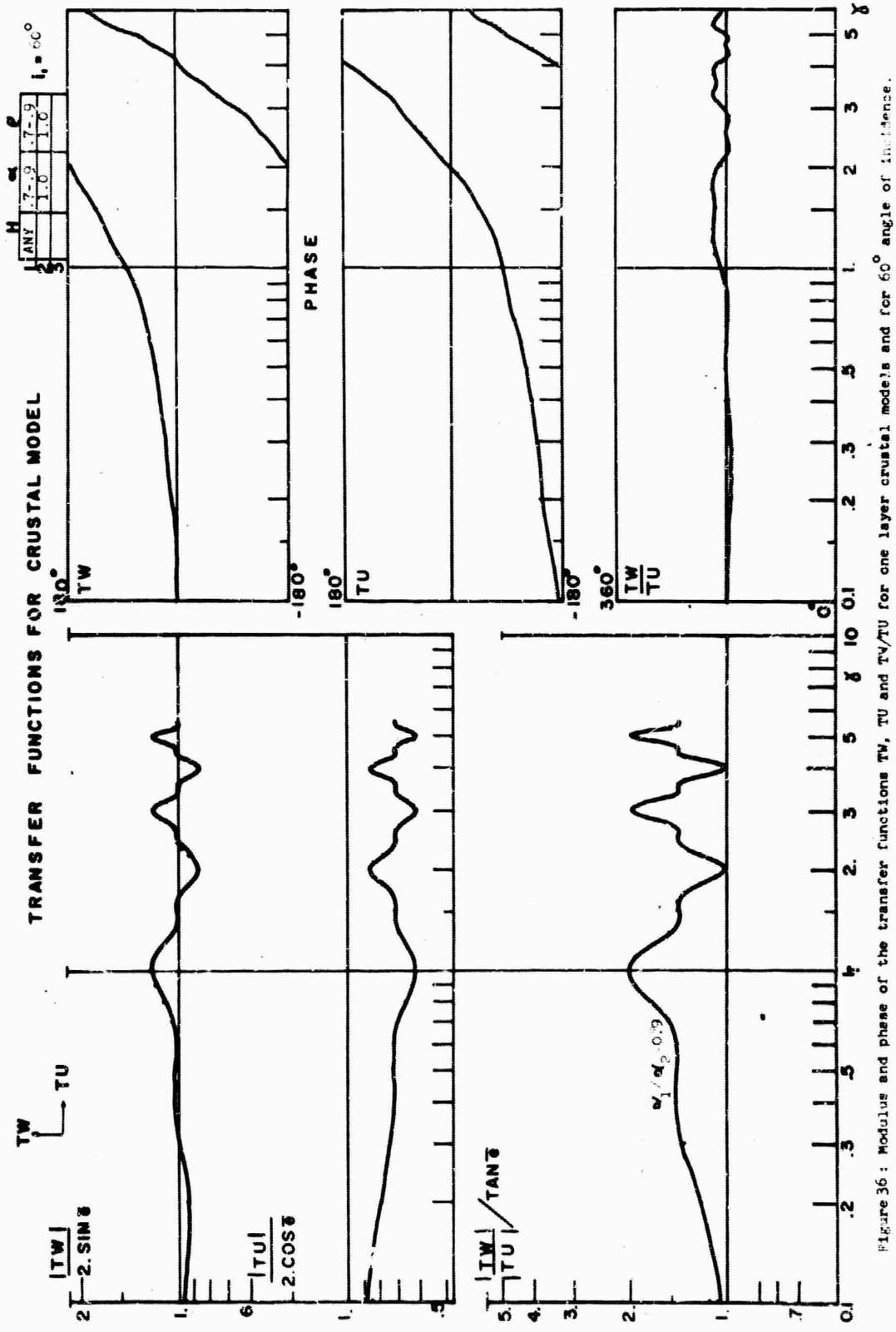

Figure 36 : Modulus and phase of the transfer functions TW, TU and TW/TU for one layer crustal models and for 60° angle of incidence.

change as the ratio between the velocities of the crust and mantle changes. Exact curves are given for the ratios α_1/α_2 equal to 0.9 and 0.7 and intermediate values may be interpolated.

In the non-realistic case in which the P velocity in the crust is greater than in the mantle, the sign of the amplitude is reversed. For illustrative purposes one such case was calculated for the angle of incidence of 25° and for the ratio $\alpha_1/\alpha_2 = 1.1$ and is presented in Figure 29.

In each figure the modulus and phase of the vertical and horizontal component transfer functions are given. These expressions are theoretically important, but in practice the spectrum of the apparent angle of emergence is the one which can be obtained most directly from observations and special attention is directed to this portion of each figure. The vertical and horizontal component are given in order to understand better the features of the apparent angle of emergence.

In these figures the values of the vertical and horizontal component are normalized so as to represent the ratio of the surface component to the corresponding component of the incident motion at the base of the layered system. In this way for infinitely long wave lengths the value of the ratio is always unity, independent of the angle of incidence of the ray. The transfer function for the apparent angle of emergence is similarly normalized to the value of the

tangent of the apparent angle of emergence corresponding to infinitely long wave lengths; this corresponds to the tangent of the apparent angle of emergence at the bottom of the layers, which may be deduced from simple ray theory without frequency considerations and given by:

$$2 \cos^2 e = 3 (1 - \sin \bar{e})$$

where e is the real angle of emergence and $\bar{e}$ the apparent one.

4.11 The vertical component transfer function.

Since the transfer function depends on several variables such as the thickness of the layer, velocities of the seismic waves, angle of incidence of the ray, and the densities of the materials, it is convenient to remark the effect of these parameters and the effect of their changes on the transfer functions. The remarks which follow may be verified by careful examination of the figures.

1) For small angles of incidence such as 5° (Figure 25) the main contribution to the vertical component after the initial P arrival pertains to the P wave reflected once at the surface and again at the crust-mantle boundary. The amplitude of this reflection depends on the contrast of velocity between crust and mantle and in each case could be obtained from the graphical solutions of Zoeppritz's

equation mentioned in section 3. In our graphs this contribution is easily detected and corresponds to the amplitude of the sinusoidal fluctuation of the vertical component transfer function. Since for small angles of incidence the reflected P is almost the only reflection of importance, it occurs without interference from other reflected phases. This is also the reason why the amplitudes of all the peaks are the same.

2) For small angles of incidence the periodicity of the contribution of the P reflection is easily calculated from the time lag with respect to the direct P arrival. The "period" of the oscillation may be obtained from formula (3-22). For an angle of incidence of 5° this "period" or peak-spacing is:

$$T_{3P}(\gamma) = \frac{\sin e_1 + \sqrt{3} \sin f_1}{2 \sin e_1} = 1.36,$$

measured in γ units. This is the period of the predominant large sinusoidal oscillation of the transfer function observable in Figure 25.

3) The larger the contrast of velocities the larger is the amplitude of the oscillations. This effect obeys an almost linear relation which allows the interpolation for intermediate values of the contrast of velocities. If the ratio of velocities is

reversed so that the larger values correspond to the crust (see Figure 29), the transfer function obtained is symmetric to the normal case, the axis of symmetry being the line TW = 1. This line corresponds to the transfer function of the model with a crust of equal P velocity to that of the mantle. This symmetry of the transfer functions for reversals of velocity implies that we may expect the transfer functions to be sensitive to low velocity channels at depth.

4) The influence of the converted SV on the vertical component is very small at small angles of incidence. This influence increases as the angle of incidence increases and is quite obvious at 20^{0} or 25^{0} where small oscillations of the transfer function are superimposed on the large ones. Nevertheless the calculation of the corresponding "period" shows that these short-period oscillations correspond not to the initial SV conversion but to combinations of P and SV reflections. For an angle of incidence of 25^{0} the different "periods" corresponding to these waves deduced from their time lags and equation (3-22) are:

$$T_{s}(\gamma) = 3.3\ \gamma \text{ units}$$
$$T_{1P,2S}(\gamma) = .77\ \gamma \text{ units}$$
$$T_{2P,1S}(\gamma) = 1.0\ \gamma \text{ units}$$

Thus in Figure 29 short period oscillations of the vertical transfer function with peaks at 1.3 and

1.8 correspond rather to the multireflected waves than to the long-period contribution of the direct SV converted wave.

5) As the angle of incidence increases not only does the vertical component of the SV wave increase relative to the horizontal component, but also the conversion factor of P into SV increases. This explains the influence of SV conversions as the angle of incidence increases.

4.12 The horizontal component transfer function.

Due to the influence of the SV conversions from the original incident P, the transfer function of the horizontal component is more complex than that of the vertical component.

The behavior of the horizontal component has a special influence on the value of the tangent of the apparent angle of emergence since the peaks of this curve correspond to the troughs of the horizontal transfer function.

Some of the main characteristics of this component transfer function curves are:

1) The main contribution to the character of the curve corresponds to the SV converted wave, at least for small angles of incidence. This conversion, nevertheless, has small transmission coefficients, as indicated by the graphical display of the computations of McCamy, et al.,

(1962) mentioned previously.

2) The period corresponding to the first SV conversion is given by the formula (3-22)

$$T_{sv} = \frac{(\sin e_1 + \sqrt{3} \sin f_1)}{(\sqrt{3} \sin f_1 - \sin e_1)}$$

For an angle of incidence of 25° the period is 3.3 γ, and this is the period of the large oscillation evident on the graph of the transfer function for this angle of incidence (see Figure 29). The periodicity of the transfer function of the horizontal component is not so clear as was that of the vertical component since there are present many oscillations of almost the same amplitude.

3) The short-period oscillations of the transfer function correspond to the horizontal components of the reflections of the P-SV type. For example, the corresponding periods of these reflections for the case of an angle of incidence of 25° are:

$T_{p,2s}(\gamma) =$ .77 γ units

$T_{p,s}(\gamma) =$ 1.0 γ units

These short-period components are very clear in the graphs (Figure 29).

4) As was the case for the vertical component, the transfer functions of larger amplitude correspond

to the cases of the larger contrasts of crust mantle P velocity. This is obvious not only in the curves of the modulus but also in the phase angle graphs.

4.13 Curves for the tangent of the apparent angle of emergence.

For practical purposes the curve for the apparent angle of emergence is the more important since it can be obtained directly from the seismograms.

The main features of the curve depend on the angle of incidence of the P wave. This angle is a function of the epicentral distance and of the depth of the focus.

Some characteristics of these curves and their dependence on the parameters of the crust may be indicated:

1) For small angles of incidence of the ray corresponding to large epicentral distances, the spectrum of the apparent angle of emergence oscillates rapidly between values above and below unity. Unity corresponds to the tangent of the apparent angle of emergence calculated from simple ray theory.

   At shorter epicentral distances the apparent angle of emergence is more stable and in general remains above unity.

2) The preceding remarks apply only to a normal type of crust where the P velocity of the crust is

lower than the P velocity in the mantle. Otherwise a reversal of signs takes place with symmetry about normal line.

3) Larger contrasts of velocities between the crust and the mantle result in larger departures of the spectrum of the apparent angle of emergence from normality. Only in the limiting case of no contrast of velocities between crust and mantle does the apparent angle of emergence coincide with the normal value at all frequencies.

4) Rays from distant teleseisms incident on the surface at less than 25° result in apparent angles of emergence below normal when very large period waves are considered. Seismic energy radiated from closer sources and emerging with angles of incidence greater than 30° has an apparent angle of emergency which slowly increases above normal as the period decreases.

5) Maxima of the apparent angle of emergence are controlled by the minima of the horizontal component transfer function. The frequencies of the maxima correspond to the frequencies at which the horizontal component of motion was destroyed by interference patterns of the primary and secondary waves. The energy emerges almost vertically at these frequencies.

6) The phase of the apparent angle of emergence indicates the phase shift between the vertical and horizontal components of the transfer functions. At zero frequency the phase is 180°. In a particle motion diagram in the vertical plane this phase relation corresponds to the linear polarization proper to the P wave. Following Haskell (1962), if the axes be chosen as indicated in Figure 37

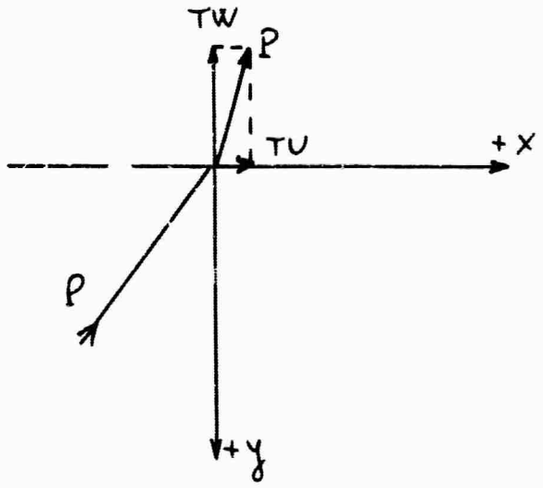

Figure 37. Components of ground motion for incident P wave.

that is, horizontal positive in the direction of advancing wave and vertical positive downward, the particle will vibrate in vertical plane and with linear motion. As the frequency of the wave increases the phase difference between the two components changes and some elliptical polarization

takes place. The ellipticity increases with the departure of the phase difference from the normal value of 180° according to Figure 38

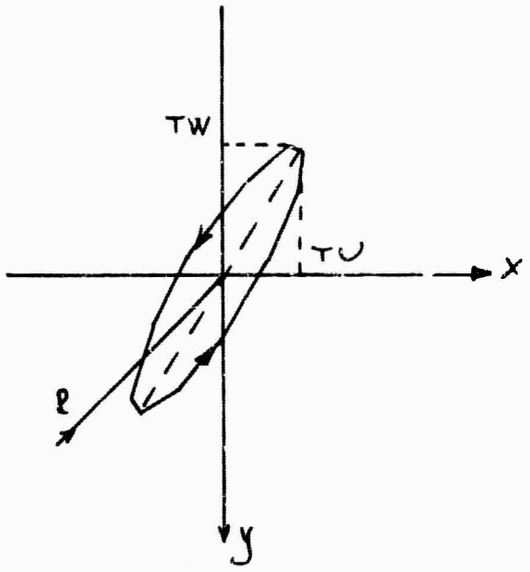

Figure 38. Particle motion diagram of P wave.

In order to present this particle motion in graphical form a FORTRAN II computer program, listed in Appendix III, was prepared. The output is presented in a series of graphs (see Figures 39 to 43). The particle motion is in the vertical plane. The graphs correspond to the one-layer model at angles of incidence of 35°, 40° and 45° for the contrasts $\alpha_1/\alpha_2 = 0.9$ and 0.7.

Not only does the ellipticity of the particle motion change with γ but also the direction of the major axis of the ellipse. The ellipticity of the ground motion is greater for large contrasts of velocity between the mantle and

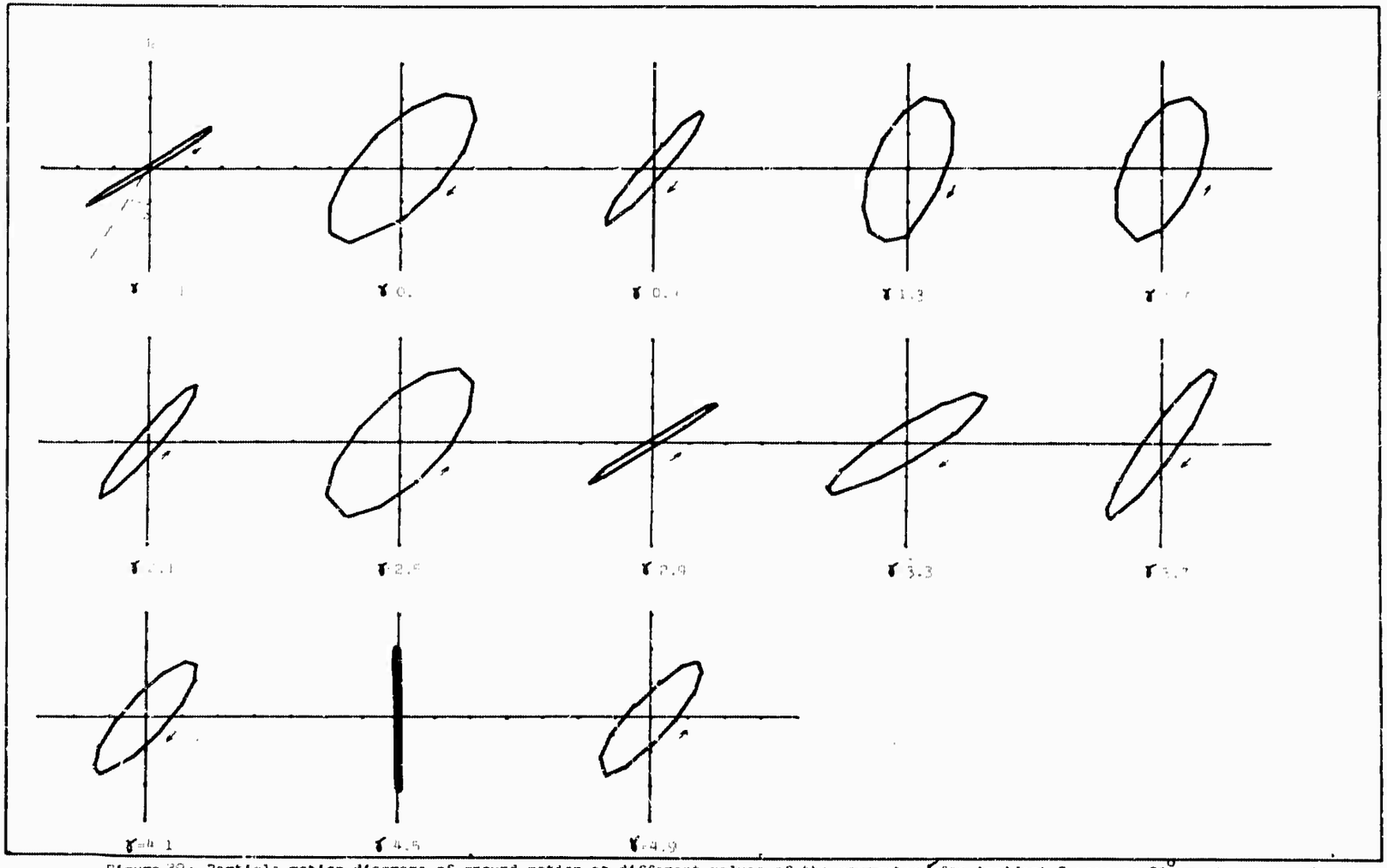

Figure 39: Particle motion diagrams of ground motion at different values of the parameter γ for incident P wave at 30° angle of incidence and for a crustal model of one layer where $\alpha_1/\alpha_2=0.7$

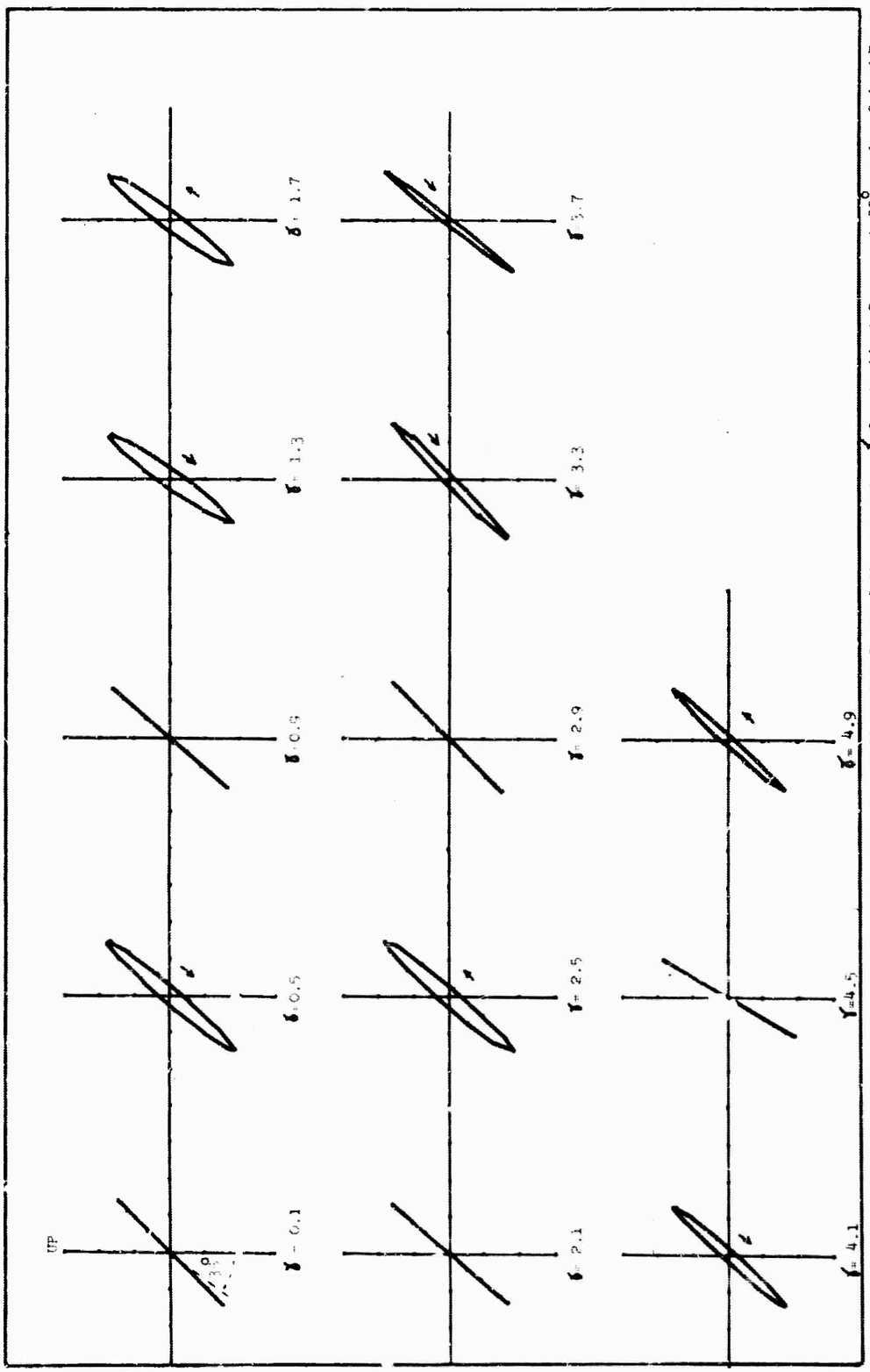

Figure 40 : Particle motion diagrams of ground motion at different values of the parameter γ for incident P wave at 35° angle of incidence and for a crustal model of one layer where $\alpha_1/\alpha_2 = 0.9$.

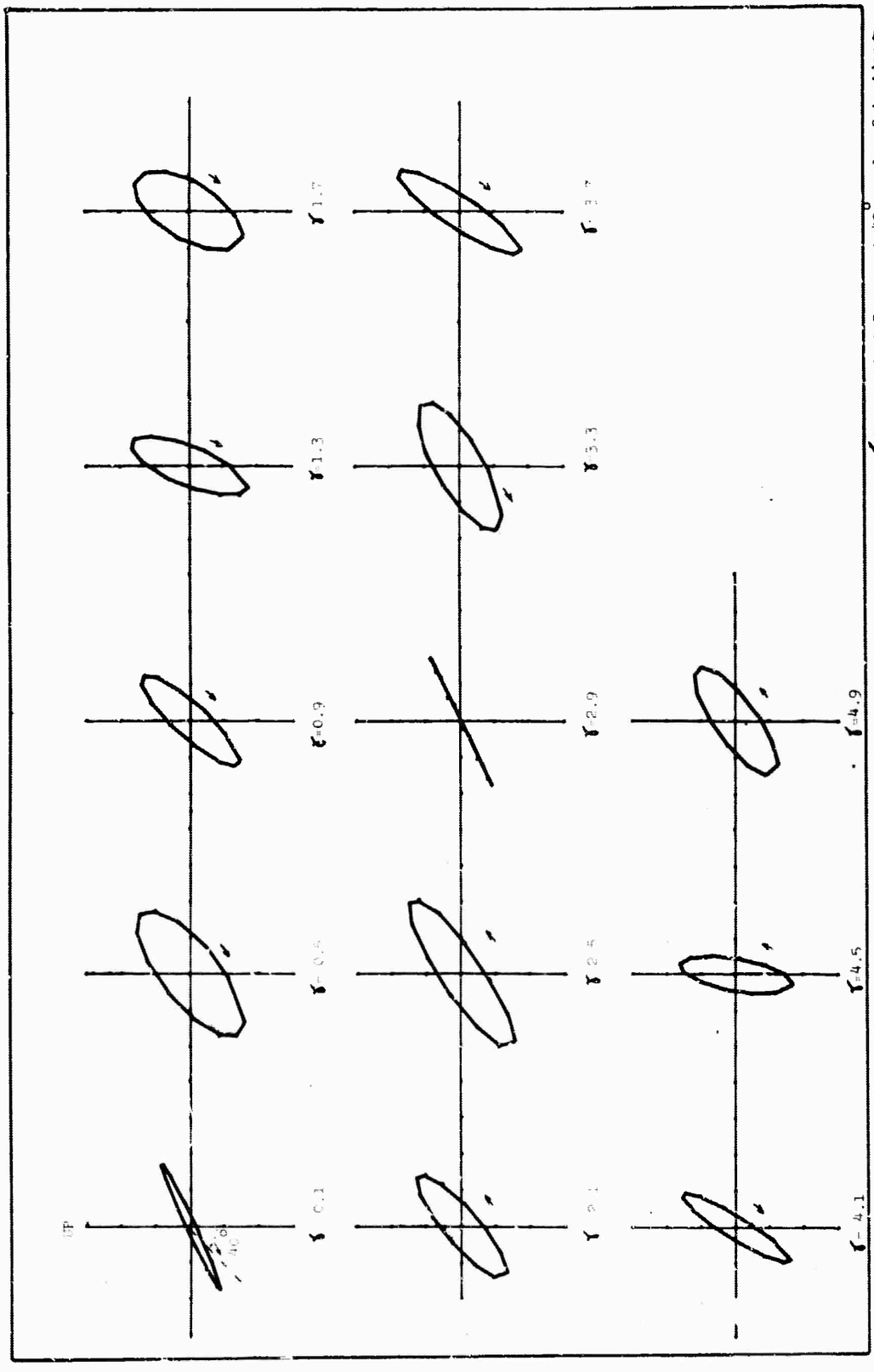

Figure 4 : Particle motion diagrams of ground motion at different values of the parameter γ for incident P wave at 40° angle of incidence and for crustal model of one layer where $\alpha_1/\alpha_2 = 0.7$.

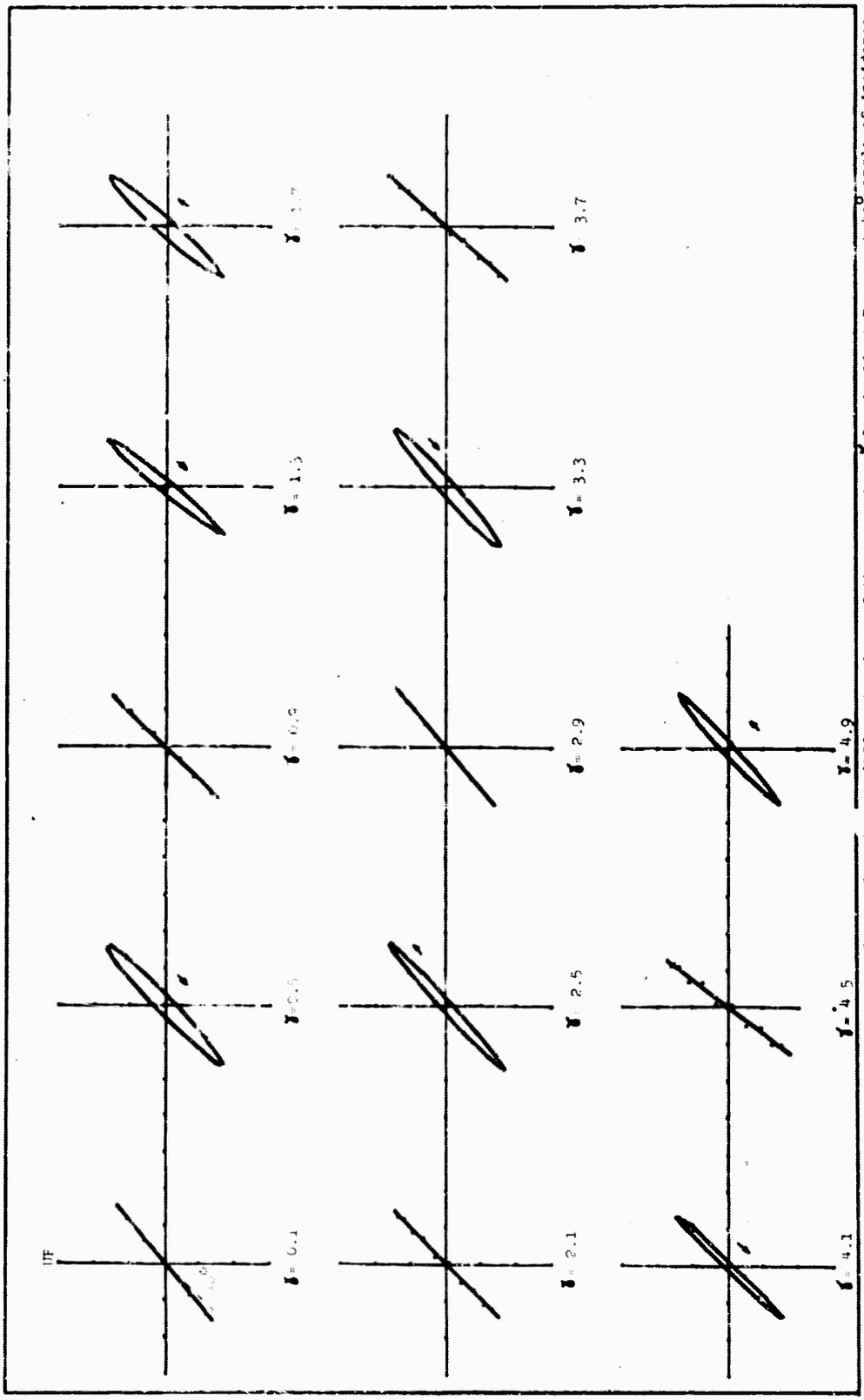

Figure 42 : Particle motion diagrams of ground motion at different values of the parameter γ for incident P wave at 40° angle of incidence and for a crustal model of one layer where $d_1/d_2 = 0.9$

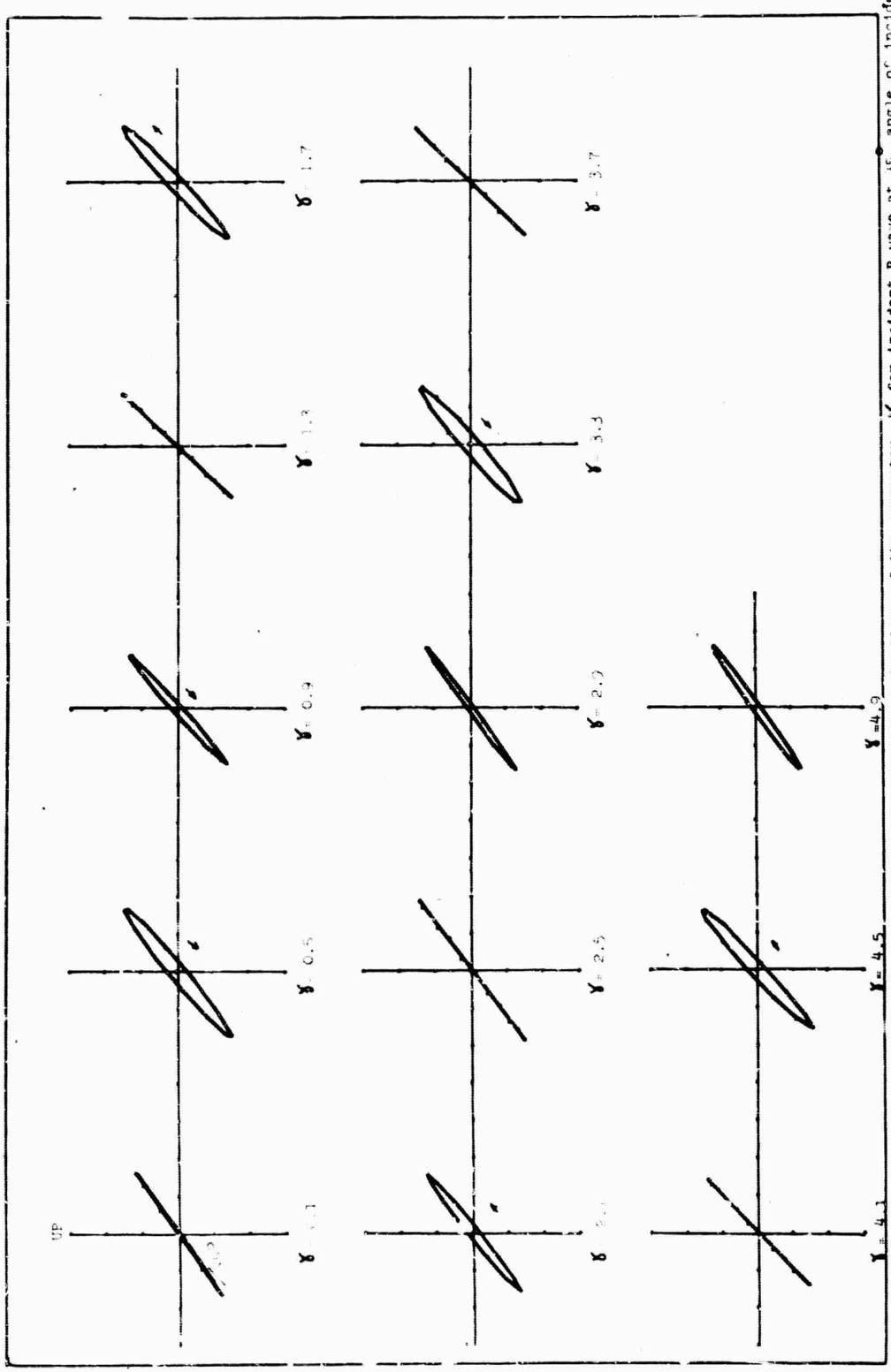

Figure 43 : Particle motion diagrams of ground motion at different values of the parameter γ for incident P wave at 45° angle of incidence and for a crustal model of one layer where $\alpha_1/\alpha_2 = 0.9$.

the crust. Nevertheless, as indicated by Haskell (1962), the character of the ground motion remains generally of the P wave type.

4.2 Two-layer crustal models

The introduction of an intermediate discontinuity in the crust in accordance with observations in many different parts of the world will increase the number of reflections and refractions which the seismic rays undergo in the crust of the earth. Some rays will be refracted at the intermediate discontinuity and so their amplitude will be affected. The time lag of these rays will also be changed and the periodicity of the transfer functions will be different. Nevertheless, observations show that these discontinuities have relatively small velocity contrasts; consequently the amplitudes and time lags introduced will be small and the deviation from the one-layer model will not be as great as might first be expected.

In addition to the above rays there will be others due to reflections at the intermediate interface. In general these waves will have reflection coefficients of small amplitude. Some of them will have small time lags, as for example the reflections of P at the interface identified in Figure 44 as $P_2 P_1 P_1 P_1$.

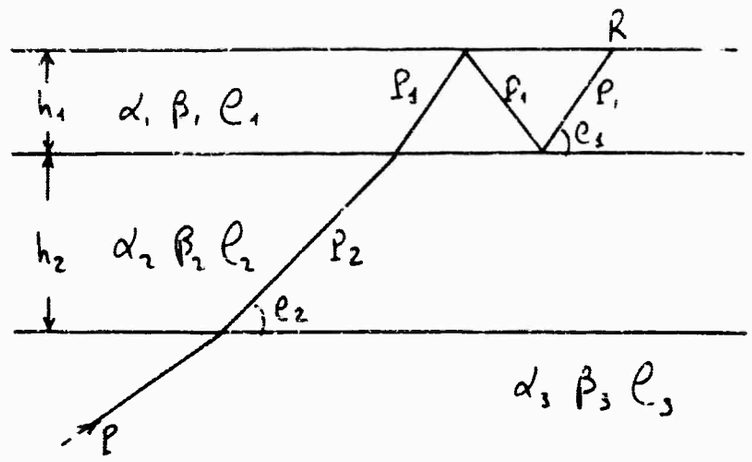

Figure 44. Multiple reflections on a two-layer crustal model.

This reflection will have small time lags as compared with the direct P, and consequently will introduce a long-period component in the transfer function curve. Other reflections will have a large time lag and their contribution will introduce short-period sinusoidal components into the periodicity of the curves.

For the two-layer case, many combinations of the layer thicknesses and velocities ratios are possible. Figures 45 to 49 present the special case of a model where the angle of incidence is 40° and $\alpha_1/\alpha_2 = 0.9$. Each family of curves corresponds to a different thickness ratio h_1/h_2.

The following remarks concerning these curves may facilitate their application to observations:

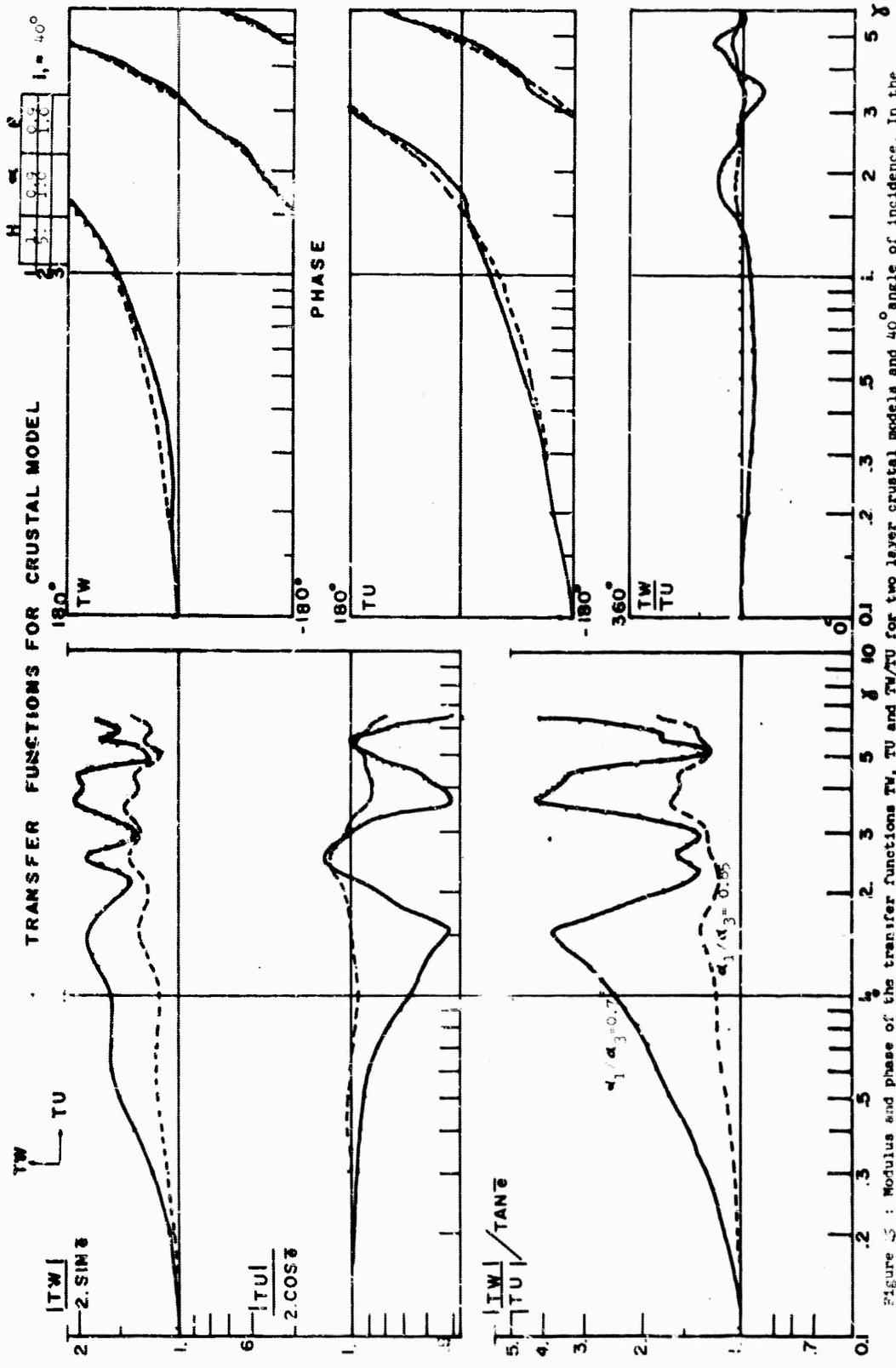

Figure 3 : Modulus and phase of the transfer functions TW, TU and TW/TU for two layer crustal models and 40° angle of incidence. In the crustal model $h_1/h_2 = 1/5$ and $d_1/d_2 = 0.9$

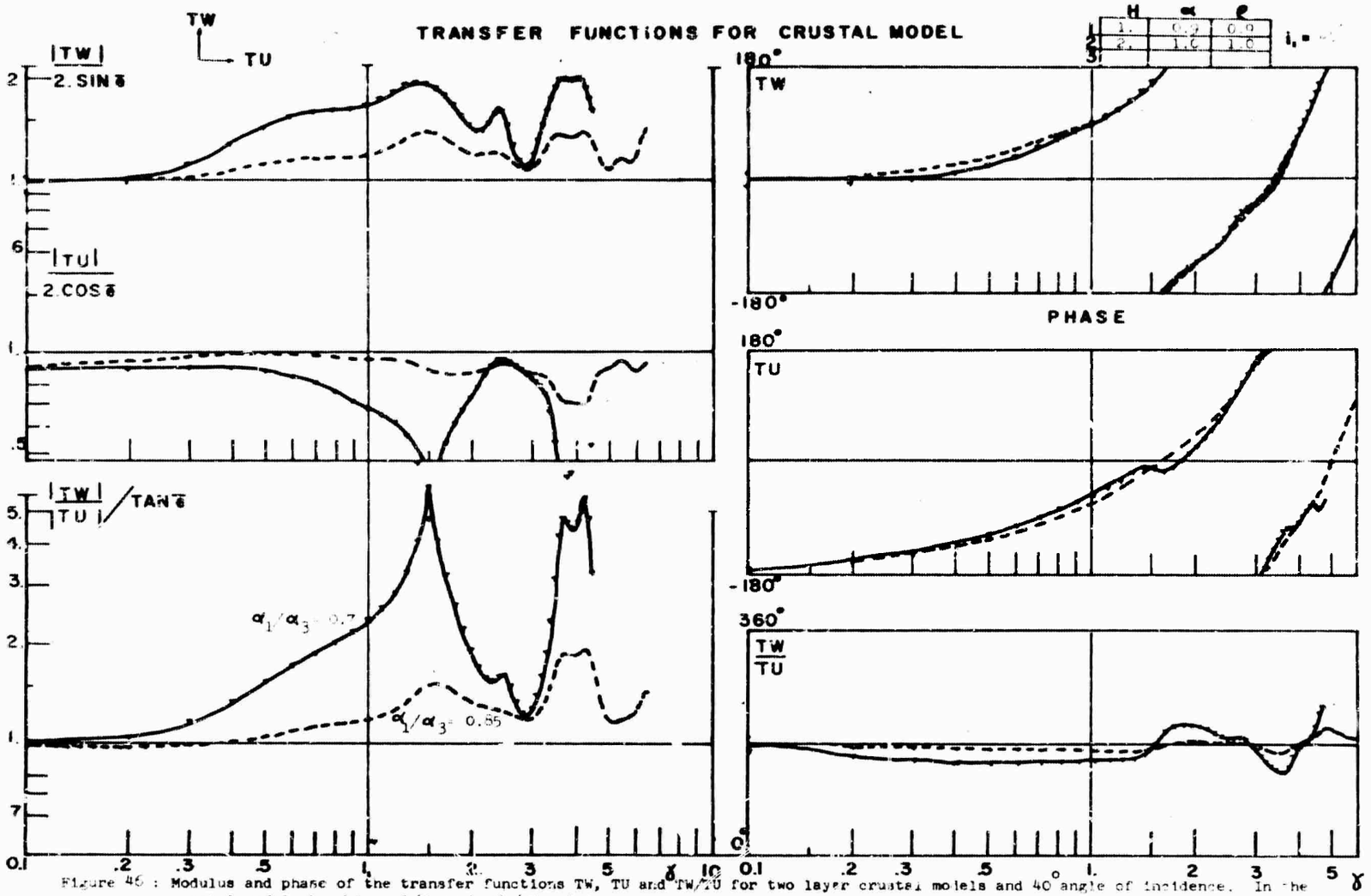

Figure 46 : Modulus and phase of the transfer functions TW, TU and TW/TU for two layer crustal models and 40° angle of incidence. In the crustal model $h_1 / h_2 = 1/2$ and $\alpha_1/\alpha_2 = 0.9$.

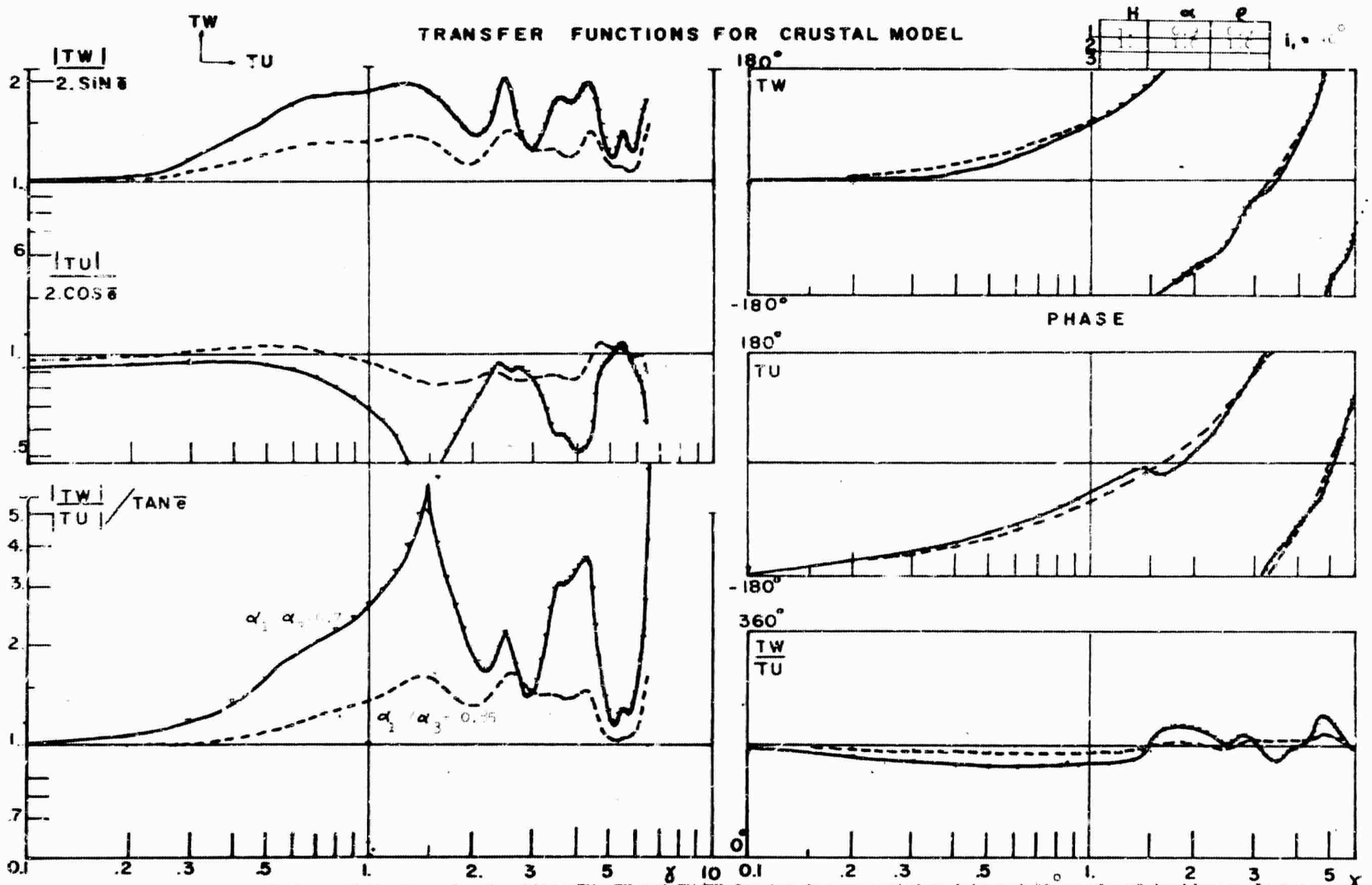

Figure 2 : Modulus and phase of the transfer functions TW, TU and TW/TU for two layer crustal models and 40° angle of incidence. In the crustal model $h_1/h_2 = 1/1$ and $\alpha_1/\alpha_2 = 0.9$.

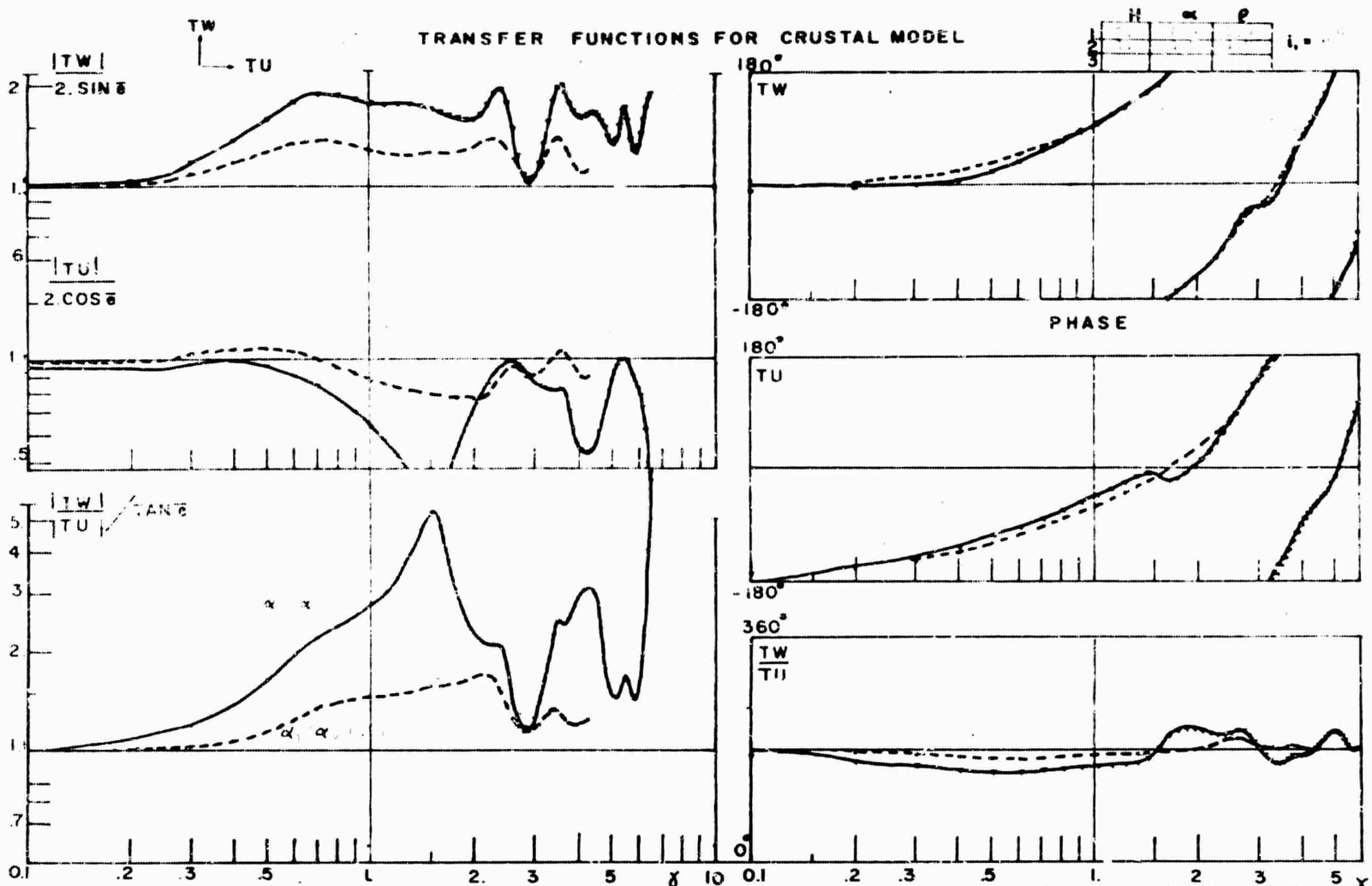

Figure 4.3 : Modulus and phase of the transfer functions TW, TU and TW/TU for two layer crustal models and 40 angle of incidence. In the crustal model $h_1/h_2 = 2/1$ and $\alpha_1/\alpha_2 = 0.9$

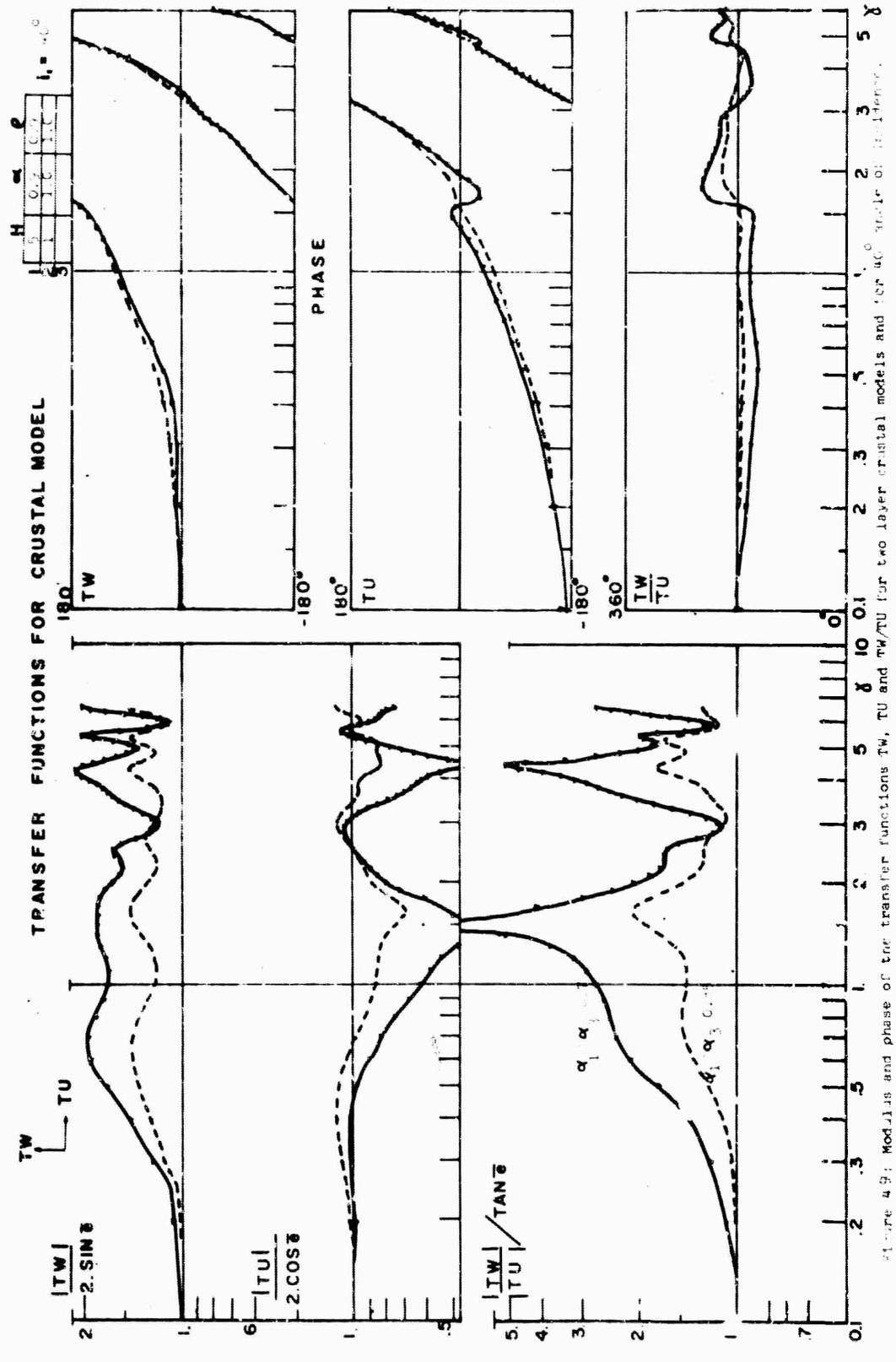

Figure 49: Modulus and phase of the transfer functions TW, TU and TW/TU for two layer crustal models and for 40° angle of incidence. In the crustal model $h_1 / \lambda_2 = 5/3$ and $\alpha_1/\alpha_2 = 0.9$.

1) In general the two-layer model transfer curves resemble the corresponding one-layer models. This is particularly true when the contrast between the P velocities in the crust and mantle is large, and also when one of the layers is very thick with respect to the other. For example, the curve of Figure 49 corresponding to $\alpha_1/\alpha_2 = 0.7$ and $h_1/h_2 = 1/5$ is very similar to the one-layer case $\alpha_1/\alpha_2 = 0.7$ presented in Figure 32.
2) The transfer function of models with layers of the same thickness, as the one presented in Figure 47 for $h_1/h_2 = 1/1$, differ considerably from the corresponding one-layer model.
3) The large amplitude components of the transfer functions are the result of the velocity contrast between the mantle and the crust.
4) The influence of intermediate layers on the transfer functions increases with frequency. This property should be of interest when the spectrum of short-period observations is obtained.
5) The periodicity of the transfer functions within a family of curves is similar in most of the cases. Nevertheless for some models the influence of the second layer is so small due to low contrast of velocities that some anomaly in the periodicity of the curves seems to be present (Figure 48).

6) Changes in the ratio of the thicknesses between the two layers of the crust influences the transfer functions. This influence is greater if the contrast of velocities between the mantle and the crust is small. Changes of thickness ratios affect only the periodicity of the transfer functions. This is true because these changes influence only the time lags of the different arrivals at the surface and not their amplitudes.

5. Spectral Analysis of the Seismic Records

As previously indicated, the tangent of the apparent angle of emergency can be obtained from the seismograms by dividing the spectrum of the vertical component by the spectrum of the horizontal component. This operation will eliminate from the spectra the influence of the frequency content of the source.

The theoretical justification for this property of the apparent angle of emergence is given by Hannon (1964) and by Phinney (1965).

To be completely valid the argument assumes that for a seismic ray the frequency content at the base of the crust is exactly the same for both horizontal and vertical components. In other words, before the mantle-crust discontinuity, no other significant discontinuity was encountered by the ray. This is only partially true since the upper mantle and mantle are not exactly homogeneous. Even so, it may reasonably be assumed that deep in the mantle velocity gradients exist and that changes in the velocity of P waves are gradual; no reflections from discontinuities can be expected for this part of the ray-path and the transfer function for this portion of the medium will be unity, according to the theoretical considerations of section 3. Should discontinuities exist in the upper

mantle the velocity contrasts across these discontinuities may reasonably be presumed to be relatively small; qualitatively, in view of the previous discussion, the effect of these discontinuities would be to introduce a small oscillatory component into the form of the transfer function. Because the velocity contrasts are small the amplitude of this component would be small. Because the time lags so introduced would be large, the periodicity of this component would be small. The net result, in general, would be a small rapidly oscillating character introduced into the form of the transfer functions riding on top of the main features of these functions due to discontinuities of the crust.

An investigation of the upper mantle structure could be attempted based on the observations we have just made in the present study; however, we do not intend to follow this procedure. In fact, we shall smooth the spectra to be obtained from seismograms, and one reason for so doing will be to exclude any oscillatory character of the transfer function of short periodicity due, possibly to the influence of the upper mantle.

5.1 Fourier analysis of longitudinal seismic waves.

In the spectral analysis of the seismograms several restrictions are imposed by the very nature of spectral analysis and by the transient aspect of the seismic body waves.

The finite length of the seismic record limits the frequency resolution of the spectrum. This resolution is a function of the total length of the seismogram used to estimate the spectrum. The resolution is given by Blackman and Tukey (1958) by the relation

$$(\text{resolution in cps}) = \frac{1}{(\text{total length in seconds})}$$

This notion of resolution is intrinsically connected with the concept of a data window and with smoothing of the spectrum. In practice, when a finite length of record is taken, if no shaping or tapering of the record is introduced the record is actually passed through a rectangular window of the form

$$D_o(t) = 1, \text{ for } t < T_m$$
$$= 0, \text{ for } t > T_m$$

where T_m is the total length of the record available.

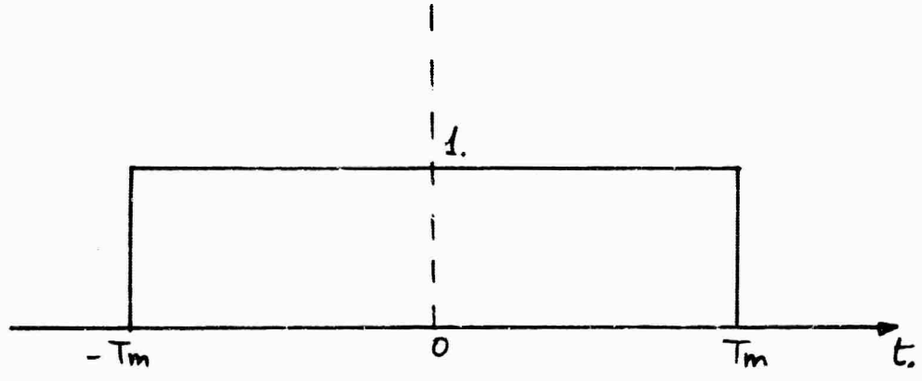

Figure 50. Rectangular time window.

When this record is Fourier analyzed the result is the convolution of the true spectrum P (f) of the signal and the

Fourier transform of the rectangular window $Q_o(f)$. This spectrum is only an estimation of the true spectrum and may be called the "average spectrum"

$$\text{ave.}\{P(f_1)\} = \int_{-\infty}^{+\infty} Q_o(f_1 - f) \cdot P(f)\, df \tag{5-2}$$

Consequently, the value estimated for the spectrum at the frequency, f_1, is the average value at this frequency and the neighboring frequencies with a weight proportional to $Q_o(f_1-f)$. The Fourier transform of the rectangular function is

$$Q_o(f) = 2T_m \frac{\sin(2\pi f T_m)}{2\pi f T_m} \tag{5-3}$$

and its graph is given in Figure 51.

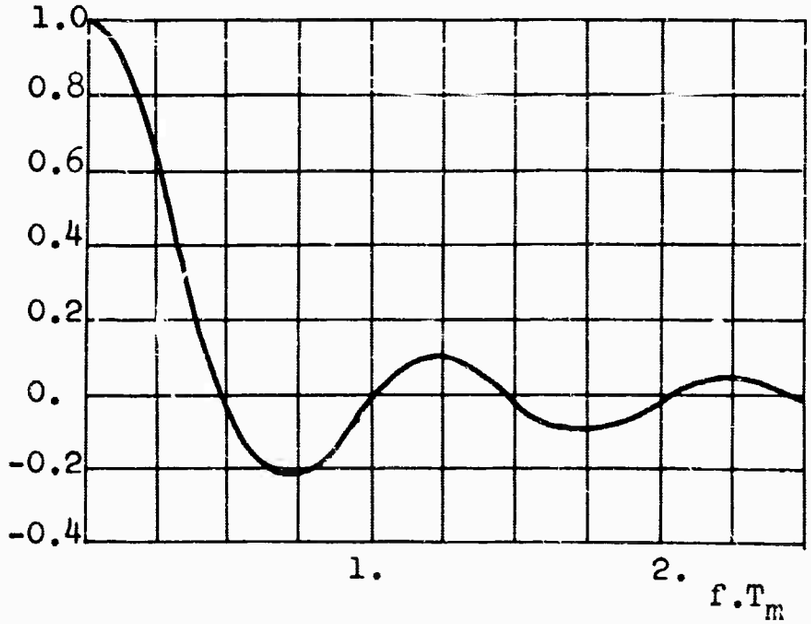

Figure 51. Fourier transform of the rectangular window

This figure illustrates the fact that if no special data window is used in the analysis of the records, in reality a rectangular window is used and the spectrum will be a poor estimation of the real spectrum. This follows since the spectral window does not behave in the manner we might desire; the estimation at each frequency is affected by the spectral amplitude values of distant frequencies.

Several data windows have been devised to remedy, at least in part, this difficulty. For example, Hirasawa and Stauder (1964) use a data window of exponential type presented by Kasahara (1957). Phinney (1964) uses for his lag window a Gaussian function. For the present analysis we have selected the use of the taper-pair window given by Blackman and Tukey (1958) and designated by them as a "hamming" window. Its form is

$$D_3(t) = 0.54 + 0.46 \cos\frac{t}{T_m} \qquad |t| < T_m$$
$$= 0 \qquad |t| > T_m \qquad (5\text{-}4)$$

and its Fourier Transform is:

$$Q_3(f) = 0.54\, Q_0(f) + 0.23 \left[Q_0\left(f + \frac{1}{2T_m}\right) + Q_0\left(f - \frac{1}{2T_m}\right) \right]$$

where Q_0 is given by (5-3).

The graph of the pair is given in Figure 52. This figure shows that for a sufficiently large value of T_m the estimation of the frequency is restricted to a narrow frequency

band without influence of the side lobes.

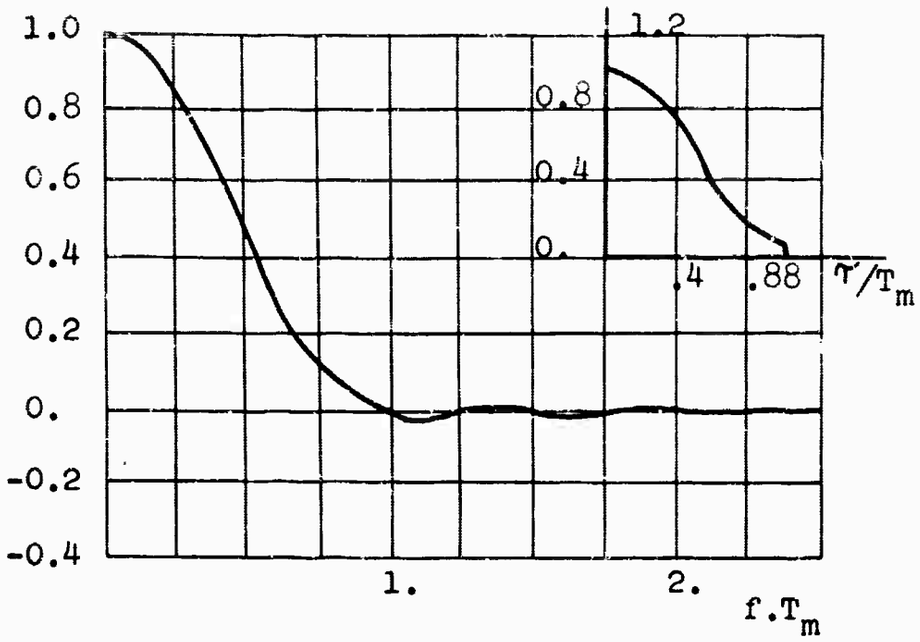

Figure 52. Hamming data window and its Fourier Transform

In addition to the smoothing aspect of the data window its use serves another purpose. The data window can be considered as a weighting function which emphasizes the first part of the P wave and minimizes the influence that later arrivals could have on the spectrum. This is very convenient in the analysis of the seismic body waves since the first arrival of the P wave is followed at short time intervals by other phases such as pP or PcP not related to the direct P wave. In practice the selection of the total length of the record to be used and the value of the window for which the weight should be zero is very critical. If too short a time is selected some important reflections will not be included and the transfer function will be incomplete.

If too long an interval is selected other phases as pP and PcP could be included and the transfer function obtained will no longer be representative of the crustal structure of the station under study.

Proper selection of the time interval of record to be used is a function of the magnitude, depth, and epicentral distance of the earthquake. Some estimation of the minimum time required may be obtained from the calculations of Ben-Menahem, et al. (1964), who computed the theoretical record corresponding to different structures and a conventional source function. The computed seismograms include the reverberations from the layers of the crust and show that at times greater than 40 seconds after the first arrival there are no longer substantial contributions to the record from the direct P.

Another limitation of spectral analysis is introduced by the folding frequency. To avoid this folding of the spectrum it is convenient to use linear digital filters with a low pass-band. This may be done using one of any number of filters. We shall here use a digital linear smoothing filter with no phase shift presented by Hamming (1962). This filter replaces the original value of the record $y_k(t)$ by a new one given by

$$y'_k = \frac{y_k + 2y_{k+1} + 3y_{k+2} + 3y_{k+3} + 2y_{k+4} + y_{k+5}}{12} \qquad (5\text{-}5)$$

The ability of this filter to reject the upper half of the spectrum is very good and its transfer function is

$$H(\omega) = \frac{\sin\left(6\pi \frac{\Delta t}{T}\right) \sin\left(8\pi \frac{\Delta t}{T}\right)}{12 \sin\left(2\pi \frac{\Delta t}{T}\right)} \qquad (5\text{-}6)$$

where T is the period of the wave. This filter puts zeros in the spectrum at 1/4, 1/3 and 1/2 of the folding frequency as is shown in Figure 53.

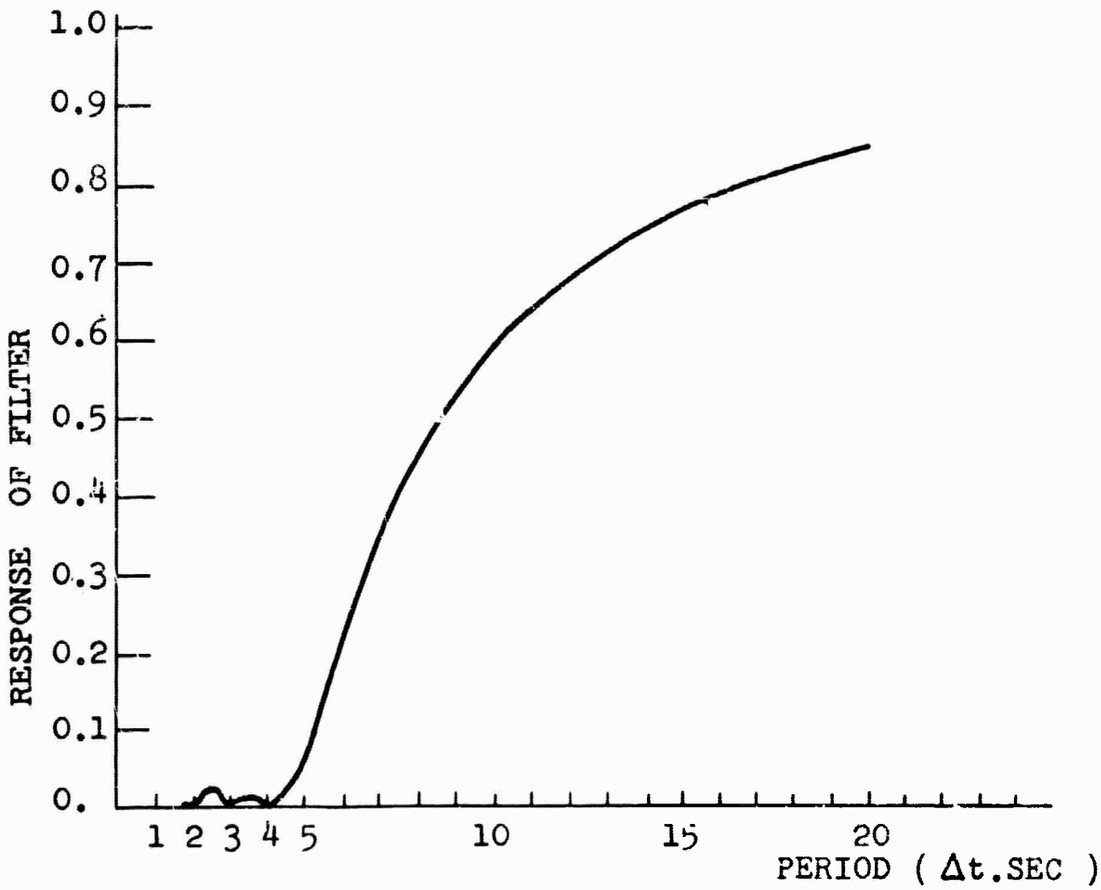

Figure 53. Frequency response of digital filter.

The transient character of the P wave does not allow us to treat it as a stationary signal. Consequently, in-

stead of calculating the autocorrelation of the signal and then taking the Fourier transform to find the power spectrum, the records are directly Fourier integrated. The numerical integration is performed using Filon's method as described by Hamming (1962).

In order to combine all these operations in a flexible FORTRAN program a main program was written which includes a series of subroutines with the different operations.

This program, called Seismic Analyzer, is listed in Appendix IV. The output of this program is the series of graphs used in the next section for crustal determinations.

6. Crustal Parameters of the Central United States

In this section, as an application of the theory and methods of analysis developed previously, we shall evaluate the thickness of the crust and the average crustal P wave velocity for the region of the central United States. The data for this evaluation will consist of the spectra of the apparent angle of emergence obtained from seismograms recorded at stations of the Saint Louis University network.

The interpretation itself will progress in two steps. First, the observational spectra will be compared to theoretical spectra for single-layered models of the crust. In this way a first approximation to the crustal parameters may be obtained. Second, two-layered models should be used in an attempt of a more precise interpretation.

6.1 Application of the one-layer model master curves.

For the one-layer models the dimensionless parameter γ becomes

$$\gamma = f \cdot \frac{h_1}{\alpha_1} (\sin e_1 + \sqrt{3} \sin f_1)$$

Since the families of master curves were calculated for constant values of f_1 and e_1 it is possible to divide γ by the expression in the parenthesis. Then

$$\gamma' = f \cdot \frac{h_1}{\alpha_1} \qquad (6\text{-}1)$$

This simplification of γ represents a translation of the curves along the γ axis when they are plotted on logarithmic paper. A set of master curves with this translation is presented in Figures 54 to 62*. In these figures only the tangent of the apparent angle of emergence is given. Each family of curves corresponds to an angle of incidence of the ray in the crustal layer. Only three members of the family are presented for the sake of simplicity and clarity. Intermediate values of the ratio may be easily interpolated.

The use of these master curves may be summarized by the following procedural steps:

1) Evaluate the tangent of the apparent angle of emergence versus frequency at a given station using the method and program presented in the preceding chapter.

The selection of the earthquakes for this type of analysis is very critical. The main criterion is that at least 40 seconds of the seismogram correspond to the direct P recording free of interference of other phases which have their origin outside of the crust below the station. In practice the phases to be avoided are pP and PcP, since these are the waves which arrive at a short time interval after the direct P phase. Records which satisfy this condition can be obtained at epicentral distances smaller

---

*To facilitate the use of these curves, they are included in a pocket at the back cover.

than 55^{o} and for earthquakes with a depth of focus greater than 150 km. The magnitude of the shocks should be such that the signal-to-noise ratio of the long-period records is sufficiently high.

2) Plot the curve of the tangent of the apparent angle of emergence versus frequency on logarithmic tracing paper of the same scale as that of the master curves.

3) From the available information of epicentral distance and depth of the focus estimate roughly the angle of incidence of the ray at the surface of the earth. This evaluation is only a guiding criterion in the selection of the correct family of master curves to be used.

4) Match the observed and theoretical curves. To obtain this matching the observed curves are laid over the theoretical curves and then moved to the right and to the left, up and down, but without rotation of the axis until the best match is achieved. In the matching special attention should be given to the central portions of the observed curves since these correspond to the central values of the response curve of the seismometer for which the observations are more accurate.

5) The value of the velocity contrast may be obtained by the interpolation between the members of the families of curves. If the velocity of the mantle in the region is known from other sources or assumed in some way, the average velocity of the P waves in the crust α_1 may be

obtained from the ratio α_1/α_2.

6) Read the value of γ' corresponding to the 0.1 cps frequency value of the observations. If we call this value γ'_1, then:

$$\gamma'_1 = 0.1 \frac{h_1}{\alpha_1} \qquad (6\text{-}2)$$

and the thickness of the crust will be:

$$h_1 = 10. \gamma'_1 \alpha_1$$

A graphic example of the method is presented in Figure 63.

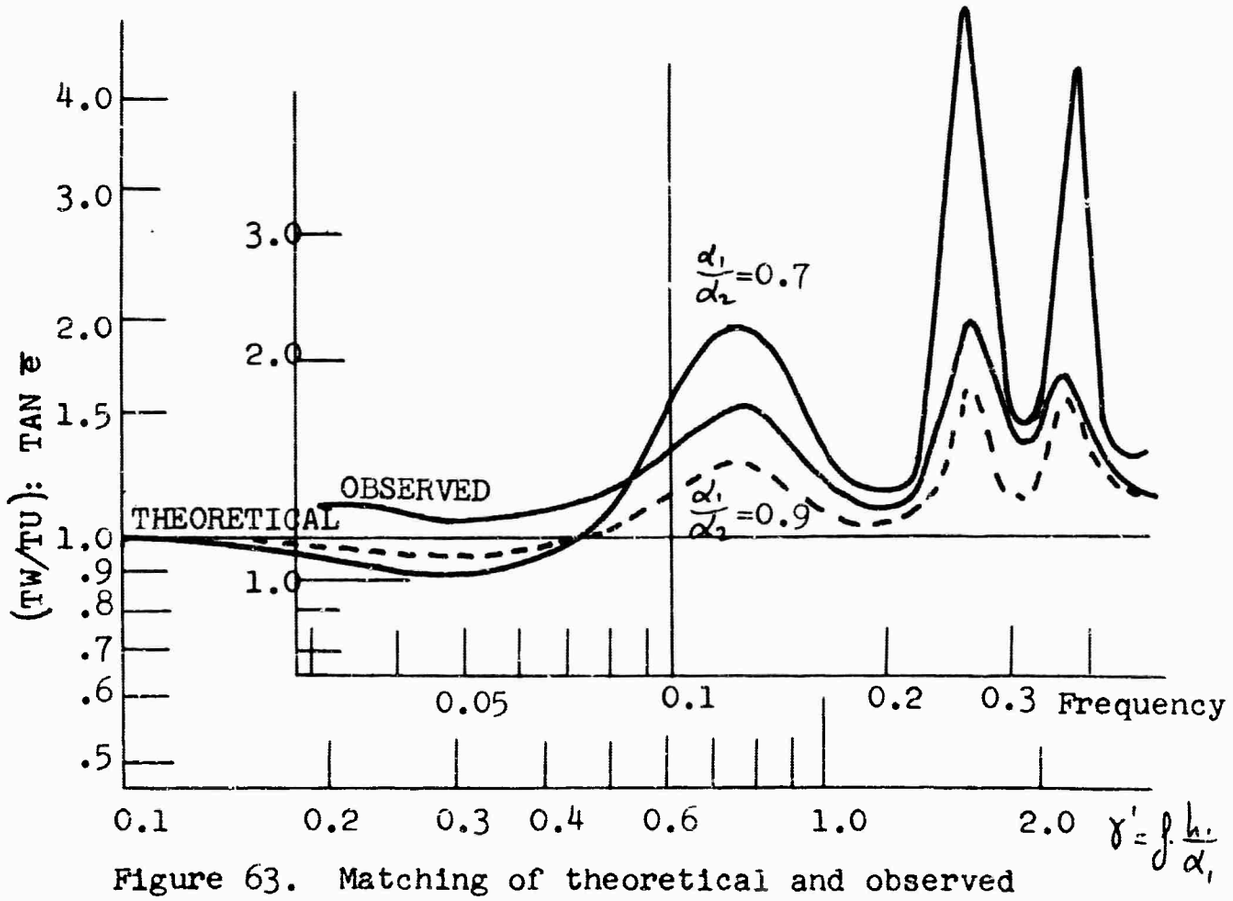

Figure 63. Matching of theoretical and observed curves.

In Figure 63

$$\alpha_1 = 0.82\ \alpha_2$$

$$\gamma_1' = 0.61$$

$$h_1 = 0.61 \times 10 \times 0.82 = 41.5$$

So assuming a value of the P velocity in the mantle of 8.2 km/sec., the average P velocity, α_1 = 6.806 km/sec. and the total thickness of the crust h_1 = 41.5 km.

6.2 Multi-layered case.

Application of the master curves for the case of two and more layer models may be done in a similar way.

In the case of two layers it is possible to transform the dimensionless parameter γ as follows:

$$\gamma = \frac{h_1}{\alpha_1}\left[(\sin e_1 + \sqrt{3}\sin f_1) + \frac{h_2/h_1}{\alpha_2\ \alpha_1}(\sin e_2 + \sqrt{3}\sin f_2)\right] \qquad (6\text{-}3)$$

Since for each family of master curves h_2/h_1 and α_2/α_1 remain constant, it is possible to divide by the quantity in brackets and present the curves in terms of $\gamma' = h_1/\alpha_1$. In this way the thickness h_1 and the velocity α_1 of the first layer may be obtained directly from the matching of the curves. We then calculate h_2 and α_2 for the second layer from the ratios h_1/h_2 and α_1/α_2.

A set of 90 master curves for two-layer models have been calculated. This set includes three velocity contrasts in the crust with values for α_1/α_2=0.90, 0.95

and 1.05. The third case corresponds to a low velocity layer at the bottom of the crust. The ratio of the layers is h_1/h_2 = 1/5, 1/2, 1/1, 2/1, 5/1.

6.3 Application to the crustal structure in Central United States.

The master curve matching technique just described was applied to long-period seismograms obtained at the seismic network of stations of Saint Louis University in the central United States. The list of stations and their coordinates is given in Table 1.

Table 1. STATIONS OF SAINT LOUIS UNIVERSITY NETWORK

	Geographic Latitude	Longitude
Bloomington	39° 11' 20"N	86° 30' 15"W
Dubuque	42° 30' 24"N	90° 41' 00"W
Florissant	38° 48' 06"N	90° 22' 12"W
Manhattan	39° 11' 59"N	96° 34' 50"W
Rolla	37° 55' 04"N	91° 52' 08"W
Saint Louis	38° 38' 10"N	90° 14' 10"W

The response characteristics of the long-period seismographs used in this study were calculated by Nuttli and McEvilly (1961) using the impedance bridge method described by Willmore.

According to the criteria previously indicated, three earthquakes of intermediate and deep focus were selected. The three components of the long-period instruments were

used to evaluate the spectrum of the angle of emergence according to the method indicated in section 5 of this study. The parameter of the three selected earthquakes according to the U.S. Coast and Geodetic Survey Bulletins are:

Date			Origin time	Epicenter		Depth	Magn.	Site
Year	Mo.	Day	Hr.min.sec.	Lat.	Long.	(Km)		
1961	Dec.	20	13-25-34.4	4.6N	75.6W	176	6 3/4	Colombia
1963	Aug.	15	17-25-05.9	13.8S	69.3W	543	7 3/4	Peru
1963	Nov.	9	21-15-30.4	9.0S	7.1W	600	6 3/4-7	Brazil

The three long-period components were digitized at a rate of one sample every 0.566 seconds, which corresponds to a folding frequency of 1 cps. The length of the time window in each case was determined from the epicentral distance and depth of the focus.

The signal-to-noise ratio of some seismograms was such that the analysis could be performed without the filtering and detrending steps.

The result of the final analysis is presented in table 2 and in Figures 64 to 75. In these figures the original records are presented together with the appearance of the phase after the filtering and weighting operations have been performed. At the left side of the graph the tangent of the apparent angle of emergence versus frequency is given together with the phase difference between vertical and horizontal components of the Fourier analysis.

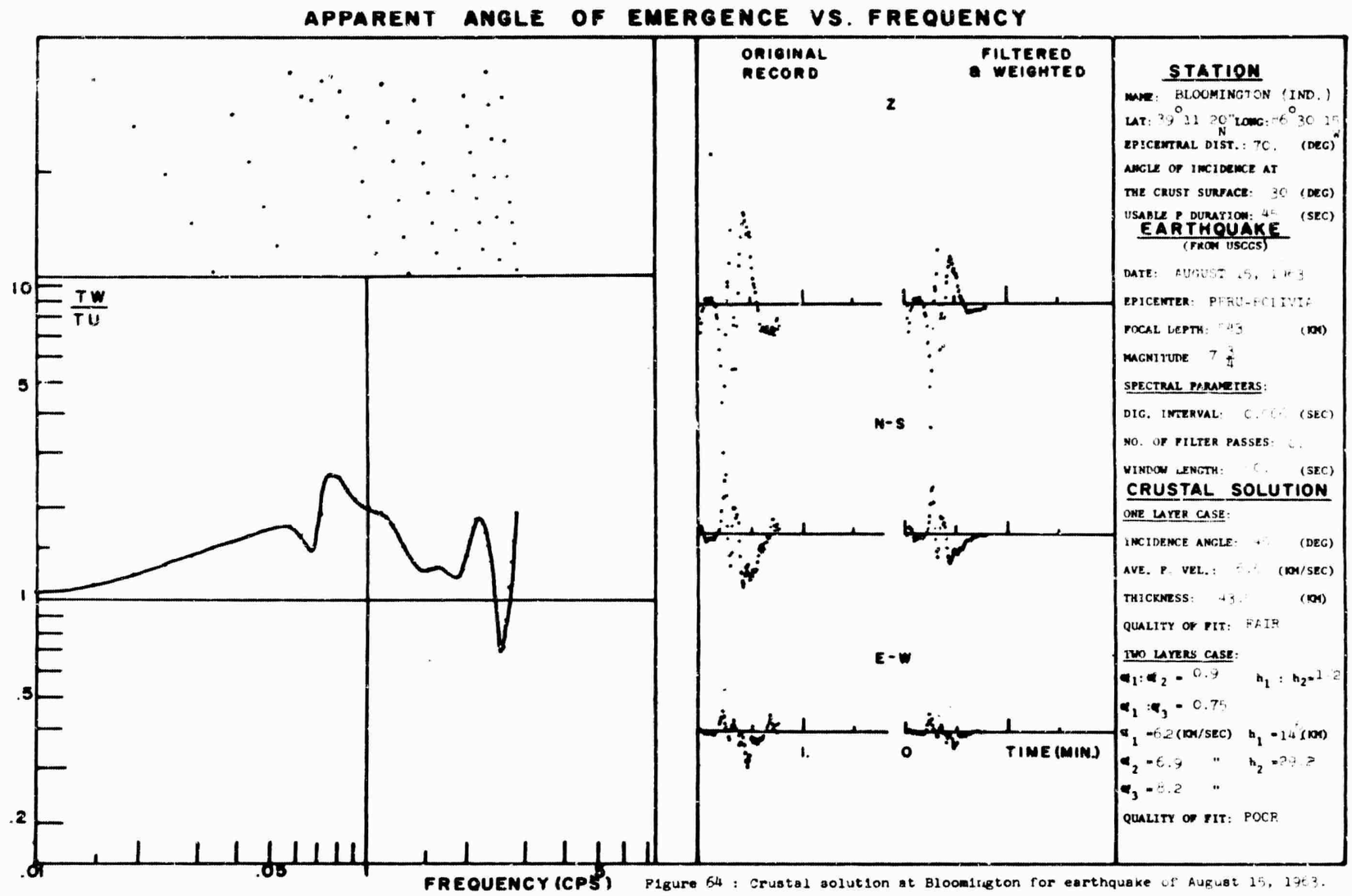

Figure 64 : Crustal solution at Bloomington for earthquake of August 15, 1963.

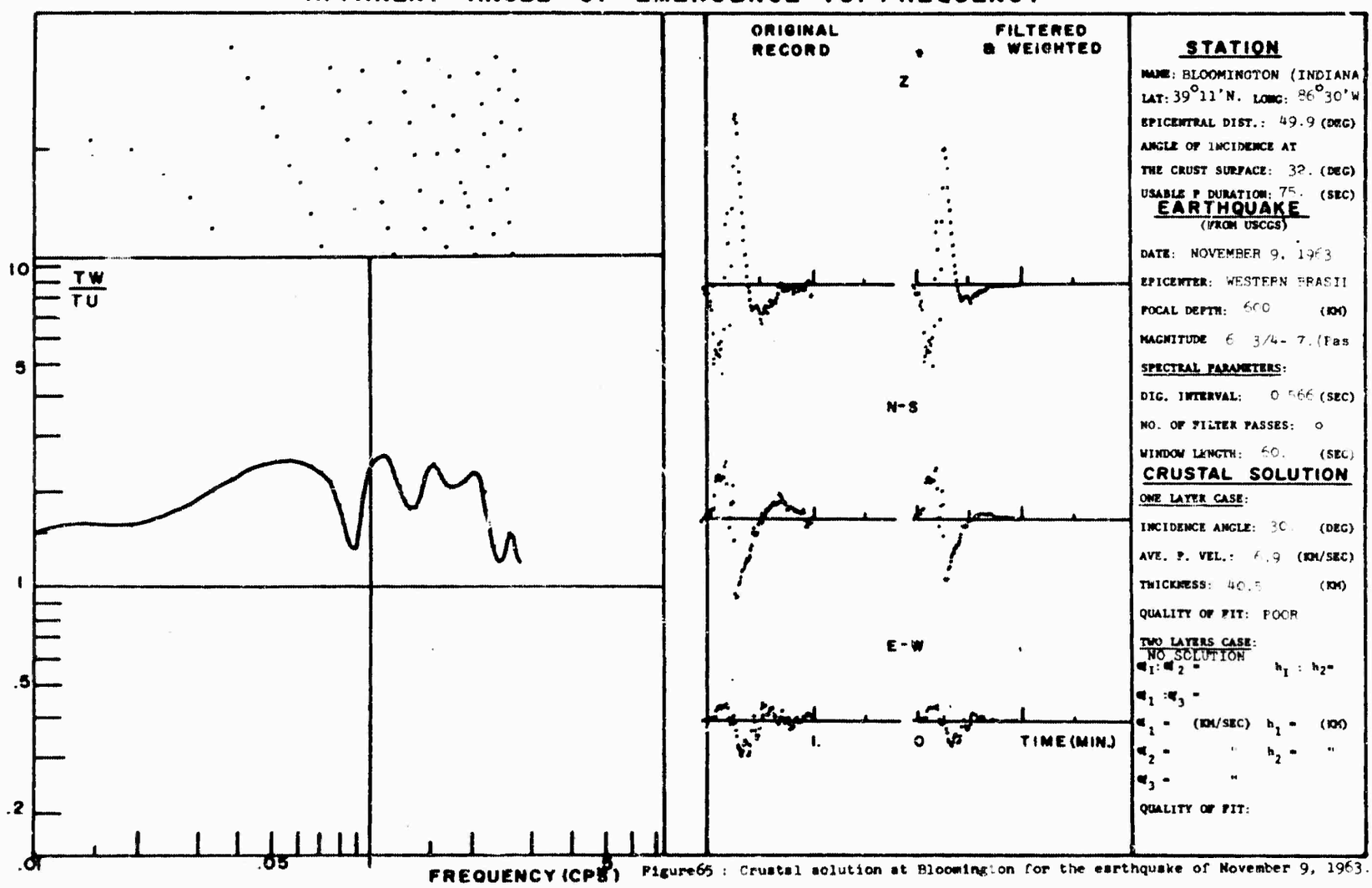

Figure65 : Crustal solution at Bloomington for the earthquake of November 9, 1963.

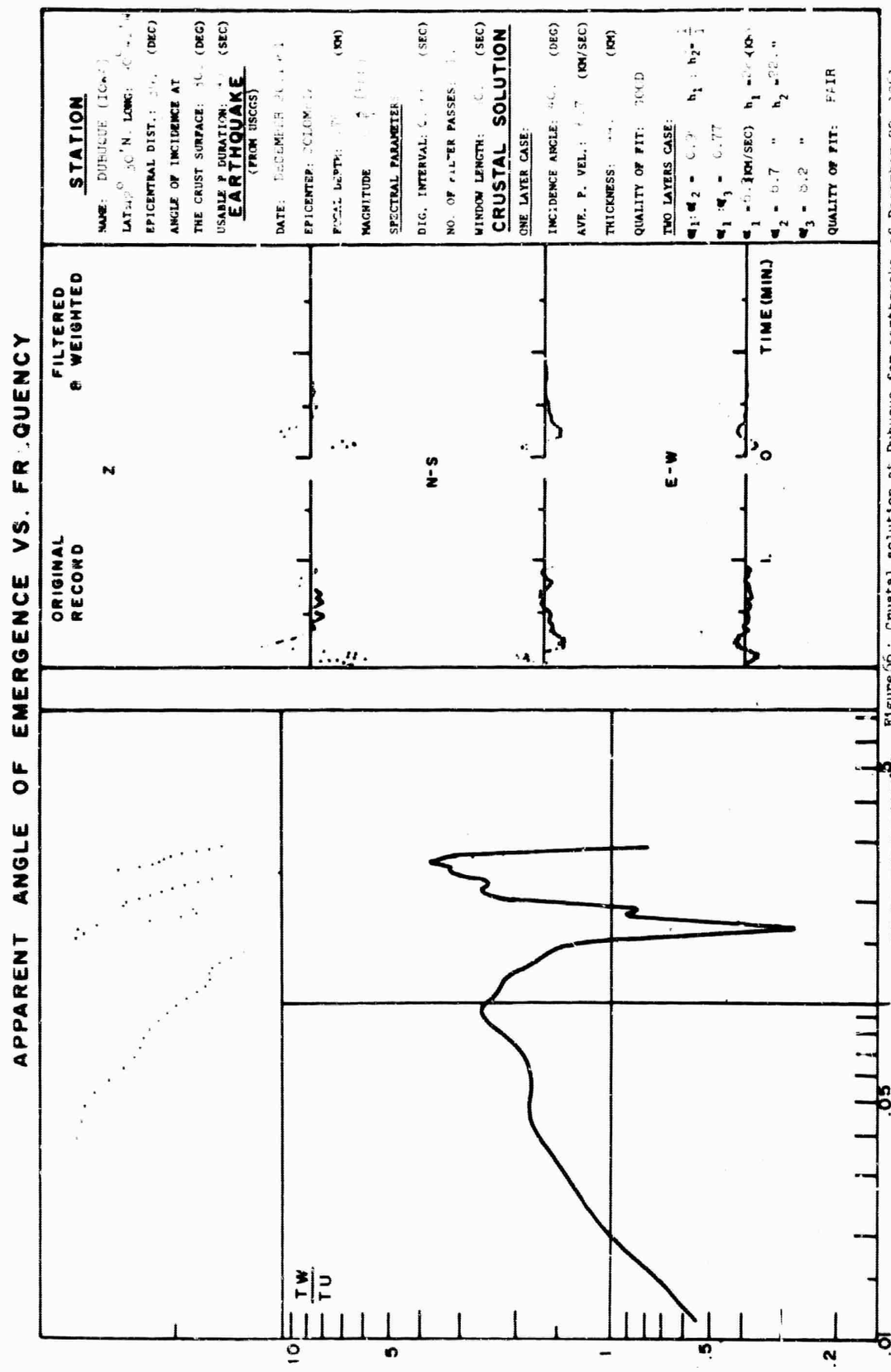

Figure 56 : Crustal solution at Dubuque for earthquake of December 20, 1961.

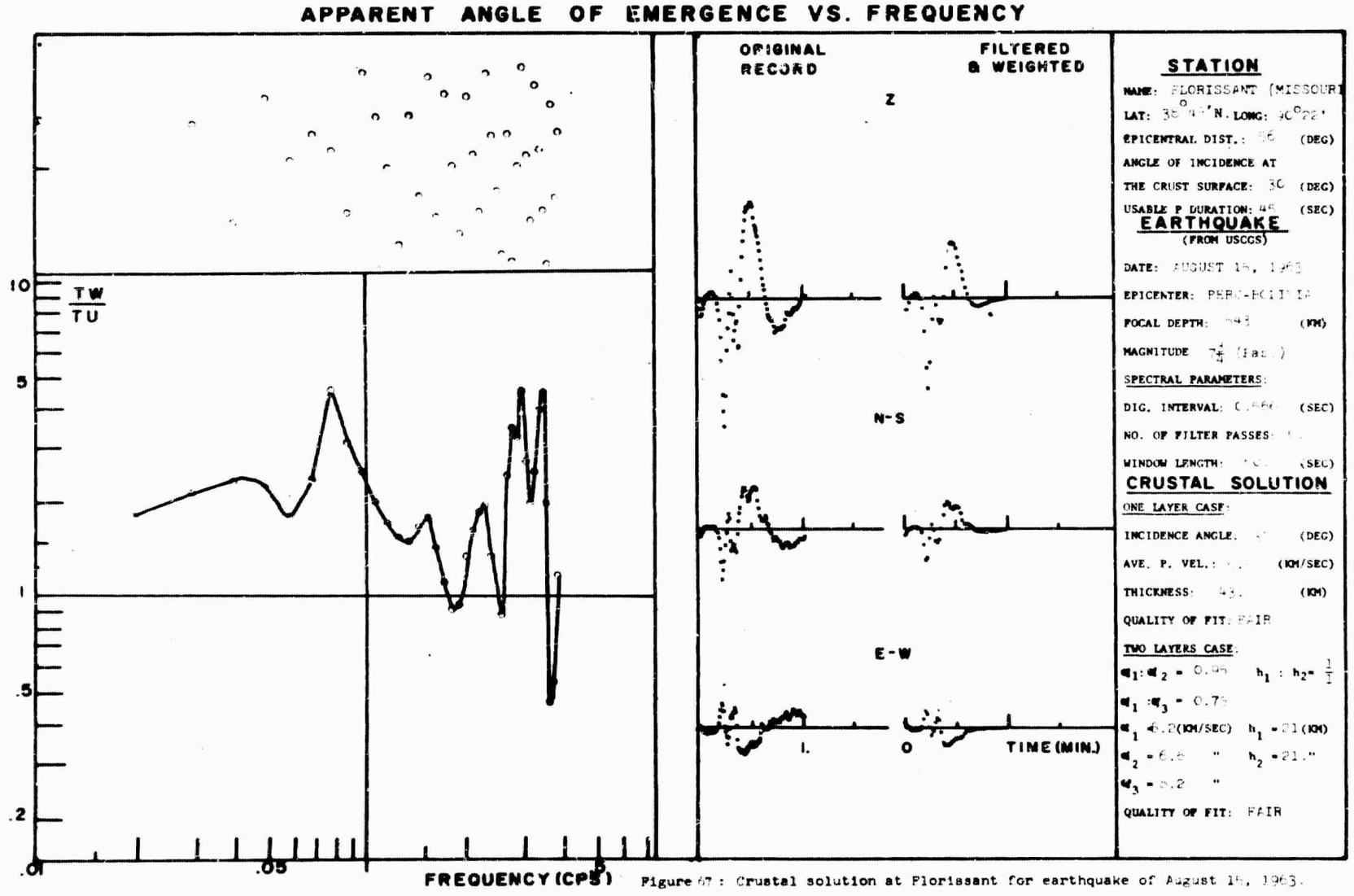

Figure 67 : Crustal solution at Florissant for earthquake of August 15, 1963.

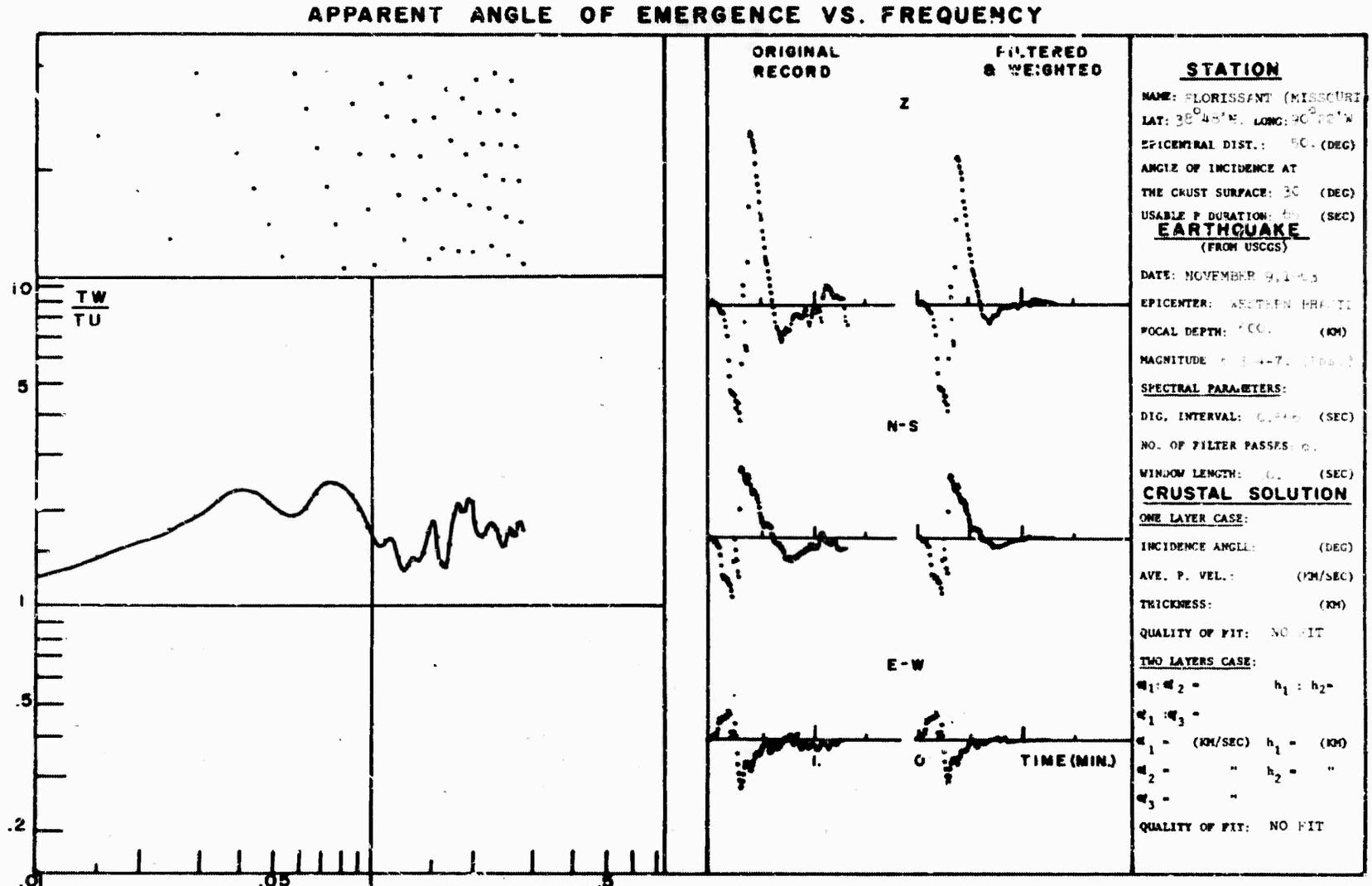

Figure 68: Crustal solution at Florissant for earthquake of November 9, 1965.

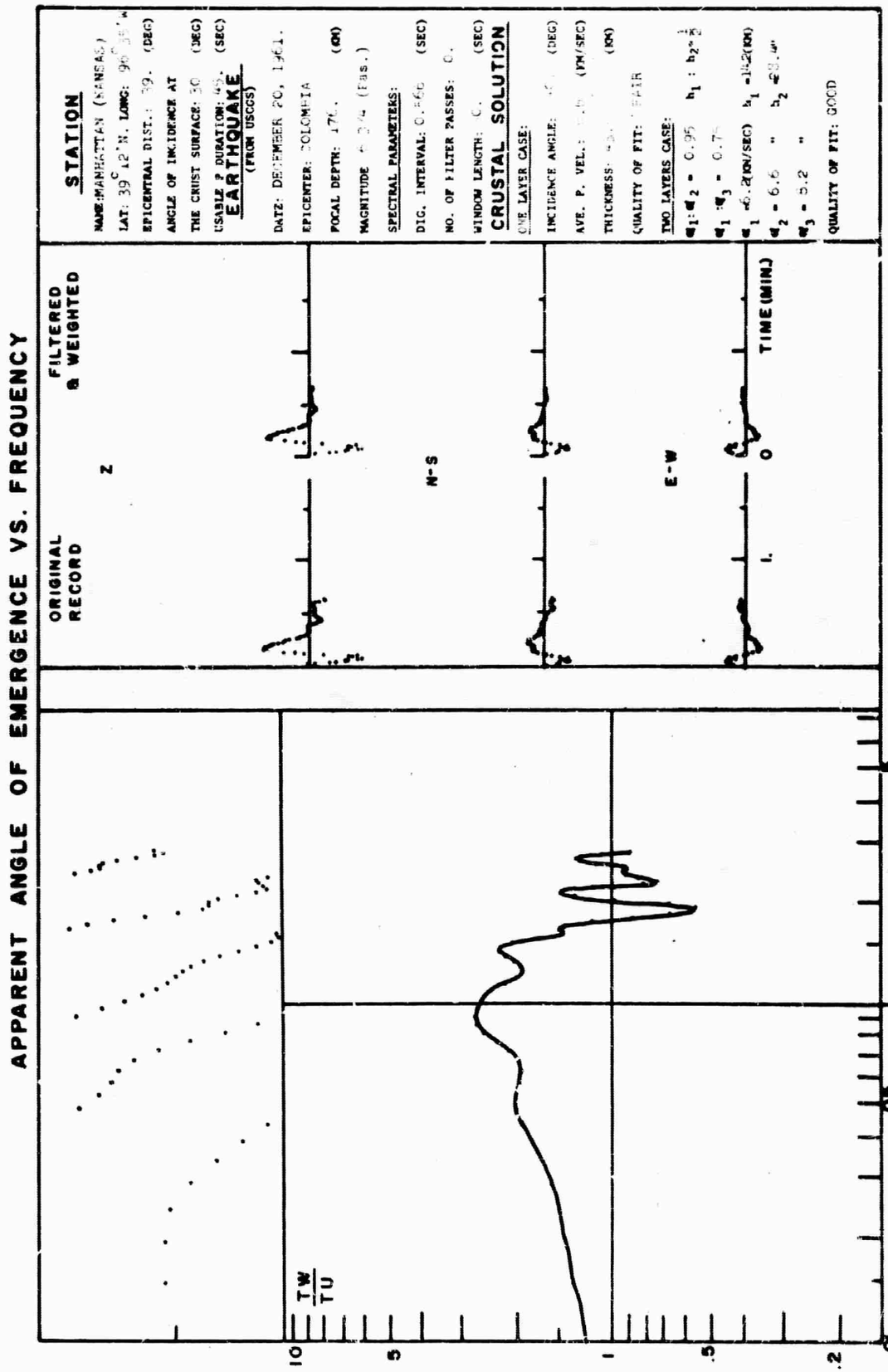

Figure 69: Crustal solution at Manhattan for earthquake of December 20, 1961

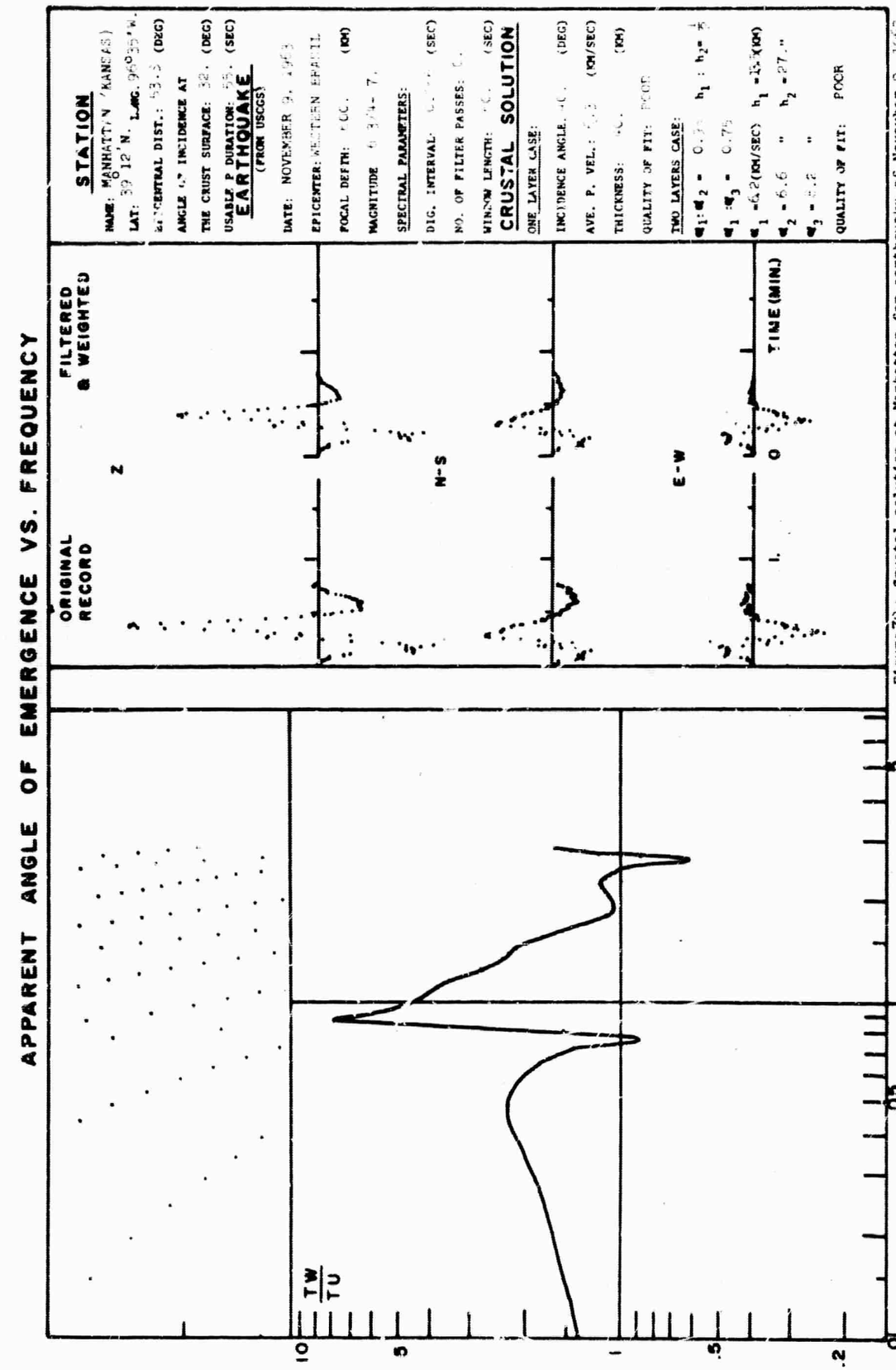

Figure 70 : Crustal solution at Manhattan for earthquake of November 9, 1963.

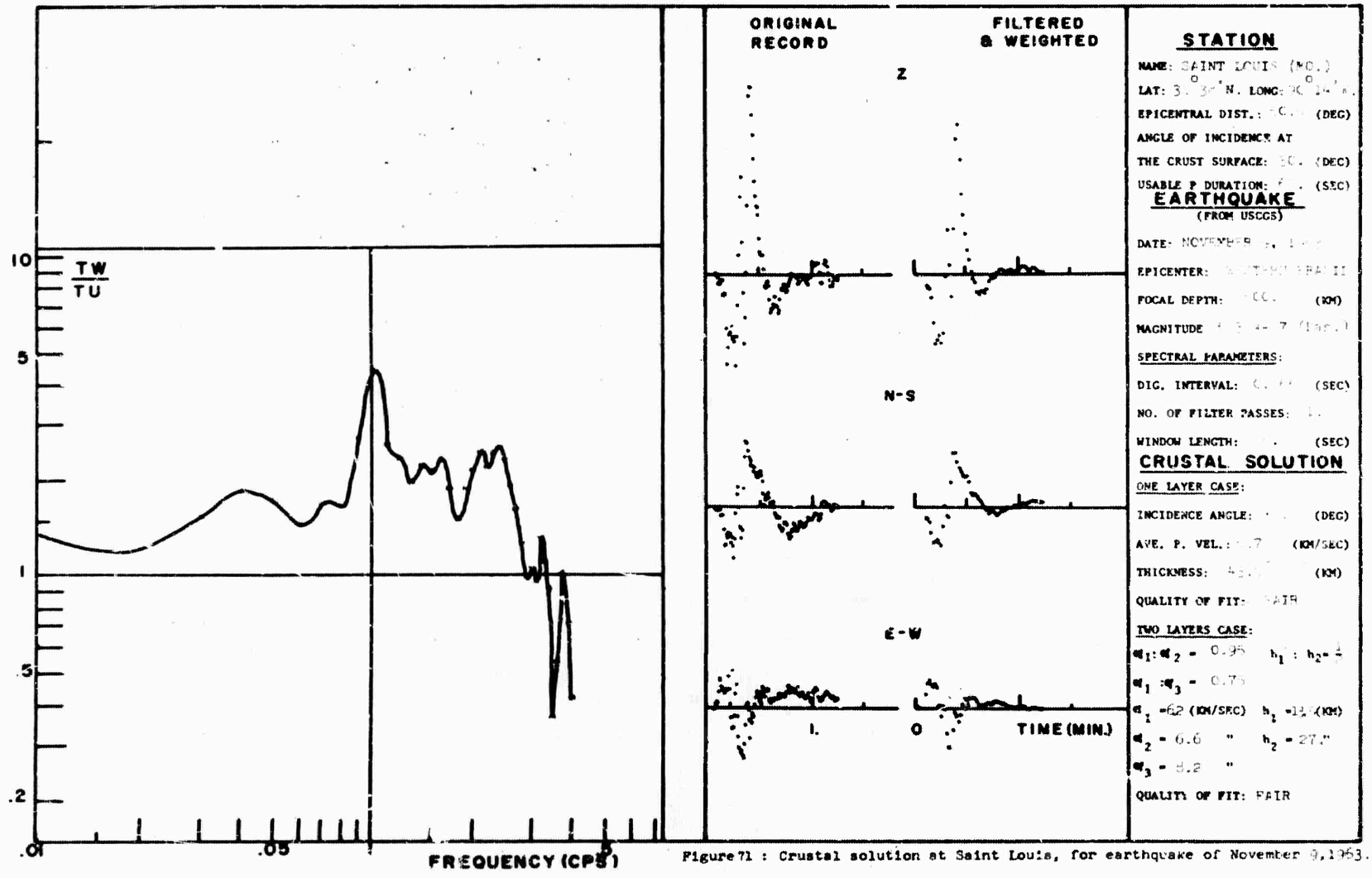

Figure 71 : Crustal solution at Saint Louis, for earthquake of November 9, 1963.

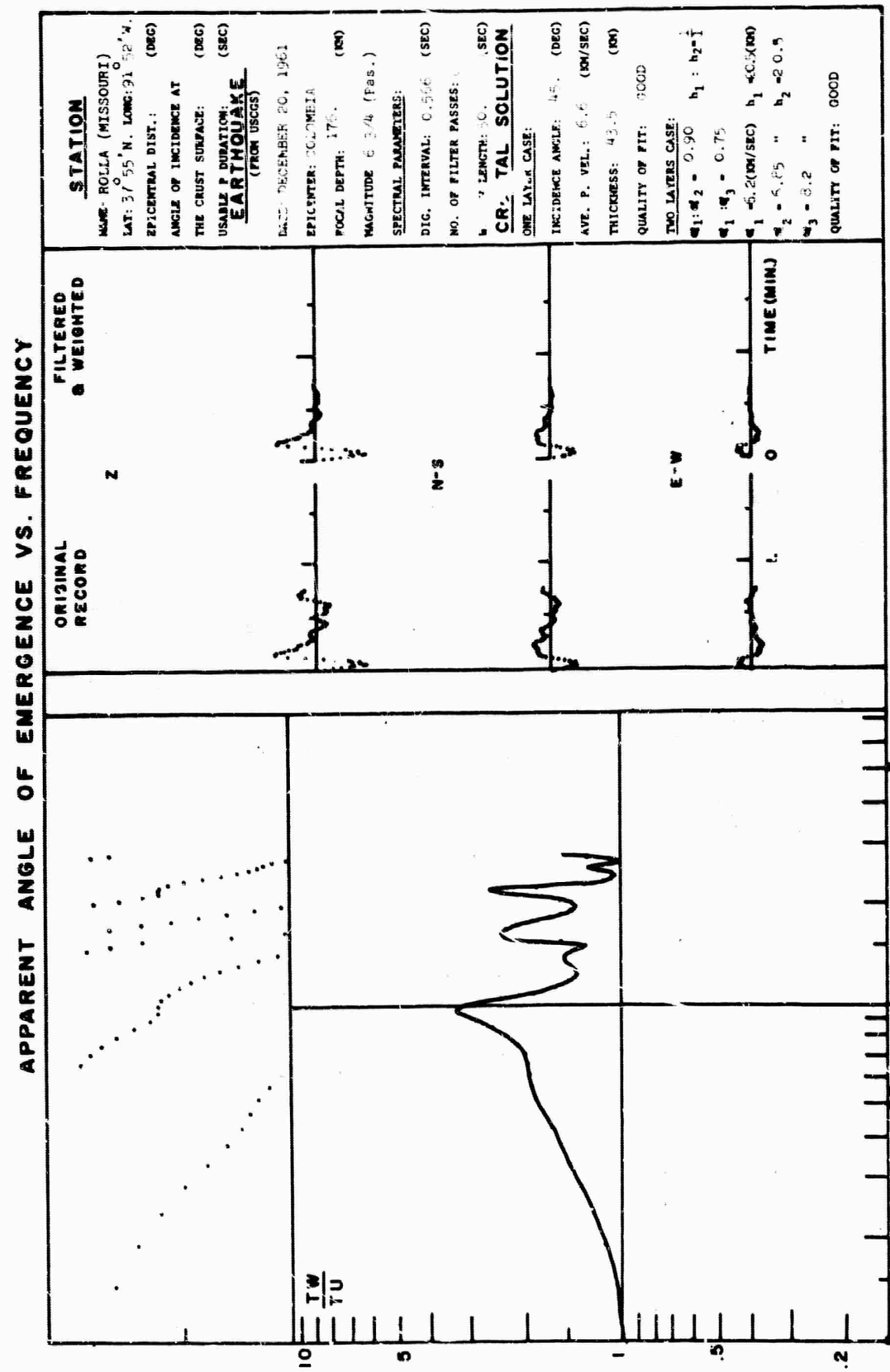

Figure 72 : Crustal solution at Rolla for earthquake of December 20, 1961.

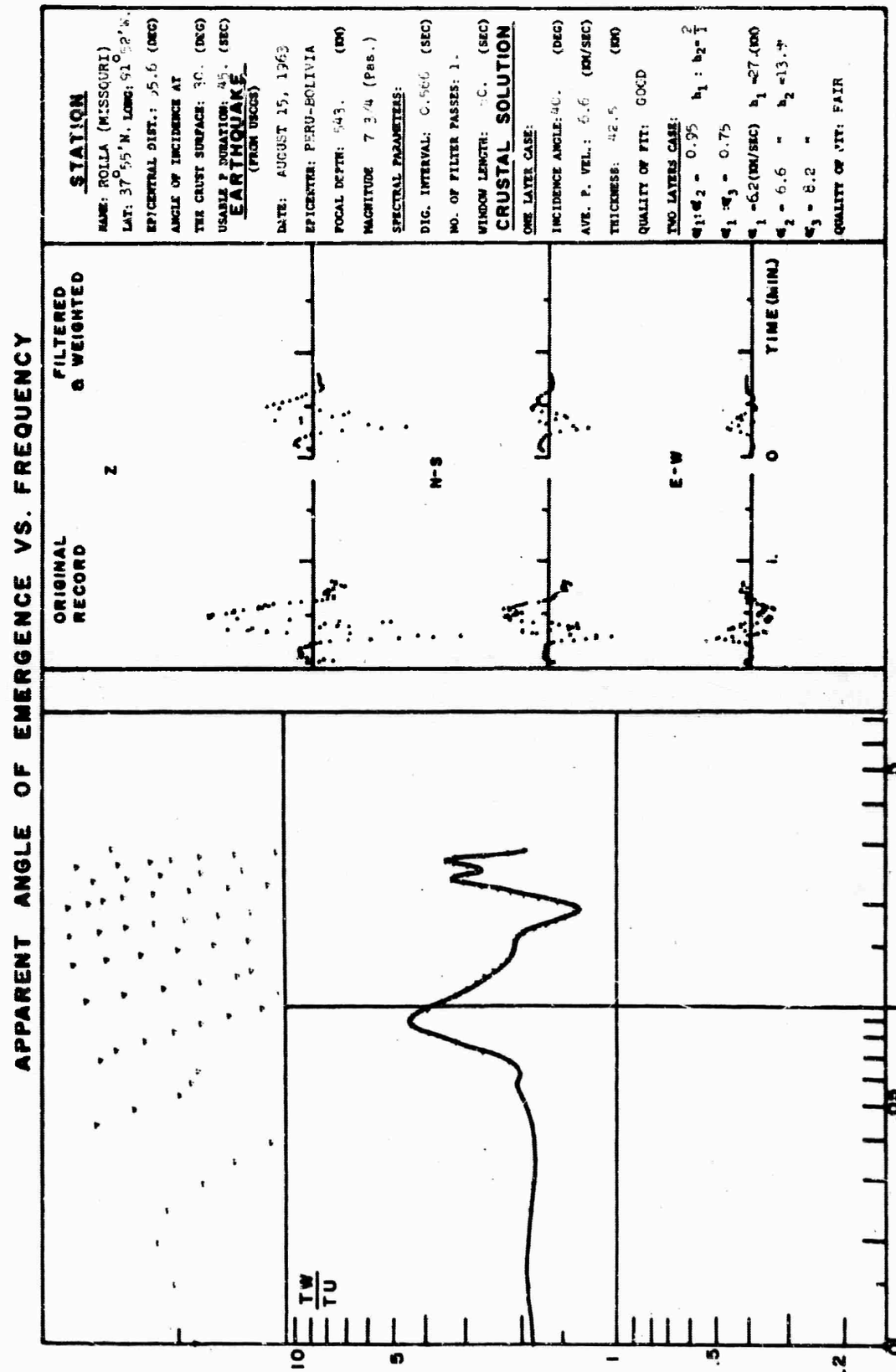

Figure 73 : Crustal solution at Rolla for earthquake of August 15,1963.

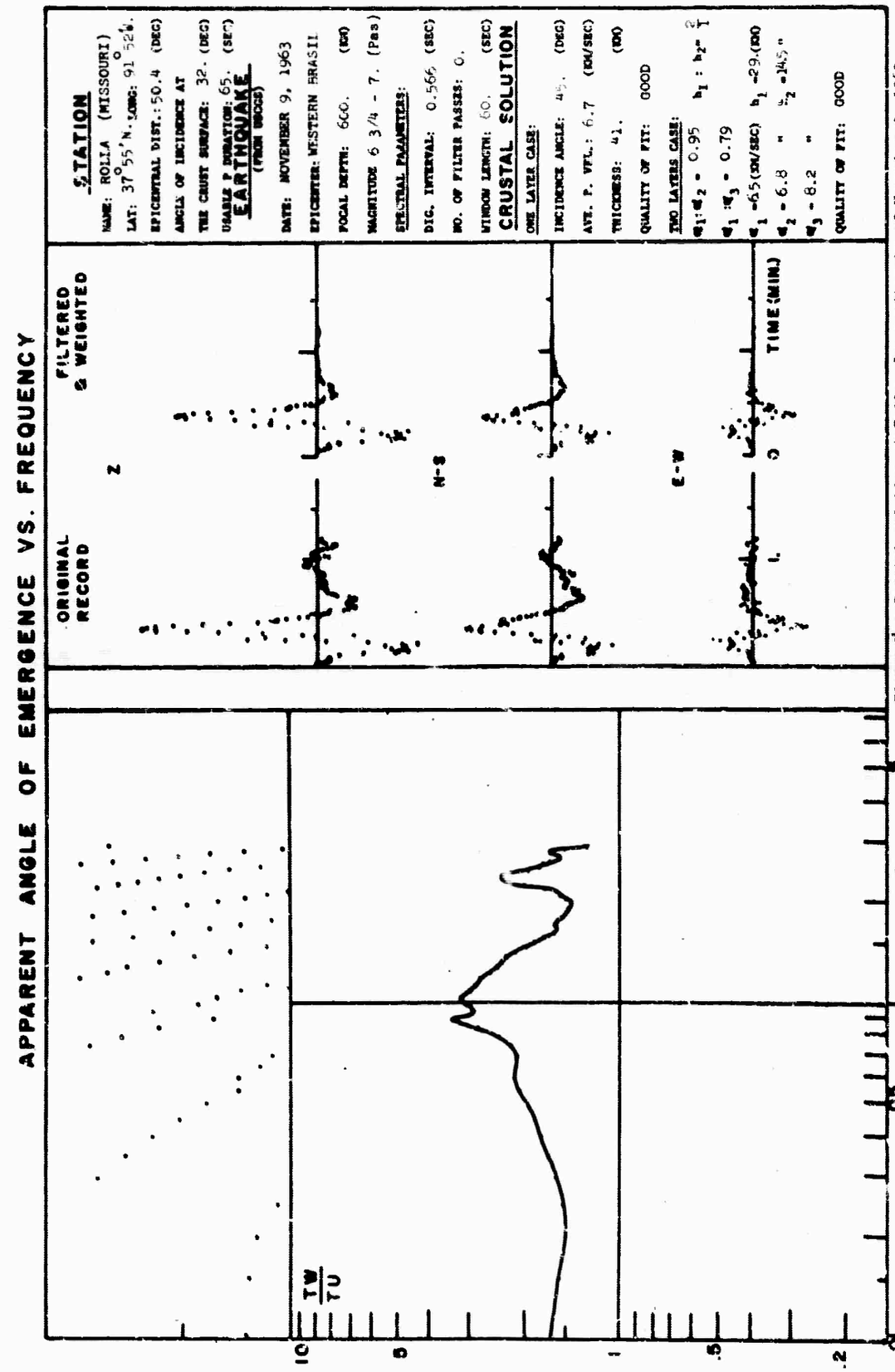

Figure 74: Crustal solution at Rolla, for earthquake of November 9, 1963.

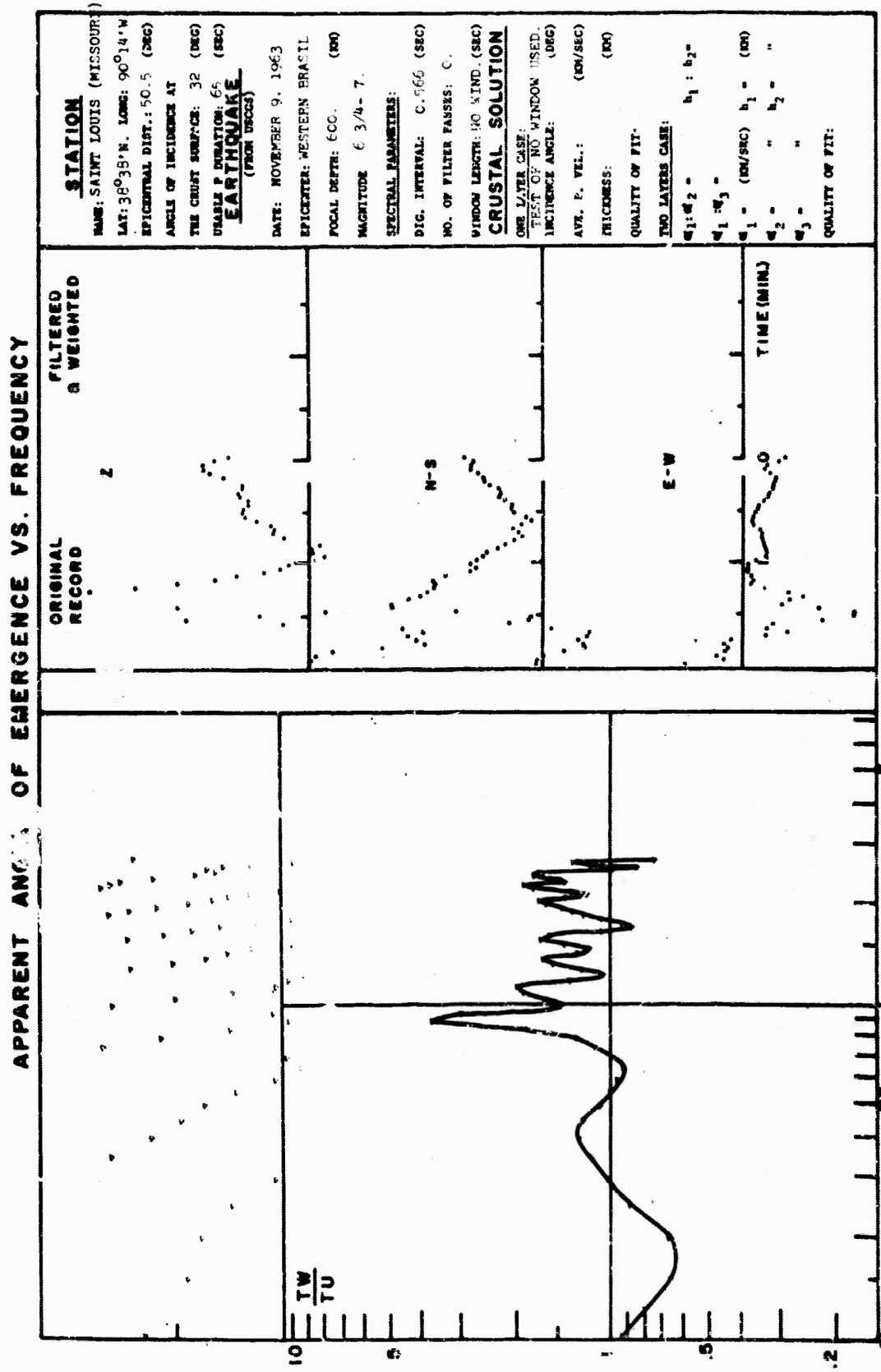

Figure 75 : Effects of no taing data window for the spectrum of the earthquake of November 9, 1963 , a Saint Louis station.

Table 2: CRUSTAL SOLUTIONS AT THE SAINT LOUIS UNIVERSITY STATIONS

SITE	EARTHQUAKE Date	ONE LAYER MODEL SOLUTION i_1 (Deg)	α_1 (km/sec)	h_1 (Km.)	Quality of fit	TWO LAYER MODEL SOLUTION i_1 (Deg)	α_1 (Km/sec)	α_2	h_1	h_2 (Km.)	Total h
Bloom.	Aug.15,1963	45	6.6	43.5	Fair	40	6.2	6.9	14.6	29.2	43.8
"	Nov. 9, "	30	6.9	41.0	Poor	No solution					
Dubuq.	Dec.20,1961	40	6.7	44.0	Good	40	6.3	6.7	22.0	22.0	44.0
Flori.	Aug.15,1963	35	6.5	43.0	Fair	35	6.2	6.6	21.0	21.0	42.0
"	Nov. 9,1963	No solution				No solution					
Manhat.	Dec.20,1961	40	6.6	43.5	Fair	35	6.2	6.5	14.2	28.4	42.6
"	Aug.15,1963	40	6.5	41.5	Fair	40	6.2	6.6	13.5	27.0	40.5
"	Nov. 9,1963	40	6.3	40.0	Poor	40	6.2	6.6	13.5	27.0	40.5
Rolla	Dec.20,1961	45	6.6	43.5	Good	40	6.2	6.8	20.5	20.5	41.0
"	Aug.15,1963	40	6.6	42.5	Good	40	6.2	6.6	27.0	13.5	40.5
"	Nov. 9,1963	45	6.7	41.0	Good	40	6.4	6.8	29.0	14.5	43.5
St.L.	Nov. 9,1963	35	6.7	43.5	Fair	35	6.2	6.6	13.5	27.0	40.5

The interpretation of the observed curves given in Table 2 gives very consistent values for the one-layer models. Considering the area covered by the stations as a unit, an average P velocity in the crust of 6.6 Km/sec is obtained. The average thickness of the crust is 42 Km.

The above results are in good agreement with values of the crust obtained by previous investigators using different techniques. A summary of these studies is presented by McEvilly (1964) and is reproduced here:

SUMMMARY OF CRUSTAL STUDIES IN THE CENTRAL U.S.

Reference	Observations	Pg	Pn	Crustal Thickness
Walter (1940)	Earthquakes near St. Louis	6.03	7.73	39
Stechschulte & Birkenhauer (1948)	Ohio earthquakes	--	8.25	--
Lehman (1955)	N.E.U.S. & Oklahoma earthquakes	--	8.16	--
Nuttli (1956)	Tennessee earthquake	6.1	8.19	--
Steinhart & Meyer (1961)	Ark.-Mo. Refraction profile	5.18	8.16	41
Stauder & Bollinger (1963)	S.E. Missouri Earthquake	6.41	8.20	--
McCamy & Meyer (1963)	Mo.-Ark. Refraction profile	6.2	8.1	45-50
McEvilly & Stauder (1963)	Body and Rayleigh waves from strip-mine explosions, Ill.	6.1	--	--
Stewart & McEvilly	USGS Mo. Refraction data--preliminary interpretation	6.1	8.15	36-40

McEvilly, using phase and group velocities of surface waves, obtains a model of 38 Km thickness and an average P velocity of 6.5 Km/sec.

The interpretation of the observed curves in terms of two layer crustal models is subject to more ambiguities and different models may be selected to match the observations. This, of course, indicates that the interpretation given in Table 2 for the two-layer case is not unique. Nevertheless all the different interpretations give a very constant value for the total thickness of the crust. The average value of this thickness for the Central United States using the two-layer models is 42 Km.

It is expected that the use of short-period records and master curves corresponding to the 0.1 and 1.0 cps frequency band will provide more detailed information on the layering of the crust and a better interpretation of observational data in terms of two or more layer models.

7. Summary and Conclusions

1) The use of the dimensionless parameter δ allows the systematization of the effects of layered systems on longitudinal seismic waves into families of transfer function curves.
2) The periodicity of the transfer function curves is determined by the relative time lags of the arrivals at the surface of the reflections and refractions within the layered system.
3) The amplitude of the transfer function curves is determined by the contrasts of the P wave velocities at the interfaces of the layered system.
4) A set of normalized master curves of the transfer functions for one- and two-layer models and for several angles of incidence has been prepared.
5) The use of deep and intermediate depth earthquakes at convenient epicentral distance allows the calculation of the spectrum of the apparent angle of emergence independently of the conditions at the source. This spectrum depends only on the structure immediately below the receiving station.
6) In most of the cases the matching of master curves and observations allows the calculation of the thickness and average P velocity of the crust with less than $\pm$ 5% incertitude.

7) Estimation of different layers within the crust from the spectrum of long-period records is neither precise nor unique. It is suspected that spectra of short-period records will give more detailed information of the structure within the crust.

8) Application of the method to the region of central United States occupied by the Saint Louis University network of seismic stations gave an average crustal thickness of 42 Km and average crustal velocity of P waves of 6.6 Km/sec.

9) The use of the dimensionless parameter γ should facilitate the calculation of the first partial derivatives of the transfer functions with respect to the parameters of the layers. Depending on the behavior of these partial derivatives the inversion problem for the spectrum of P body waves may be attempted. This inversion problem should find the best fit, in a least squares sense, between observations and theoretical curves.

List of References

Anderson, Don L.
1964 "Universal Dispersion Tables. 1. Love Waves Across Oceans and Continents on a Spherical Earth," Bull. Seis. Soc. Am., 54, 681-762.

Ben-Menahem, Ari, Stewart Smith and Ta Liang Teng
1965 "A Procedure for Source Studies from Spectrum of Long-Period Seismic Body Waves," Bull. Seis. Soc. Am., 55, 203-235.

Birch, Francis
1964 "Density and Composition of Mantle and Core," J. Geophys. Res., 69, 4377-4388.

Blackman, R. B., and J. W. Tukey
1[illegible] The Measurement of Power Spectra. Dover, New York 190 p.

Brune, J., and J. Dorman
1963 "Seismic Waves and Earth Structure in the Canadian Shield," Bull. Seis. Soc. Am., 53, 167-210.

Costain, John [illegible]., Kenneth L. Cook and S. T. Algermissen.
1963 "Amplitude, Energy and Phase Angles of Plane SV Waves and Their Applications to Earth Crustal Studies," Bull. Seis. Soc. Am., 53, 1039-1074.

Dorman, J.
1962 "Period Equation for Waves of Rayleigh Type on a Layered Liquid- Solid Half- Space," Bull. Seis. Soc. Am., 52, 389-397.

Dorman, J., and M. Ewing
1962 "Numerical Inversion of Surface Wave Dispersion Data and Crust-Mantle Structure in the New York-Pennsylvania Area," J. Geophys. Res., 67, 5227-5241.

Dunkin, J.W.
1965 "Computation of Modal Solutions in Layered, Elastic Media at High Frequencies," Bull. Seis. Soc. Am., 55, 335-358.

Fernandez, S.J.
1963 "Variations in Amplitude of Short-Period P Waves," The Geotechnical Corporation Technical Report No. 63-106 for Contract AF 49(638)-1150.

Fuchs, Karl
1965 "The Transfer Function for P-Waves for a System Consisting of a Point Source in a Layered Medium," Saint Louis University Technical Report for Contract AF 19(604)-7399.

Gutenberg, B.
1934 "Periods of the Ground in Southern California Earthquakes," Earthquake Investigations in California: 1934-1935, U.S. Coast and Geodetic Survey, Spec. Publ. 201, 163-225.

1957 "Effects of Ground on Earth's Motion," Bull. Seis. Soc. Am., 47, 221-249.

Gutenberg, B. and C. F. Richter
1936 "Deep Focus Travel Time Curves. Material for the Study of Deep Focus Earthquakes," Bull. Seis. Soc. Am., 26, 341-390.

1946 "Earthquake Magnitude, Intensity, Energy and Acceleration," Bull. Seis. Soc. Am., 46, 105-143.

Halperin, E.I.
1962 "On the Change in the Direction of the Displacement of the Particle during the Passage of Seismic Waves through a Zone of Low Velocities," Izvest. Akad. Nauk, SSSR, Ser. Geofiz., 5, 585-594.

Hamming, Richard W.
1962 Numerical Methods for Scientists and Engineers, McGraw-Hill Book Co., New York, 411 p.

Hannon, Willard J.
1964a "Some Effects of a Layered System on Dilatational Waves," Saint Louis University, Technical Report 3, for Contract AF 19(604)-7399.

1964b "An Application of the Haskell-Thomson Matrix Method to the Synthesis of the Surface Motion Due to Dilatational Waves," Bull. Seis. Soc. Am., 54, 2067-2083.

Harkrider, David
1964 "Surface Waves in a Multilayered Elastic Media I. Rayleigh and Love Waves from Buried Sources in a Multilayered Elastic Half-Space." Bull. Seis. Soc. Am., 54, 627-680.

Haskell, N. A.
1953 "The Dispersion of Surface Waves on a Multilayered Media," Bull. Seis. Soc. Am., 43, 17-34.

1962 "Crustal Reflections of Plane P and SV Waves," J. Geophys. Res., 67, 4751-4767.

Hirasawa, Tomowo, and W. Stauder, S.J.
1964 "Spectral Analysis of Body Waves from the Earthquake of February 18, 1956," Bull. Seis. Soc. Am., 54, 2017-2055.

Imamura, A.
1929 "On the Earth-vibrations Induced in Some Localities at the Arrival of Seismic Waves," Bull. Earthq. Res. Inst. (Tokyo) 7, 489-494.

Inouye, Win
1934 "Comparison of EarthShakings above Ground and Underground," Bull. Earthq. Res. Inst. (Tokyo), 12, 712-741.

Ishimoto, Mishio
1931a "Un seismographe accélérometrique et ses enregistrements," Bull. Earthq. Res. Inst. (Tokyo), 9, 316-332.

1931b "Caractéristiques des ondes séismiques," Bull. Earthq. Res. Inst. (Tokyo), 9, 473-484.

1932 "Comparisson accelerometrique des secousses sismiques dans deus parties de la ville de Tokyo," Bull. Earthq. Res. Inst. (Tokyo), 10, 171-187.

1934 "Observations accélérometriques des secousses sismiques dans les villes de Tôkyô et Yokohama," Bull. Earthq. Res. Inst. (Tokyo), 12, 234-248.

Ivanova, T. C.
1959 "Experimental Data on the Influence of a Layer in the Upper Part of a Cross-Section on the Angles of Emergence of Waves of Various Frequencies," Trans. (Trudy) Inst. Physics of the Earth, Akad. Nauk, SSSR, No. 6, (173).

Ivanova, T.C.
1960 "On the Application of Seismic Frequency Sounding for the Investigation of the Upper Part of a Cross Section," Izvest., Akad. Nauk, SSSR, Ser. Geofiz., 2, 223-228.

Jeffreys, H., and K. E. Bullen
1958 Seismological Tables, British Assoc. for the Advancement of Science, London, 50 P.

Kanai, K.
1952 "Relation between the Nature of Surface Layer and the Amplitudes of Earthquake Motions," Bull. Earthq. Res. Inst. (Tokyo), 30, 30-39.

1953a "Relation between the Nature of Surface Layer and the Amplitudes of Earthquake Motions, Part II," Bull. Earthq. Res. Inst. (Tokyo) 31, 219-226.

1953b "Relation between the Nature of Surface Layer and the Amplitudes of Earthquake Motions, Part III," Bull. Earthq. Res. Inst. (Tokyo) 31, 275-279.

Kanai, K., T. Tanaka and T. Suzuki
1953 "Relation between the Earthquake Damage and the Nature of the Ground," Bull. Earthq. Res. Inst. (Tokyo), 31, 57-61.

Kanai, K., and S. Yoshizawa
1956 "Relation between the Amplitude of Earthquake Motions and the Nature of the Surface Layer, Part IV," Bull. Earthq. Res. Inst. (Tokyo), 34, 167-183.

Kasahara, K.
1960 "The Nature of Seismic Origins as Inferred from Seismological and Geodetic Observations," Bull. Earthq. Res. Inst. (Tokyo), 35, 473-532.

Malinovskaya, L.N.
1959 "On the Calculation of the Theoretical Seismograms Due to Interference of Oscillations," in Symposium: "Problems of the Dynamic Theory of Seismic-Wave Propagation," No. 3, Gostoptekhizdat, Leningrad University, Leningrad.

McCamy, K., R. Meyer and T. J. Smith
1962 "General Applicable Solutions of Zoeppritz' Amplitude Equations," Bull. Seis. Soc. Am., 52, 923-955.

Matumoto, T.
1953 "Transmission and Reflection of Seismic Waves through a Multilayered Elastic Medium," Bull. Earthq. Res. Inst. (Tokyo), 31, 261-273.

1960 "On the Spectral Structure of Earthquake Waves," Bull. Earthq. Res. Inst. (Tokyo), 38, 13-27.

McEvilly, T.V.
1964 "Central U.S. Crust-Upper Mantle Structure from Love and Rayleigh Wave Phase Velocity Inversion," Bull. Seis. Soc. Am., 54, 1997-2015.

Nasu, Nobuji
1931 "Comparative Studies of Earthquake Motions Above-Ground and in a Tunnel, Part I," Bull. Earthq. Res. Inst. (Tokyo), 9, 454-472.

Neumann, Frank
1954 Earthquake Intensity and Related Ground Motion. University of Washington Press, Seattle, 77p.

Nuttli, O.
1964a "Some Observations Relating to the Effect of the Crust on Long-Period P-Wave Motion," Bull. Seis. Soc. Am., 54, 141-149.

1964b "The Determination of S-Wave Polarization Angles for an Earth Model with Crustal Layering," Bull. Seis. Soc. Am., 54, 429-1440.

Nuttli, O. and T. V. McEvilly
1961 "The Response Characteristics of the Long-Period Seismographs of the Saint Louis University Network," Earthquake Notes, 32, 27-36.

Nuttli, O., and J. D. Whitmore
1961 "An Observational Determination of the Variation of the Angle of Incidence of P Waves with Epicentral Distance," Bull. Seis. Soc. Am., 51, 269-276.

Phinney, R.A.
1964 "Structure of the Earth's Crust from Spectral Behavior of Long-Period Body Waves," J. Geophys, Res., 69, 2997-3017.

1965 "Theoretical Calculation of the Spectrum of First Arrivals in Layered Elastic Media," Princeton University, Technical Report for AFOSR Contract No. AF 49(638)-1243.

Pod'Yapol'ski, G. S.
1961 "Refraction and Reflection Indices for an Elastic Wave at a Layer," Izvest., Akad. Nauk SSSR Ser. Geofiz., 520-533.

Savarensky, E.E.
1952 "On the Angles of Emergence of Seismic Radiation and Several Related Questions," Trans. (Trudy) Geophys. Inst., Akad. Nauk, SSSR. No. 15 (142).

Steinhart, J.S., and R. P. Meyer
1959 Explosion Studies of Continental Structure, Carnegie Institution of Washington, Publication 622, Washington, D.C., 409 p.

Sezawa, K.
1930 "Possibility of the Free Oscillations of the Surface Layer Excited by the Seismic Waves," Bull. Earthq. Res. Inst. (Tokyo), 8, 1-11.

Sezawa, K., and K. Kanai
1932a "Possibility of Free Oscillations of Strata Excited by Seismic Waves, III," Bull. Earthq. Res. Inst. (Tokyo), 10, 1-18.

1932b "Possibility of Free Oscillations of Strata Excited by Seismic Waves, IV," Bull. Earthq. Res. Inst. 10, 273-298.

1932c "Reflection and Refraction of Seismic Waves in a Stratified Body, I. Bull. Earthq. Res. Inst. (Tokyo), 10, 805-816.

1934 "Reflection and Refraction of Seismic Waves in a Stratified Body, II, Bull. Earthq. Res. Inst. (Tokyo), 12, 269-276.

1937 "On the Free Vibrations of a Surface Layer Due to An Obliquely Incident Disturbance," Bull. Earthq. Res. Inst., (Tokyo), 15, 375-383.

Suzuki, T.
1932 "On the Angle of Incidence of the Initial Motion Observed at Hongo and Mitaka," Bull. Earthq. Res. Inst. (Tokyo), 10, 517-530.

Takahasi, R., and K. Hirano
1941 "Seismic Vibration of Soft Ground," Bull. Earthq. Res. Inst. (Tokyo), 19, 534.

Thomson, W. T.
1950 "Transmission of Elastic Waves through a Stratified Solid Medium," J. Appl. Phys., 21, 89-93.

Willmore, P.L.
1959 "The Application of the Maxwell Impedance Bridge to the Calibration of Electromagnetic Seismographs," Bull. Seis. Soc. Am., 49, 53-80.

Zoeppritz, K.
1919 "Uper Erdbebenwellen VII b," Gottingen Nachrichten; 66-84.

APPENDIX I

```
**    FERNANDEZ                    GPH18    TRANSFE
C     THIS PROGRAM IS DESIGNED TO CALCULATE THE TRANSFER
C     FUNCTIONS OF A LAYERED SYSTEM FOR THE VERTICAL AND
C     HORIZONTAL COMPONENTS OF DILATATIONAL WAVES AND
C     THEIR RATIO. THIS RATIO IS THE TANGENT OF THE
C     APPARENT ANGLE OF EMERGENCE.
C     THE TRANSFER FUNCTIONS MAY BE CALCULATED IN TERMS
C     OF FREQUENCY OR IN TERMS OF A DIMENSIONLESS
C     PARAMETER GAMMA.
C     THE PROGRAM WILL PLOT ALSO THE MODULUS AND THE PHASE
C     OF THE TRANSFER FUNCTIONS IN ORDINARY OR LOGARITHMIC
C     SCALE. THE VALUES OF THE TRANSFER FUNCTIONS OF THE
C     PLOT ARE NORMALIZED TAKING AS UNITY THE CORRESPONDING
C     COMPONENT OF MOTION AT THE BOTTOM OF THE LAYER SYSTEM.
C     THE APPARENT SURFACE VELOCITY MUST BE GREATER THAN
C     THE P VELOCITY IN THE TOP LAYER AND THE S VELOCITY
C     IN ANY LAYER.
C     THE ANGLE OF INCIDENCE  OF THE INPUT CORRESPONDS TO
C     THE ANGLE OF THE RAY AT THE SURFACE.

      DIMENSION D(50),A(50),B(50),RHO(50),DGAM(50)
     1,DGAM1(50),DRA(50),DRB(50),DH(50),FLAND(50)
      SIGNF(VAR)=ABSF(VAR)/VAR
C     READ THE SCALE FACTORS AND CONSTANTS FOR THE PLOT OF
C     THE FUNCTIONS.
      READ 192,XS,YS,YPS,X02
      READ 192,Y01,Y02,Y03,Y04
192   FORMAT(4F10.0)
1030  PUNCH 1
1     FORMAT(1X,18HTRANSFER FUNCTIONS)
C     UNDER STUDY
C     READ THE IDENTIFICATION OF THE CRUSTAL MODEL
      READ 1101
      PUNCH 1101
1101  FORMAT(1X,20H                    )
C     NOL=NUMBER OF LAYERS+1, AT=1 IF GAMMA DESIRED,PLOTR=1
C     IF PLOT OF RATIO ONLY DESIRED, PLOTO=1 IF PLOT NOT
C     IN LOGARITHMIC SCALE DESIRED
      READ 2,NOL,AT,PLOTR,PLOTO
2     FORMAT(I3,3F3.0)
      PUNCH 2,NOL,AT,PLOTR,PLOTO
      PUNCH 707
707   FORMAT(10HTHICK.(KM),1X,14HP VEL.(KM/SEC),1X,14HS
     1VEL.(KM/SEC),1X,12HDEN.(GM/CMC),1X,5HLANDA,/)
C     READ THE LAYER PARAMETERS. D=THICKNESS, A=P VELOCITY,
C     B=S VELOCITY,RHO= DENSITY
      DO 3 I=1,NOL
      READ 500,D(I),A(I),B(I),RHO(I)
```

```
500   FORMAT(1X,F9.4,3F10.4)
      FLAND(I)=RHO(I)*A(I)*A(I)/3.
3     PUNCH 501,D(I),A(I),B(I),RHO(I),FLAND(I)
501   FORMAT(5F10.4)
      N=NOL
      N1=NOL-1
      N2=NOL-2
C     READ ANGI1=INITIAL ANGLE OF INCIDENCE AT THE SURFACE
C     DANGI= INCREMENT OF THE ANGLE OF INCIDENCE ,
C     NOANG=NUMBER OF ANGLES OF INCIDENCE TO BE CALCULATED
7001  READ 4,ANGI1,DANGI,NOANG
4     FORMAT(2F10.5,I3)
C     GMIN=MINIMUM VALUE OF GAMMA DESIRED, GINC= INCREMENT
C     OF GAMMA,NOF= NUMBER  OF VALUES OF GAMMA DESIRED.
C     IF THE CALCULATIONS ARE IN TERMS OF FREQUENCY ,
C     LET GMIN= MINIMUM FREQUENCY DESIRED, ETC.
      READ 4,GMIN,GINC,NOF
5104  ANGIP=ANGI1-DANGI
831   DO 311 IA=1,NOANG
      GAF=GMIN-GINC
5004  ANGIP=ANGIP+DANGI
      SINI1=SINF(ANGIP/57.29578)
      SININ=A(NOL)*SINI1/A(1)
      C=A(NOL)/SININ
      SINE=(1.-2.*(SININ**2)/3.)
      COSE=SQRTF(1.-SINE**2)
      TANE=SINE/COSE
      EM=ATANF(TANE)*57.29578
      AIM=90.-EM
      PUNCH 742
742   FORMAT(9HAP.VELOC.,2X,10HTAN.EMERG.,14HANG. INC.
     1 BOT.,15HANG. INC. SURF.)
      PUNCH 741,C,TANE,AIM,ANGIP
741   FORMAT(4F12.3)
      DO 1346 M=1,NOL
      COVA=C/A(M)
      COVB=C/B(M)
      DGAM(M)=2./(COVB**2 )
      DGAM1(M)=DGAM(M)-1.
      DRA(M)= SQRTF(ABSF(COVA**2- 1.))
      DRB(M) =SQRTF(ABSF(COVB**2-1.))
1346  DH(M) =RHO(M)*C*C
      TH=0.
      APTH=0.
      PUNCH TAPE 237
237   FORMAT(1H=)
      IF (AT)285,286,286
286   DO 287 L=1,N1
      TH=TH+D(L)/A(L)
287   APTH=APTH+D(L)*(SQRTF(1.-(A(L)*SINI1/A(1))**2)+
     11.732005*SQRTF(1.-(B(L)*SINI1/A(1))**2))/A(L)
285   CONTINUE
```

```
      PUNCH 499
499   FORMAT(10X,28HCONSTANTS OF PROPORTIONALITY,/)
      PUNCH 708
708   FORMAT(5HLAYER,1X,11HTHICK.RATIO,1X,7HP RATIO,1X,
     17HS RATIO,2X,10HDEN. RATIO,2X,7HL RATIO,/)
      DO 502 I=1,NOL
      PK=D(I)/TH
      QK=A(I)/A(NOL)
      VK=B(I)/B(NOL)
      RK=RHO(I)/RHO(NOL)
      SK=FLAND(I)/FLAND(NOL)
502   PUNCH 503,I,PK,QK,VK,RK,SK
503   FORMAT(1X,I2,5X,F9.4,4F10.4,/)
      PUNCH 1620
1620  FORMAT(1X,6HPERIOD,3X,4HFREQ,3X,4HHF/A,3X,2HTW,5X,
     13HPHW,6X,2HTU,5X,3HPHU,3X,5HTW/TU,1X,4HNORM,2X,
     15HPHASE)
      DO 310 IFR=1,NOF
      GAF=GAF+GINC
      IF(AT) 290,291,292
290   FREQ=GAF
      GO TO 293
291   FREQ=GAF*A(NOL)/TH
      GO TO 293
292   FREQ=GAF/APTH
293   CONTINUE
      PER=1./FREQ
      WVNO=6.2831853*FREQ/C
      A11=1
      A12=0
      A21=0
      A22=1
      A31=0
      A32=0
      A41=0
      A42=0
C     COMPUTE ELEMENTS OF A MATRIX FOR REMAINING LAYERS
      DO 1345 M=1,N1
      GAM=DGAM(M)
      GAMM1=DGAM1(M)
      RA=DRA(M)
      RB=DRB(M)
      H=DH(M)
      P=WVNO*D(M)*RA
      Q=WVNO*D(M)*RB
      SINP=SINF(P)
      W=SINP/RA
      X=RA*SINP
      COSP=COSF(P)
      SINQ=SINF(Q)
      Y=SINQ/RB
      Z=RB*SINQ
      COSQ=COSF(Q)
      RHOM=RHO(M)
      BM=B(M)
```

```
      DM=D(M)
      B11=GAM*COSP-GAMM1*COSQ
      B12=GAMM1*W+GAM*Z
      B13=-(COSP-COSQ)/H
      B14= (W+Z)/H
      B21= GAM*X+GAMM1*Y
      B22=-GAMM1*COSP+GAM*COSQ
      B23 =-(X+Y)/H
      B24 =B13
      B31 =H*GAM*GAMM1*(COSP-COSQ)
      B32 =H*(GAMM1*GAMM1*W+GAM*GAM*Z)
      B33 =B22
      B34 =B12
      B41 =-H*(GAM*GAM*X+GAMM1*GAMM1*Y)
      B42 =B31
      B43 =B21
      B44 =B11
      EA11 =B11*A11 + B12*A21 + B13*A31 + B14*A41
      EA12 = B11*A12 + B12*A22 + B13*A32 + B14*A42
      EA21 = B21*A11 + B22*A21 + B23*A31 + B24*A41
      EA22 = B21*A12 + B22*A22 + B23*A32 + B24*A42
      EA31 = B31*A11 + B32*A21 + B33*A31 + B34*A41
      EA32 = B31*A12 + B32*A22 + B33*A32 + B34*A42
      EA41 = B41*A11 + B42*A21 + B43*A31 + B44*A41
      EA42 = B41*A12 + B42*A22 + B43*A32 + B44*A42
      A11 = EA11
      A12 = EA12
      A21 = EA21
      A22 = EA22
      A31 = EA31
      A32 = EA32
      A41 = EA41
      A42 = EA42
1345  CONTINUE
1349  A21 = -A21
      A41 = -A41
      GAM = DGAM(N)
      GAMM1 = DGAM1(N)
      RA = DRA(N)
      RB = DRB(N)
      H = DH(N)
C     COMPUTE ELEMENTS OF E INVERSE FOR THE  LAST LAYER
      B11 = -GAM*COVA**2
      B13 = 1./(RHO(N)*A(N)*A(N))
      B22 = GAMM1*COVA**2/RA
      B24 = B13/RA
      B44 = 1./(H*GAM)
      B33 = -B44/RB
      B31 = -B33*GAMM1*H
      B42 = 1.
      EA11=B11*A11+B13*A31
      EA12=B11*A12+B13*A32
```

```
      EA21=B22*A21+B24*A41
      EA22=B22*A22+B24*A42
      EA31=B31*A11+B33*A31
      EA32=B31*A12+B33*A32
      EA41=B42*A21+B44*A41
      EA42=B42*A22+B44*A42
      DR= EA21*EA32 - EA11*EA42 - EA12*EA41 + EA22*EA31
      DI = EA11*EA32 + EA21*EA42 - EA12*EA31 - EA22*EA41
      DENSQ = DR*DR + DI*DI
      UPNR = EA32*DI - EA42*DR
      UPNI = EA32*DR + EA42*DI
      WPNI = EA41*DR + EA31*DI
      WPNR = -EA31*DR + EA41*DI
      PWDTP=((2./DENSQ)*SQRTF(WPNR*WPNR+WPNI*WPNI))*COVA
      PPHWP=ATANF(-WPNI/WPNR)-(1.-SIGNF(WPNR))*
     1SIGNF(WPNI)*1.57079
      PUDTP=  ((2./DENSQ)*SQRTF(UPNR*UPNR + UPNI*UPNI))*
     1COVA
      PPHUP =ATANF(-UPNI/UPNR)-(1.-SIGNF(UPNR))*
     1SIGNF(UPNI)*1.57079
      PAUOW=PWDTP/PUDTP
      DPAUOW=PAUOW/TANE
      PPHUW=PPHWP-PPHUP
      ABPH=ABSF(PPHUW)-3.1416
      IF(ABPH)1248,1248,1251
1251  IF(PPHUW)1252,1252,1253
1252  PPHUW=PPHUW+6.2832
      GO TO 1248
1253  PPHUW=PPHUW-6.2832
1248  IF(PPHUW)395,395,396
395   PPHUW=PPHUW+3.1416
      GO TO 1250
396   PPHUW=PPHUW-3.1416
1250  PUNCH 834,PER,FREQ,GAF,PWDTP,PPHWP,PUDTP,PPHUP,PAUOW,
     1DPAUOW,PPHUW
834   FORMAT(F7.1,F6.3,F7.4,5F7.2,F8.2,F7.2)
      IF (PLOTO)740,740,745
740   GAFLO=LOGF(GAF)/2.302585
      IX=GAFLO*XS
      IF(PLOTR)232,232,233
232   PWDTP=PWDTP/(2.*SINE)
      FIY=LOGF(10.*PWDTP)/2.302585
      IY=FIY*YS+Y01
      CALL XYPLOT(IX,IY)
      PUDTP=PUDTP/(2.*COSE)
      FIY=LOGF(10.*PUDTP)/2.302585
      IY=FIY*YS+Y02
      CALL XYPLOT(IX,IY)
233   FIY=LOGF(10.*DPAUOW)/2.302585
      IY=FIY*YS+Y03
      CALL XYPLOT(IX,IY)
```

```
      IX=GAFLO*XS+X02
      IF(PLOTR)230,230,231
230   IY=PPHWP*YPS+5.*Y04
      CALL XYPLOT(IX,IY)
      IY=PPHUP*YPS+3.*Y04
      CALL XYPLOT(IX,IY)
231   IY=PPHUW*YPS+Y04
      CALL XYPLOT(IX,IY)
      GO TO 310
745   IX=FREQ*XS
      IY=PWDTP*YS+Y01
      CALL XYPLOT(IX,IY)
      IY=PUDTP*YS+Y02
      CALL XYPLOT(IX,IY)
      IY=PAUOW*YS+Y03
      CALL XYPLOT(IX,IY)
      IX=FREQ*XS+X02
      IY=PPHWP*YPS+5.*Y04
      CALL XYPLOT(IX,IY)
      IY=PPHUP*YPS+3.*Y04
      CALL XYPLOT(IX,IY)
      IY=PPHUW*YPS+Y04
      CALL XYPLOT(IX,IY)
310   CONTINUE
311   CONTINUE
      PUNCH 709
709   FORMAT(//)
C     CONTROL CARD NEGATIVE=NEW ANGLE. IF CONTROL CARD = 0,
C     A NEW CRUSTAL MODEL . IF CONTROL CARD = A POSITIVE
C     NUMBER, THE PROGRAM WILL END.
1020  READ 7000,CNTRL
7000  FORMAT(1X,F9.2)
      IF(CNTRL)7001,1030,1021
1021  PRINT 990
990   FORMAT(1X,21HEND OF CASE,THANK YOU)
      END
```

APPENDIX II

```
**    FERNANDEZ                    GPH18    PARTDIF

*0705
C     THIS PROGRAM IS DESIGNED TO CALCULATE THE
C     TRANSFER FUNCTIONS OF THE VERTICAL AND HORIZONTAL
C     COMPONENTS OF LONGITUDINAL SEIZMIC WAVES IN A
C     LAYERED MEDIUM, AND THE FIRST PARTIAL DERIVATIVES
C     OF THESE TRANSFER FUNCTIONS WITH RESPECT TO THE
C     THICKNESS, THE ELASTIC PARAMETERS AND THE DENSITIES
C     OF ANY OF THE LAYERS OF THE SYSTEM.  BESIDES THIS
C     PROGRAM CALCULATES THE TRANSFER FUNCTION FOR THE
C     APPARENT ANGLE OF EMERGENCE, THIS IS, THE RATIO
C     OF THE VERTICAL TO THE HORIZONTAL COMPONENT AND
C     ITS FIRST PARTIAL DERIVATIVES.
      DIMENSION D(5),FL(5),A(5),RHO(5),DGAM(5),DGAM1(5),
     1DRA(5),B(5),DH(5),ELTAD(4),ELTAL(4),ELTAR(4),PA11
     2(4),  PA12(4),PA13(4),PA14(4),PA21(4),PA22(4),
     3PA23(4),PA24(4),PA31(4),PA32(4),PA33(4),PA34(4),
     4PA42(4),PA43(4),PA44(4),PEA11(4),PEA12(4),PEA21(4),
     5PEA22(4),PEA31(4),PEA32(4),PA41(4)
      DIMENSION PEA41(4),PEA42(4),DPDPR(4),DPDQL(4),
     1DPDQR(4),DPDGL(4),DRB(5),DPDGR(4),DDRAL(4),DDRAR
     2(4),DDRBR(4),DPDPL(4),DDRBL(4)
      SIGNF(VAR)=ABSF(VAR)/VAR
C     READ CARD TO IDENTIFY THE CRUSTAL MODEL UNDER STUDY
1030  READ 1101
      PUNCH 1101
1101  FORMAT(10H          )
C     READ IN THE NUMBER OF LAYERS PLUS ONE OF THE SYSTEM
      READ 2,NOL
2     FORMAT(I3)
      PUNCH 2,NOL
C     READ IN LAYER CONSTANTS,D(I)= THICKNESS OF THE ITH
C     LAYER, FL(I)=PARAMETER LANDA OF THE ITH LAYER,
C     RHO(I),DENSITY OF THE ITH LAYER
      PUNCH 6123
6123  FORMAT(1X,9HTHICKNESS,3X,5HLANDA,4X,7HDENSITY,1X,
     1 10HP VELOCITY,2X,10HS VELOCITY,/)
      DO 3 I=1,NOL
      READ 483,D(I),FL(I),RHO(I)
483   FORMAT(3F10.4)
      A(I)=SQRTF(3.*FL(I)/RHO(I))
      B(I)=SQRTF(FL(I)/RHO(I))
3     PUNCH 500,D(I),FL(I),RHO(I),A(I),B(I)
500   FORMAT(5F10.4)
      N=NOL
```

```
C       READ AGIP1= INITIAL ANGLE OF INCIDENCE,DANGI=
C       INCREMENT OF THE ANGLE NOANG=NUMBER OF ANGLES TO
C       BE CALCULATED
        READ 4, AGIP1,DANGI,NOANG
4       FORMAT(2F10.4,I3)
C       READ IN INITIAL VALUES OF FREQUENCY,INCREMENT OF
C       FREQ, NUMBER OF FREQ.
        READ 4,FMIN,FINC,NOF
7001    ANGIP= AGIP1-DANGI
C       READ IN CHANGES IN THE LAYERS PARAMETERS. IF THE
C       PARTIAL DERIVATIVE IS DESIRED WITH RESPECT TO THE
C       PARAMETER, MAKE ELTAD(I)=1. ETC. IF NOT=0 NO MORE
C       THAN 4 PARTIAL DERIVATIVES MAY BE CALCULATED IN ONE
C       PASS OF THE PROGRAM BECAUSE OF MEMORY CAPABILITIES
C       OF THE 1620 COMPUTER
        DO 100 I=1,N1
        READ 101, ELTAD(I), ELTAL(I), ELTAR(I)
100     PUNCH 101, ELTAD(I), ELTAL(I), ELTAR(I)
101     FORMAT (3F10.4)
        PUNCH 6319
6319    FORMAT(2X,5HFREQ.,3X,5HGAMMA,7X,2HTW,17X,2HTU,17X,
     1  5HTW/TU,/)
        DO 310 IA=1,NOANG
        FREQ=FMIN-FINC
5004    ANGIP=ANGIP+DANGI
        PUNCH 305,ANGIP
305     FORMAT(F8.3)
        C=A(NOL)/SINF(ANGIP/57.295780)
C       COMPUTE REUSABLE VARIABLES FOR THE LAYERS
        DO 1346 M=1,NOL
        DH(M) =RHO(M)*C*C
        COVA=C/A(M)
        COVB=C/B(M)
        DRA(M)=SQRTF(ABSF(COVA**2-1.))
        DRB(M)=SQRTF(ABSF(COVB**2-1.))
        COVP=1./DRA(M)
        COVS=1./DRB(M)
        DPDGL(M)=2./DH(M)
        DPDGR(M)=-2.*FL(M)/(DH(M)*RHO(M))
        DDRAL(M)=-DH(M)*COVP/(6.*FL(M)*FL(M))
        DDRAR(M)=C*C*COVP/(6.*FL(M))
        DDRBL(M)=-DH(M)*COVS/(2.*FL(M)*FL(M))
        DDRBR(M)=C*C*COVS/(2.*FL(M))
        DPDPL(M)=-DH(M)*D(M)*COVP/(6.*FL(M)*FL(M))
        DPDPR(M)=D(M)*C*C*COVP/(6.*FL(M))
        DPDQL(M)=-DH(M)*D(M)*COVS/(2.*FL(M)*FL(M))
        DPDQR(M)=D(M)*C*C*COVS/(2.*FL(M))
        DGAM(M)=2.*FL(M)/DH(M)
1346    DGAM1(M)=DGAM(M)-1.
        DO 310 IFR=1,NOF
        FREQ=FREQ+FINC
```

```
      GAF=FREQ*D(1)/A(1)
      WVNO=6.2831853*FREQ/C
      A11=1
      A12=0
      A21=0
      A22=1
      A31=0
      A32=0
      A41=0
      A42=0
      ND=0
C     COMPUTE THE ELEMENTS OF A MATRIX FOR REMAINING LAYERS
      DO 1345 M=1,N1
      GAM=DGAM(M)
      GAMM1=DGAM1(M)
      RA=DRA(M)
      RB=DRB(M)
      H=DH(M)
      P=WVNO*D(M)*RA
      Q=WVNO*D(M)*RB
      SINP=SINF(P)
      W=SINP/RA
      X=RA*SINP
      COSP=COSF(P)
      SINQ=SINF(Q)
      Y=SINQ/RB
      Z=RB*SINQ
      COSQ=COSF(Q)
      RHOM=RHO(M)
      ZZ=RB*COSQ
      XX=RA*COSP
      YY=COSQ/RA
      WW=COSP/RA
      YYY=COSQ/RB
      DM=D(M)
      NDM=0
      B11=GAM*COSP-GAMM1*COSQ
      B12=GAMM1*W+GAM*Z
      B13=-(COSP-COSQ)/H
      B14= (W+Z)/H
      B21= GAM*X+GAMM1*Y
      B22=-GAMM1*COSP+GAM*COSQ
      B23 =-(X+Y)/H
      B24 =B13
      B31 =H*GAM*GAMM1*(COSP-COSQ)
      B32 =H*(GAMM1*GAMM1*W+GAM*GAM*Z)
      B33 =B22
      B34 =B12
```

```
      B41 =-H*(GAM*GAM*X+GAMM1*GAMM1*Y)
      B42 =B31
      B43 =B21
      B44 =B11
      IF( ELTAD(M))10,11,10
C     CALCULATE THE PARTIAL DERIVATIVES OF THE MATRIX
C     ELEMENTS RESPECT TO THE THICKNESS OF THE CORRES-
C     PONDENT LAYER
10    ND=ND+1
      NDM=NDM+1
      PA11(ND)=WVNO*(-GAM*X+GAMM1*Z)
      PA12(ND)=WVNO*(GAMM1*COSP+GAM*RB**2*COSQ)
      PA13(ND)=(X-Z)*WVNO/H
      PA14(ND)=WVNO*(COSP+RB**2*COSQ)/H
      PA21(ND)=-WVNO*(GAM*RA**2*COSP+GAMM1*COSQ)
      PA22(ND)=WVNO*(GAMM1*X-GAM*Z)
      PA23(ND)= WVNO*(RA**2*COSP+COSQ)/H
      PA24(ND)=PA13(ND)
      PA31(ND)=-H*GAMM1*GAM*WVNO*(X-Z)
      PA32(ND)=H*(GAMM1**2*WVNO*COSP+GAM**2*RB**2*COSQ
     1*WVNO)
      PA33(ND)=PA22(ND)
      PA34(ND)=PA12(ND)
      PA41(ND)=H*(GAM**2*RA**2*WVNO*COSP+GAMM1**2*WVNO
     1*COSQ)
      PA42(ND)=PA31(ND)
      PA43(ND)=PA21(ND)
      PA44(ND)=PA11(ND)
11    CONTINUE
      IF( ELTAL(M))18,19,18
C     CALCULATE THE PARTIAL DERIVATIVES OF THE MATRIX
C     ELEMENTS IN RESPECT TO THE LANDA OF THE RESPECTIVE
C     LAYER
18    ND=ND+1
      NDM=NDM+1
      PDPL=DPDPL(M)*WVNO
      PDQL=DPDQL(M)*WVNO
      PDGL=DPDGL(M)
      PDRAL= DDRAL(M)
      PDRBL= DDRBL(M)
      PA11(ND)=PDGL*(COSP-COSQ)-GAM*SINP*PDPL+GAMM1*SINQ*PDGL
      PA12(ND)=PDGL*(W+Z)+GAMM1*(COSP*PDPL-W*PDRAL)/RA+GAM*
     1(PDRBL*SINQ+ZZ*PDQL)
      PA13(ND)=(SINP*PDPL-SINQ*PDQL)/H
      PA14(ND)=(WW*PDPL-SINP*PDRAL/(RA*RA)+PDRBL*SINQ+
     1ZZ*PDQL)/H
      PA21(ND)=-(X*PDGL+GAM*SINP*PDRAL+GAM*XX*PDPL+GAMM1*
     1(YYY*PDQL-(SINQ*PDRBL)/(RB*RB))+Y*PDGL)
```

```
      PA22(ND)=PDGL*(COSQ-COSP)+PDPL*GAMM1*SINP-GAM*SINQ
     1*PDQL
      PA23(ND)=(SINP*PDRAL+XX*PDPL+YYY*PDQL-(SINQ*PDRBL)/
     1(RB*RB))/H
      PA24(ND)=PA13(ND)
      PA31(ND)=H*(PDGL*(COSP-COSQ)*(2.*GAM-1.)+GAM*GAMM1*
     1(SINQ*PDQL-SINP*PDPL))
      PA32(ND)=H*(2.*PDGL*(GAMM1*W+GAM*Z)+GAMM1**2*(COSP*
     1PDPL/RA-SINP*PDRAL/(RA**2))+GAM**2*(RB*COSQ*PDQL
     2+SINQ*PDRBL))
      PA33(ND)=PA22(ND)
      PA34(ND)=PA12(ND)
      PA41(ND)=H*(2.*PDGL*(GAM*X+GAMM1*Y)+GAM**2 *(SINP*
     1PDRAL+XX*PDPL)+GAMM1**2*(YYY*PDQL-Y*PDRBL/RB))
      PA42(ND)=PA31(ND)
      PA43(ND)=PA21(ND)
      PA44(ND)=PA11(ND)
19    CONTINUE
      IF( ELTAR(M))22,23,22
C     CALCULATE THE PARTIAL DERIVATIVES OF THE MATRIX
C     ELEMENTS RESPECT TO THE DENSITY OF THE CORRESPONDENT
C     LAYER
22    ND=ND+1
      NDM=NDM+1
      PDPR=DPDPR(M)*WVNO
      PDQR=DPDQR(M)*WVNO
      PDGR=DPDGR(M)
      PDRAR= DDRAR(M)
      PDRBR= DDRBR(M)
      PA11(ND)=PDGR*(COSP-COSQ)-GAM*SINP*PDPR+GAMM1*SINQ
     1*PDQR
      PA12(ND)=PDGR*W+GAMM1*(COSP*PDPR-W*PDRAR)/RA+PDGR*
     1Z+GAM*(PDRBR*SINQ+ZZ*PDQR)
      PA13(ND)=-B13/RHOM+(SINP*PDPR-SINQ*PDQR)/H
      PA14(ND)=-B14/RHOM+(WW*PDPR-SINP*PDRAR/(RA*RA)+PDRBR
     1*SINQ+ZZ*PDQR)/H
     1Y+GAMM1*(YYY*PDQR)-(GAMM1*SINQ*PDRBR/RB**2))
      PA21(ND)=-(X*PDGR+GAM*SINP*PDRAR+GAM*XX*PDPR+PDGR*
      PA22(ND)=PDGR*(COSQ-COSP)+GAMM1*SINP*PDPR-GAM*
     1SINQ*PDQR
      PA23(ND)=-B23/RHOM+(SINP*PDRAR+XX*PDPR+YYY*PDQR-
     1(Y*PDRBR)/RB)/H
      PA24(ND)=PA13(ND)
      PA31(ND)=B31/RHOM+H*((COSP-COSQ)*(GAMM1+GAM)*PDGR
     1 +GAM*GAMM1*(SINQ*PDQR-SINP*PDPR))
      PA32(ND)=B32/RHOM+H*(2.*PDGR*(GAMM1*W+GAM*Z)
     1+GAMM1**2 *(WW*PDPR-W*PDRAR/RA)+GAM**2 *
     2(SINQ*PDRBR+ZZ*PDQR))
      PA33(ND)=PA22(ND)
      PA34(ND)=PA12(ND)
      PA41(ND)=B41/RHOM+H*(2.*PDGR*(GAM*X+GAMM1*Y)+GAM**2*
     1(SINP*PDRAR+XX*PDPR)+GAMM1**2 *(YYY*PDQR-Y
     2*PDRBR/RB))
      PA42(ND)=PA31(ND)
```

```
      PA43(ND)=PA21(ND)
      PA44(ND)=PA11(ND)
23    CONTINUE
C     MULTIPLY MATRICES
      EA11 =B11*A11 + B12*A21 + B13*A31 + B14*A41
      EA12 = B11*A12 + B12*A22 + B13*A32 + B14*A42
      EA21 = B21*A11 + B22*A21 + B23*A31 + B24*A41
      EA22 = B21*A12 + B22*A22 + B23*A32 + B24*A42
      EA31 = B31*A11 + B32*A21 + B33*A31 + B34*A41
      EA32 = B31*A12 + B32*A22 + B33*A32 + B34*A42
      EA41 = B41*A11 + B42*A21 + B43*A31 + B44*A41
      EA42 = B41*A12 + B42*A22 + B43*A32 + B44*A42
      NF=ND-NDM
      NF1=NF+1
      IF(NDM)54,55,54
54    DO 30 I=NF1,ND
      PEA11(I)=PA11(I)*A11+PA12(I)*A21+PA13(I)*A31+
     1PA14(I)*A41
      PEA12(I)=PA11(I)*A12+PA12(I)*A22+PA13(I)*A32+
     1PA14(I)*A42
      PEA21(I)=PA21(I)*A11+PA22(I)*A21+PA23(I)*A31+
     1 PA24(I)*A41
      PEA22(I)=PA21(I)*A12+PA22(I)*A22+PA23(I)*A32+
     1PA24(I)*A42
      PEA31(I)=PA31(I)*A11+PA32(I)*A21+PA33(I)*A31+
     1PA34(I)*A41
      PEA32(I)=PA31(I)*A12+PA32(I)*A22+PA33(I)*A32+
     1PA34(I)*A42
      PEA41(I)=PA41(I)*A11+PA42(I)*A21+PA43(I)*A31+
     1PA44(I)*A41
30    PEA42(I)=PA41(I)*A12+PA42(I)*A22+PA43(I)*A32+
     1PA44(I)*A42
55    CONTINUE
      A11 = EA11
      A12 = EA12
      A21 = EA21
      A22 = EA22
      A31 = EA31
      A32 = EA32
      A41 = EA41
      A42 = EA42
      IF(NF)50,1344,50
50    DO 31 I=1,NF
      PEA11(I)=B11*PA11(I)+B12*PA21(I)+B13*PA31(I)+
     1B14*PA41(I)
      PEA12(I)=B11*PA12(I)+B12*PA22(I)+B13*PA32(I)+
     1B14*PA42(I)
      PEA21(I)=B21*PA11(I)+B22*PA21(I)+B23*PA31(I)+
     1B24*PA41(I)
```

```
      PEA22(I)=B21*PA12(I)+B22*PA22(I)+B23*PA32(I)+
     1B24*PA42(I)
      PEA31(I)=B31*PA11(I)+B32*PA21(I)+B33*PA31(I)+
     1B34*PA41(I)
      PEA32(I)=B31*PA12(I)+B32*PA22(I)+B33*PA32(I)+
     1B34*PA42(I)
      PEA41(I)=B41*PA11(I)+B42*PA21(I)+B43*PA31(I)+
     1B44*PA41(I)
31    PEA42(I)=B41*PA12(I)+B42*PA22(I)+B43*PA32(I)+
     1B44*PA42(I)
1344  CONTINUE
      IF(ND)60,1345,60
60    DO 38 I=1,ND
      PA11(I)=PEA11(I)
      PA12(I)=PEA12(I)
      PA21(I)=PEA21(I)
      PA22(I)=PEA22(I)
      PA31(I)=PEA31(I)
      PA32(I)=PEA32(I)
      PA41(I)=PEA41(I)
38    PA42(I)=PEA42(I)
1345  CONTINUE
1349  A21 = -A21
      A41 = -A41
      GAM = DGAM(N)
      GAMM1 = DGAM1(N)
      RA = DRA(N)
      RB=DRB(N)
      H=DH(N)
C     COMPUTE THE ELEMENTS FOR THE E INVERSE OF THE LAST
C     LAYER
      B11=-GAM*COVA**2
      B13 = 1./(RHO(N)*A(N)*A(N))
      B22 = GAMM1*COVA**2/RA
      B24 = B13/RA
      B44 = 1./(H*GAM)
      B33 = -B44/RB
      B31 = -B33*GAMM1*H
      B42 = 1.
      EA11=B11*A11+B13*A31
      EA12=B11*A12+B13*A32
      EA21=B22*A21+B24*A41
      EA22=B22*A22+B24*A42
      EA31=B31*A11+B33*A31
      EA32=B31*A12+B33*A32
      EA41=B42*A21+B44*A41
      EA42=B42*A22+B44*A42
      DR= EA21*EA32 - EA11*EA42 - EA12*EA41 + EA22*EA31
      DI = EA11*EA32 + EA21*EA42 - EA12*EA31 - EA22*EA41
      DENSQ = DR*DR + DI*DI
      UPNR = EA32*DI - EA42*DR
      UPNI = EA32*DR + EA42*DI
      UDTP = ((2./DENSQ)*SQRTF(UPNR*UPNR + UPNI*UPNI))*COVA
      PHUPD=ATANF(-UPNI/UPNR)-(1.-SIGNF(UPNR))*
```

```
     1SIGNF(UPNI)* 1.57079
      WPNI = EA41*DR + EA31*DI
      WPNR = -EA31*DR + EA41*DI
      WDTP =((2./DENSQ)*SQRTF(WPNR*WPNR+WPNI*WPNI))*COVA
      AUOW=WDTP/UDTP
      PHWPD=ATANF(-WPNI/WPNR)-(1.-SIGNF(WPNR))*
     1SIGNF(WPNI)*1.57079
      PHUOW=PHWPD-PHUPD
      ABPH=ABSF(PHUOW)-3.1416
      IF(ABPH)610,610,611
611   IF(PHUOW)612,610,613
612   PHUOW=PHUOW+6.2832
      GO TO 610
613   PHUOW=PHUOW-6.2832
610   PUNCH 303,  FREQ,GAF,WDTP,PHWPD,UDTP,PHUPD,AUOW,PHUOW
303   FORMAT(2F8.4,6F9.4)
C     FOR INVERSE MATRIX OF LAST LAYER
      DO 32 I=1,ND
      PA21(I)=-PA21(I)
      PA41(I)=-PA41(I)
      PEA11(I)=B11*PA11(I)+B13*PA31(I)
      PEA12(I)=B11*PA12(I)+B13*PA32(I)
      PEA21(I)=B22*PA21(I)+B24*PA41(I)
      PEA22(I)=B22*PA22(I)+B24*PA42(I)
      PEA31(I)=B31*PA11(I)+B33*PA31(I)
      PEA32(I)=B31*PA12(I)+B33*PA32(I)
      PEA41(I)=B42*PA21(I)+B44*PA41(I)
      PEA42(I)=B42*PA22(I)+B44*PA42(I)
      PDR=PEA21(I)*PEA32(I)-PEA11(I)*PEA42(I)-
     1PEA12(I)*PEA41(I)+PEA22(I)*PEA31(I)
      PDI=PEA11(I)*PEA32(I)+PEA21(I)*PEA42(I)-
     1PEA12(I)*PEA31(I)-PEA22(I)*PEA41(I)
      PUR=DR*PEA42(I)+DI*PEA32(I)-EA42*PDR-EA32*PDI
      PUI=DI*PEA42(I)-DR*PEA32(I)-EA42*PDI+EA32*PDR
      PWR=-DR*PEA31(I)-DI*PEA41(I)+EA41*PDI+EA31*PDR
      PWI=DR*PEA41(I)-DI*PEA31(I)-EA41*PDR+EA31*PDI
      D2R=DR*DR-DI*DI
      D2I=2.*DR*DI
      PUPNR=PUR*D2R+PUI*D2I
      PUPNI=PUI*D2R-PUR*D2I
      PDENSQ=D2R*D2R+D2I*D2I
      PUDTP=(2./PDENSQ)*COVA*SQRTF(PUPNR*PUPNR+PUPNI*PUPNI)
      PPHUPD=ATANF(-PUPNI/PUPNR)-(1.-SIGNF(PUPNR))*
     1SIGNF(PUPNI)*1.57079
      PWPNR=PWR*D2R+PWI*D2I
      PWPNI=-PWR*D2I+PWI*D2R
      PWDTP=(2./PDENSQ)*COVA*SQRTF(PWPNR*PWPNR+PWPNI*PWPNI)
      PPHWPD=ATANF(-PWPNI/PWPNR)-(1.-SIGNF(PWPNR))*
     1SIGNF(PWPNI)*1.57079
      PRR=-EA42*PEA31(I)+EA32*PEA41(I)+PEA42(I)*EA31-
     1EA41*PEA32(I)
      PRI=EA32*PEA31(I)+EA42*PEA41(I)-EA41*PEA42(I)-
     1EA31*PEA32(I)
      P2R=EA42**2-EA32**2
```

```
      P2I=2.*EA42*EA32
      PRPHR=PRR*P2R-PRI*P2I
      PRPNI=PRR*P2I+PRI*P2R
      PRDESQ=P2R*P2R+P2I*P2I
      PMUOW=(1./PRDESQ)*SQRTF(PRPNR*PRPNR+PRPNI*PRPNI)
      PPHUOW=ATANF(-PRPNI/PRPNR)-(1.-SIGNF(PRPNR))*
     1SIGNF(PRPNI)*1.57079
      PUNCH 307,I,FREQ,GAF,PWDTP,PPHWPD,PUDTP,PPHUPD,PMUOW
     1,PPHUOW
307   FORMAT(I2,2F8.4,6F9.4)
32    CONTINUE
310   CONTINUE
C     CONTROL CARD TO CONTROL RECYCLE
1020  READ 7000,CNTRL
7000  FORMAT(F10.2)
      IF(CNTRL)7001,1030,1021
1021  CONTINUE
      END
```

APPENDIX III

```
**      FERNANDEZ                    GPH 18   DIAGR
C       THIS PROGRAM IS DESIGNED TO PLOT THE PARTICLE
C       MOTION DIAGRAMS OF THE GROUND MOTION CORRESPONDING
C       TO AN INCIDENT LONGITUIDINAL WAVE THROUGH A
C       LAYERED SYSTEM, AT DIFFERENT VALUES OF THE
C       PARAMETER GAMMA


        DIMENSION PWDTP(16),PUDTP(16),PHWOU(16)
14      PUNCH TAPE 100
100     FORMAT(1H=)
        IX= 3800
        IY= 0
        CALL XYPLOT(IX,IY)
        IX=0
        IY=2500
        CALL XYPLOT(IX,IY)
        DO 3 LG=1,16
C       READ THE VERTICAL AMPLITUDE(PWDTP) THE HORIZONTAL
C       AMPLITUDE (PUDTP) AND THE PHASE DIFFERENCE(PHWOU)
        READ 2 ,PWDTP(LG),PUDTP(LG),PHWOU(LG)
2       FORMAT(20X,F7.2,7X,F7.2,22X,F7.2)
        IF (PWDTP(LG))4,10,4
4       CONTINUE
        DO 20 L=1,3
        READ 21, ZRO
21      FORMAT(20X,F7.2)
20      CONTINUE
3       CONTINUE
10      NE=LG-1
        LG=0
        DO 7 JY=4,20,8
        OY=2400-JY*100
        DO 6 JX=5,33,7
        OX=JX*100
        LG=LG+1
        DO 200 NS=1,7
        FNS=NS
        IX=OX-400.+FNS*100.
        IY=OY
200     CALL XYPLOT(IX,IY)
        DO 201 MS=1,7
        IX=OX
        FMS=MS
        IY=OY-400.+FMS*100.
```

```
201     CALL XYPLOT(IX,IY)
        IF (NE LG)12,11,11
11      DO 5 I=1,12
        FI=I-1
        W=FI/2.
        IX=PUDTP(LG)*100.*COSF(W+PHWOU(LG)+3.1415)+ OX
        IY=-PWDTP(LG)*100.*COSF(W) + OY
5       CALL XYPLOT(IX,IY)
6       CONTINUE
7       CONTINUE
12      CONTINUE
        READ 500, MORE
500     FORMAT(I2)
        IF (MORE)13,13,14
13      PRINT 15
15      FORMAT(21HEND OF RUN, THANK YOU)
        END
```

APPENDIX IV

SEISMIC ANALYZER PROGRAM

MAIN PROGRAM

The main program

1) Reads the scale factors of the different graphs of the output.
2) Reads the identification of the earthquake and the characteristics of the spectral analysis to be performed, such as data window length, digitization interval, frequency resolution of the spectrum, number of passes of the record through the digital filter and the limits of the frequency of the spectrum.

This part of the program controls the use of all the subprograms, which are optional and can be omitted if desired.

Finally, this main program reads the frequency amplitude and phase response of the three instruments of the station and the digitized values of the seismograms of the three components.

The program can be recycled to perform the operations with another set of records.

FILTER SUBPROGRAM

This is an optional subprogram whose use is controlled

by the Main Program.

Its object is:

1) To remove the zero-shift of the record by a correction based on the average of all the data points.
2) To remove the linear trend that could be introduced in the records by mislocation of the zero line. In practice this step traces a straight line through the points and relocates all the points about this line.
3) To apply the linear digital filter indicated before.

WINDOW SUBPROGRAM

This is an optional subprogram whose use is controlled by the main program.

Its object is:

1) To weight the seismic record in such a way that amplitudes near the first arrival of the P wave are emphasized and later arrivals minimized. This is done according to the "hamming" operation described before. The time interval of the window is controlled by the main program and is optional for each case.
2) To smooth out the spectrum.
3) To plot the seismogram after these operations have been performed.

At this point the seismogram of the P wave is ready for Fourier integration.

FOURIER INTEGRAL SUBPROGRAM

This is an optional subprogram that can be used in two different forms: a) cosine Fourier integral for power spectrum calculation from autocorrelation data, or b) complex Fourier integral. This optional control is given in the Main Program.

Its object is:

1) To calculate the Fourier integral of the records. The numerical integration is performed using Filon's method.
2) To correct the amplitudes and phases of the Fourier analysis by the frequency response of the instrument for amplitudes and phase.
3) To print an output of the individual spectra of the three components. Though this output is not necessary for the object of this dissertation, nevertheless it can be used in related investigations.

RATIO SUBPROGRAM

This is an optional program whose use is controlled by the Main Program.

Its object is:

1) To divide the vertical component of ground motion (as represented by the output of the previous

program) by the horizontal component. The result is printed and plotted on a logarithmic scale.

2) To find the phase difference between the vertical and the horizontal components at the different frequencies of the Fourier analysis. The results are printed and plotted on a logarithmic scale.

In addition to the above, the program gives the total vector amplitude of ground motion at the frequencies of the Fourier analysis.

By a convenient control the program may be recycled to analyze several records in succession.

```
**    FERNANDEZ        GPH 18   SEISMIC ANALYZER.MAIN

C     THIS PROGRAM IS DESIGNED TO DIVIDE THE SMOOTHED
C     SPECTRA OF THE VERTICAL AND HORIZONTAL COMPONENTS OF
C     THE P WAVES AND TO PLOT THE  TANGENT OF THE APPARENT
C     ANGLE OF EMERGENCE VERSUS FREQUENCY.
C     THE PROGRAM IS COMPOSED OF A MAIN PROGRAM AND FOUR
C     OPTIONAL SUBPROGRAMS.

      DIMENSION Y( 900),FMOD(3, 60),GAIN(3),COR(100),
     1XRS(3),XRO(3),YRS(3),YRO(3),XFS(3),XFO(3),YFS(3)
     2,YFO(3),XCS(3),XCO(3),YCS(3),YCO(3),PHA(3, 60)
      COMMON Y,FMOD,NT,COR,FMIN,FINC,NOF,GAIN,H,FNFL,
     1PLOTF ,XCS,XCO,YCO,SMOTH,M,TM,YCS,XFS,XFO,YFS,YFO,
     2XSS,XSO,YSS,YSO,NAC,TL,COMP,JC,INDS,PHA,T1,T2,T3,
     3T4,T5,T6,CT1,CT2,CT3,CT4,CT5,CT6,TF1,TF2,TF3,TF4,
     4TF5,TF6,CTF1,CTF2,CTF3,CTF4,CTF5,CTF6
C     READ THE SCALE FACTORS(XS,ETC) AND ORIGIN POINT
C     (O1,ETC) FOR THE PLOT.
      DO 270 I=1,3
      READ 1,XRS(I),XRO(I),YRS(I),YRO(I),XFS(I),XFO(I)
      READ 1 ,YFS(I),YFO(I),XCS(I),XCO(I),YCS(I),YCO(I)
1     FORMAT(6F10.0)
270   CONTINUE
      READ 411,XSS,XSO,YSS,YSO
411   FORMAT(4F10.0)
C     READ A CARD WITH THE OPERATIONS AND SUBPROGRAMS
C     TO BE USED.
C     IF FNFL= POSITIVE NUMBER THE FILTER PASS IS USED.
C     IF PLOTRE= POSITIVE NUMBER, THE DIGITIZED RECORD IS
C     PLOTTED. IF PLOTFI= POSITIVE NUMBER THE FILTERED
C     RECORD IS PLOTTED. IF SMOOTH= POSITIVE NUMBER THE
C     SUBPROGRAM WINDOW IS USED. IF FOURT=POSITIVE NUMBER,
C     THE SUBPROGRAM  FTRAN IS USED. IF WURAT=POSITIVE
C     NUMBER, THE SUBPROGRAM RATIO IS USED.
      READ 31, FNFL,PLOTR,PLOTF,SMOTH,FOURT,WURAT
31    FORMAT(6F10.0)
C     READ A CARD WITH THE PARAMETERS OF THE SPECTRUM
C     COMP= POSITIVE NUMBER FOR FOURIER COMPLEX INTEGRAL
C     FMIN=MINIMUM FREQUENCY,F C=INCREMENT OF THE FREQUENCY
C     ,NOF=NUMBER OF POINTS TO BE CALCULATED,NAC=POSITIVE
C     NUMBER  FOR PLOT OF SMOOTH RECORD.
C     INDS=POSTIVE FOR LISTING OF INDIVIDUAL SPECTRA.
      READ 30,FMIN,FINC,NOF,NAC,INDS,COMP
30    FORMAT(2F10.3,3I3,F10.0)
      PUNCH TAPE 3
3     FORMAT(1H=)
```

```
C       IDENTIFICATION OF SPECTRUM
22      READ 2
        PUNCH 2
2       FORMAT(49H
C       GAIN OF RECORDS AT CENTRAL FREQUENCY,1=Z,2=N-S,
C       3=E-W COMPONENTS. TL LENGTH OF THE WINDOW IN SECONDS.
C       CALC=0 IF NOT CALIBRATION CURVE IS USED TO FIND
C       GROUND MOTION,CALC=1 IF THE RESPONSE CURVE IS USED
C       THE RESPONSE CURVE OF THE INSTRUMENTS IS GIVEN
C       WITH THE DATA
        READ 4,GAIN(1),GAIN(2),GAIN(3),H1,TL,CALC
4       FORMAT(3F10.0,F10.7,2F10.3)
C       READ THE MAGNIFICATION ,CT1,ETC,THE  PHASE DELAY,
C      CTF1,ETC AND THE CORRESPONDING PERIODS,T1, ETC;
C       FOR SIX SELECTED POINTS OF THE RESPONSE CURVE.
C       INTERMEDIATE VALUES OF THE PERIOD ARE INTERPOLATED
        DO 5 JC=1,3
        IF (CALC) 283,284,283
283     READ 99,T1,CT1,T2,CT2,T3,CT3
        READ 99,T4,CT4,T5,CT5,T6,CT6
        READ 99,TF1,CTF1,TF2,CTF2,TF3,CTF3
        READ 99,TF4,CTF4,TF5,CTF5,TF6,CTF6
99      FORMAT(6F10.2)
284     CONTINUE
        DO 6 I=1,1600,14
        READ 24,Y(I),Y(I+1),Y(I+2),Y(I+3),Y(I+4),Y(I+5)
       1Y(I+6),Y(I+7),Y(I+8),Y(I+9),Y(I+10),Y(I+11),Y(I+12
       2),Y(I+13)
C       THE LAST CARD OF EACH COMPONENT MUST BE A CARD
C       WITH 9999
24      FORMAT(14F5.0)
        IF(Y(I)-9999.)6,7,6
6       CONTINUE
7       NT=I-2
        H=H1
        IF(PLOTR) 8,8,9
9       DO 10 I=1,NT
        FI=I-1
        IX=FI*H*XRS(JC)+XRO(JC)
        IY=Y(I)*YRS(JC)+YRO(JC)
        CALL XYPLOT(IX,IY)
10      CONTINUE
8       IF(FNFL)13,13,12
12      CALL FILTE(FNFL)
13      IF (SMOTH)15,15,16
16      CALL WINDO(COR)
15      IF (FOURT) 17,17,18
18      CALL FTRAN (COR)
17      CONTINUE
5       CONTINUE
        IF(WURAT) 19,19,20
20      CALL RATIO(FQ)
```

```
19      PUNCH TAPE 3
        READ 34, MORE
34      FORMAT(F10.0)
        IF (MORE) 21,21,22
21      PRINT 23
        PUNCH 23
23      FORMAT(20HEND OF RUN,THANK YOU)
        PAUSE
        END


**      FERNANDEZ                    GPH 18   FILTER SUB.

        SUBROUTINE FILTE(FZ)
C       THIS IS AN OPTIONAL SUBROUTINE CONTROLED BY THE
C       MAIN PROGRAM. ITS OBJECT IS TO DETREND THE RECORD
C       AND TO FILTER IT.
        DIMENSION Y( 900),FMOD(3, 60),GAIN(3),COR(100),
       1XRS(3),XRO(3),YRS(3),YRO(3),XFS(3),XFO(3),YFS(3)
       2,YFO(3),XCS(3),XCO(3),YCS(3),YCO(3),PHA(3, 60)
        COMMON Y,FMOD,NT,COR,FMIN,FINC,NOF,GAIN,H,FNFL,
       1PLOTF ,XCS,XCO,YCO,SMOTH,M,TM,YCS,XFS,XFO,YFS,YFO,
       2XSS,XSO,YSS,YSO,NAC,TL,COMP,JC,INDS,PHA,T1,T2,T3,
       3T4,T5,T6,CT1,CT2,CT3,CT4,CT5,CT6,TF1,TF2,TF3,TF4,
       4TF5,TF6,CTF1,CTF2,CTF3,CTF4,CTF5,CTF6
        NH=NT/2
        FNL=NH
        YL=0.
        DO 463 I=1,NH
463     YL=YL+Y(I)
        YL=YL/FNL
        YR=0.
        NJ=NH+1
        FNR=NT-NH
        DO 464 I=NJ,NT
464     YR=YR+Y(I)
        YR=YR/FNR
        T0=0.
470     NTR=1
        NFL=FNFL
        IF(NFL)461,461,462
462     FNT=NT
        NF=NT-5
        C1=2.*(YR-YL)/FNT
        C2=(YR-YL)/2.
        N=0
        DO 465 I=1,NF,2
        FI=I
        N=N+1
465     Y(N)=(Y(I)+Y(I+5)+2.*(Y(I+1)+Y(I+4))+3.*
       1(Y(I+2)+Y(I+3)))/12.-(FI+2.5)*C1+C2
        NT=N
        FT=2.5*H
```

```
      TO=TO+FT
      H=2.*H
      Y(N+1)=0.
      Y(N+2)=0.
      IF(NFL-NTR)466,466,467
467   NL=N/2
      YL=0.
      DO 468 I=1,NL
468   YL=YL+Y(I)
      NR1=NL+1
      YR=0.
      DO 469 I=NR1,N
469   YR=YR+Y(I)
      FNL=NL
      FNR=N-NL
      YL=YL/FNL
      YR=YR/FNR
      NTR=NTR+1
      GO TO 470
466   FT=TO
      IF(PLOTF )115,115,116
116   DO 471 I=1,N
      FI=I-1
      IX=(FI*H+FT)*XFS(JC)+XFO(JC)
      IY=Y(I)*YFS(JC)+YFO(JC)
      CALL XYPLOT(IX,IY)
471   FT=FT+H
461   CONTINUE
115   CONTINUE
      RETURN
       END


**    FERNANDEZ                    GPH18  WINDOW SUB.

C     THIS IS AN OPTIONAL SUBROUTINE CONTROLED BY THE
C     MAIN PROGRAM. ITS OBJECT IS TO PASS THE RECORD
C     THROUGH A DATA WINDOW OF VARIABLE LENGTH.
      SUBROUTINE WINDO(HAM)

      DIMENSION Y( 900),FMOD(3, 60),GAIN(3),COR(100),
     1XRS(3),XRO(3),YRS(3),YRO(3),XFS(3),XFO(3),YFS(3)
     2,YFO(3),XCS(3),XCO(3),YCS(3),YCO(3),PHA(3, 60)
      COMMON Y,FMOD,NT,COR,FMIN,FINC,NOF,GAIN,H,FNFL,
     1PLOTF ,XCS,XCO,YCO,SMOTH,M,TM,YCS,XFS,XFO,YFS,YFO,
     2XSS,XSO,YSS,YSO,NAC,TL,COMP,JC,INDS,PHA,T1,T2,T3,
     3T4,T5,T6,CT1,CT2,CT3,CT4,CT5,CT6,TF1,TF2,TF3,TF4,
     4TF5,TF6,CTF1,CTF2,CTF3,CTF4,CTF5,CTF6
C     TOTAL LENGTH OF THE RECORD=TL
      DO 43 I=1,NT
      BI=I-1
      T=H*BI
      IF (T-TL) 83,83,84
```

```
83      WD=0.54+0.46*COSF(3.14159*T/TL)
        GO TO 85
84      WD=0.
85      Y(I)=Y(I)*WD
C       IF PLOT OF THE RECORD IS DESIRED LET NAC=1
        IF (NAC)  81,81,82
82      IX=T*XCS(JC)+XCO(JC)
        IY=Y(I)*YCS(JC)+YCO(JC)
        CALL XYPLOT(IX,IY)
81      CONTINUE
43      CONTINUE
        RETURN
         END

**      FERNANDEZ                    GPH 18   FOURIER INTEGRAL

        SUBROUTINE FTRAN(R)
C       THIS IS AN OPTIONAL SUBROUTINE. ITS OBJECT IS TO
C        FOURIER ANALYZE THE RECORDS AND TO CONVERT TO
C       GROUND MOTION THE AMPLITUDE.
        DIMENSION Y( 900),FMOD(3, 60),GAIN(3),COR(100),
       1XRS(3),XRO(3),YRS(3),YRO(3),XFS(3),XFO(3),YFS(3)
       2,YFO(3),XCS(3),XCO(3),YCS(3),YCO(3),PHA(3, 60)
        COMMON Y,FMOD,NT,COR,FMIN,FINC,NOF,GAIN,H,FNFL,
       1PLOTF ,XCS,XCO,YCO,SMOTH,M,TM,YCS,XFS,XFO,YFS,YFO,
       2XSS,XSO,YSS,YSO,NAC,TL.COMP,JC,INDS,PHA,T1,T2,T3,
       3T4,T5,T6,CT1,CT2,CT3,CT4,CT5,CT6,TF1,TF2,TF3,TF4,
       4TF5,TF6,CTF1,CTF2,CTF3,CTF4,CTF5,CTF6
        SIGNF(VAR)=ABSF(VAR)/VAR
        IF(INDS)1002,1002,1003
1003    PUNCH 1001,JC
1001    FORMAT(26H    SPECTRUM FOR COMPONENT,2X,I1,//)
        PUNCH 1000
1000    FORMAT(49H       FREQ.       PERIOD      AMPLITUDE
       1    PHASE     )
1002    IDE=(NT-2)/2
        IDE=2*IDE
        FREQ=FMIN-FINC
        DO 3 I=1,NOF
        FREQ=FREQ+FINC
        PER=1./FREQ
        W=6.28318*FREQ
        SWDT=SINF(W*H)
        CWDT=COSF(W*H)
        ZETA=W*H
        ALFA=(ZETA**2+ZETA*SWDT*CWDT-2.*(SWDT**2))/ZETA**3
        BETA=2.*(ZETA*(1.+CWDT**2)-2.*SWDT*CWDT)/ZETA**3
        GAMA=4.*(SWDT-ZETA*CWDT)/ZETA**3
        SWT=0.
        CWT=1.
        S=0.
        C=Y(1)/2.
        DO 1 J=2,IDE,2
```

```
      N=J
      SA=SWT
      SWT=SWT*CWDT+SWDT*CWT
      CWT=CWT*CWDT-SA*SWDT
      C=C+GAMA*Y(J)*CWT
      IF(COMP)4,4,5
5     S=S+GAMA*Y(J)*SWT
4     CONTINUE
      SA=SWT
      SWT=SWT*CWDT+SWDT*CWT
      CWT=CWT*CWDT-SA*SWDT
      IF(COMP)6,6,7
7     S=S+BETA*Y(J+1)*SWT
6     CONTINUE
1     C=C+BETA*Y(J+1)*CWT
      SA=SWT
      SWT=SWT*CWDT+SWDT*CWT
      CWT=CWT*CWDT-SA*SWDT
      C=C+Y(IDE+1)*CWT/2.
      S=S+Y(IDE+1)*SWT/2.
      IF(COMP)8,8,9
8     FMOD(JC,I)=2.*H*(Y(IDE+1)*SWT*ALFA+C)
      FMOD(JC,I)=SQRTF(FMOD(JC,I))
      PHA(JC,I)=0.
      GO TO 10
9     C=Y(IDE+1)*SWT*ALFA+C
      S=-(Y(IDE+1)*CWT+Y(1))*ALFA+S
      FMOD(JC,I)=SQRTF((S*S+C*C)*.1591549)*H
      PHA(JC,I)=ATAN(-S/C)-(1.-SIGNF(C))*SIGNF(S)*1.5707963
C     CORRECT FOR INSTRUMENT RESPONSE
      IF(CALC)119,10,119
119   T=PER
      IF(T2-T)120,120,121
121   CTI=CT1+(CT2-CT1)*(T-T1)/(T2-T1)
      GO TO 140
120   IF (T3-T)122,122,123
123   CTI=CT2+(CT3-CT2)*(T-T2)/(T3-T2)
      GO TO 140
122   IF(T4-T)124,124,125
125   CTI=CT3+(CT4-CT3)*(T-T3)/(T4-T3)
      GO TO 140
124   IF(T5-T)126,126,127
127   CTI=CT4+(CT5-CT4)*(T-T4)/(T5-T4)
      GO TO 140
126   CTI=CT5+(CT6-CT5)*(T-T5)/(T6-T5)
140   CONTINUE
      FMOD(JC,I)=FMOD(JC,I)*1000./CTI
      IF (T2-T)150,150,151
151   CTFI=CTF1+(CTF2-CTF1)*(T-TF1)/(TF2-TF1)
      GO TO 160
150   IF(T3-T)152,152,153
153   CTFI=CTF2+(CTF3-CTF2)*(T-TF2)/(TF3-TF2)
      GO TO 160
```

```
152     IF (T4-T)154,154,155
155     CTFI=CTF3+(CTF4-CTF3)*(T-TF3)/(TF4-TF3)
        GO TO 160
154     IF (T5-T)156,156,157
157     CTFI=CTF4+(CTF5-CTF4)*(T-TF4)/(TF5-TF4)
        GO TO 160
156     CTFI=CTF5+(CTF6-CTF5)*(T-TF5)/(TF6-TF5)
160     PHA(JC,I)=PHA(JC,I)-CTFI
        GO TO 170
C       NORMALIZE VALUES TO VERTICAL COMPONENT
10      FMOD(JC,I)=FMOD(JC,I)*GAIN(JC)/GAIN(1)
170     CONTINUE
        IF(INDS)13,13,15
15      PUNCH 16,FREQ,PER,FMOD(JC,I),PHA(JC,I)
16      FORMAT(4F12.4)
13      CONTINUE
3       CONTINUE
        RETURN
        END


**      FERNANDEZ                   GPH 18     RATIO SUB.

        SUBROUTINE RATIO(FQ)
C       THIS SUBROUTINE HAS AS ITS OBJECT TO DIVIDE THE
C       SPECTRUM OF THE VERTICAL COMPONENT BY THE  VECTORIAL
C       SUM OF THE SPECTRA OF THE HORIZONTAL COMPONENTS.
        DIMENSION Y( 900),FMOD(3, 60),GAIN(3),COR(100),
       1XRS(3),XRO(3),YRS(3),YRO(3),XFS(3),XFO(3),YFS(3)
       2,YFO(3),XCS(3),XCO(3),YCS(3),YCO(3),PHA(3, 60)
        COMMON Y,FMOD,NT,COR,FMIN,FINC,NOF,GAIN,H,FNFL,
       1PLOTF ,XCS,XCO,YCO,SMOTH,M,TM,YCS,XFS,XFO,YFS,YFO,
       2XSS,XSO,YSS,YSO,NAC,TL,COMP,JC,INDS,PHA,T1,T2,T3,
       3T4,T5,T6,CT1,CT2,CT3,CT4,CT5,CT6,TF1,TF2,TF3,TF4,
       4TF5,TF6,CTF1,CTF2,CTF3,CTF4,CTF5,CTF6
        SIGNF(VAR)=ABSF(VAR)/VAR
        PUNCH 6324
6324    FORMAT( 2X,43HSPECTRUM OF THE APPARENT ANGLE
       1OF EMERGENCE,/)
        PUNCH 6325
6325    FORMAT(2X,6HPERIOD,5X,5HFREQ.,4X,7HMODULUS,5X,
       15HPHASE,2X,11HTOTAL AMPL.,/)
        DO 1 I=1,NOF
        RJ=I-1
        FREQ=FMIN+RJ*FINC
        PER=1 /FREQ
        HMOD=SQRTF(FMOD(2,I)**2+FMOD(3,I)**2)
        WOU=FMOD(1,I)/HMOD
        PR=FMOD(2,I)*COSF(PHA(2,I))+FMOD(3,I)*COSF(PHA(3,I))
        PI=FMOD(2,I)*SINF(PHA(2,I))+FMOD(3,I)*SINF(PHA(3,I))
        PHAH=ATAN(-PI/PR)-(1.-SIGNF(PR))*SIGNF(PI)*1.5707963
        DPHA=PHA(1,I)-PHAH
```

```
      ABPH=ABSF(DPHA)-3.1416
      IF(ABPH)610,610,611
611   IF(DPHA)612,610,613
612   DPHA=DPHA+6.2832
      GO TO 610
613   DPHA=DPHA-6.2832
610   AMPT= SQRTF(HMOD(1,1)**2+HMOD**2)
      PUNCH 2,PER,FREQ,WOU,DPHA,AMPT
2     FORMAT(4F10.4,F10.2)
      FREQ=LOGF(FREQ)/2.302585
      IX=FREQ*XSS+XSO
      WOU=LOGF(WOU)/2.302585
      IY=WOU*YSS+YSO
      CALL XYPLOT(IX,IY)
      IY=DPHA*100.+2100.
      CALL XYPLOT(IX,IY)
1     CONTINUE
      RETURN
      END
```

Acknowledgements

The author wishes to thank the Reverend William V. Stauder, S.J., for his guidance and advice during the course of this study, and also Professor Otto W. Nuttli, and Dr. Willard J. Hannon.

This research was supported in part through Air Force Cambridge Research Laboratories Contract AF 19(604)-7399 as part of the Advanced Research Projects Agency's Project VELA-Uniform.

During the course of these studies the author enjoyed a fellowship from the "Organizacion de los Estados Americanos" Pan American Union.

The author is grateful to Reverend Ramon Cabre, S.J., of San Calixto Seismic Observatory, LaPaz, Bolivia, for his encouragement and help, and to St. Cronan's Catholic Church for its hospitality during his studies in Saint Louis.

Figure 54: Master curves for one layer crustal model and for 15° angle of incidence.

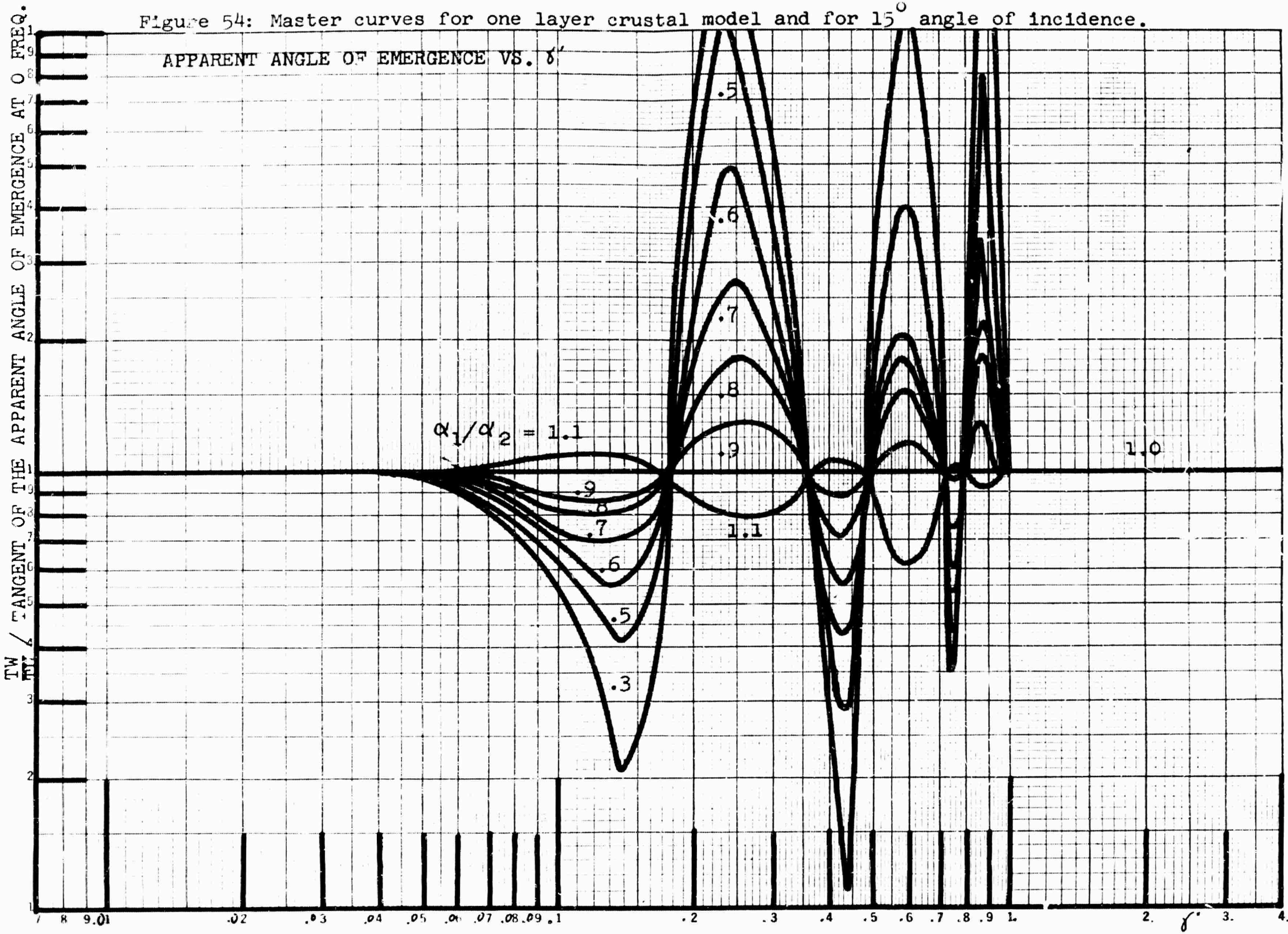

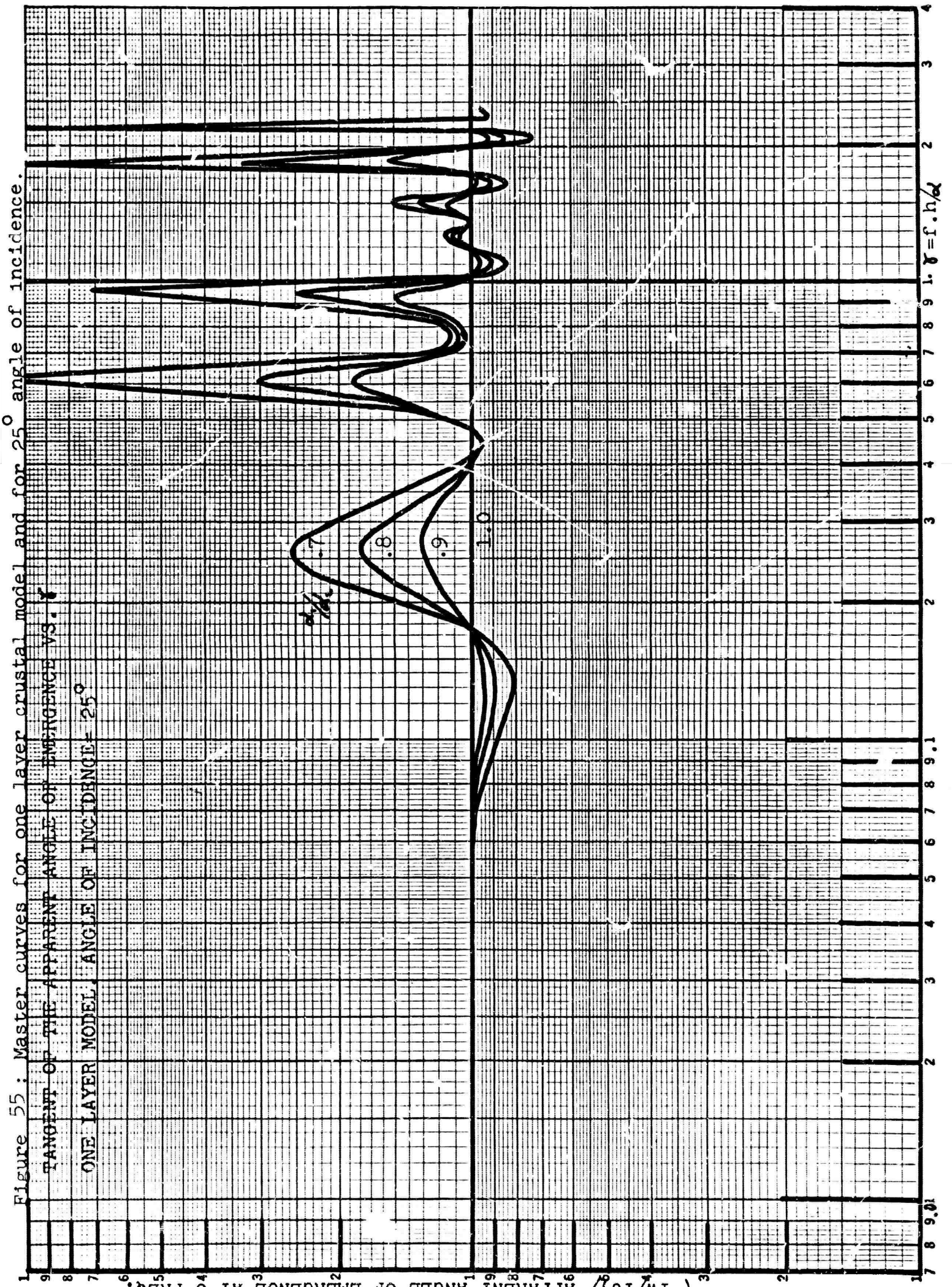

Figure 55 : Master curves for one layer crustal model and for 25° angle of incidence.

Figure56 : Master curves for one layer crustal model and for 30° angle of incidence.

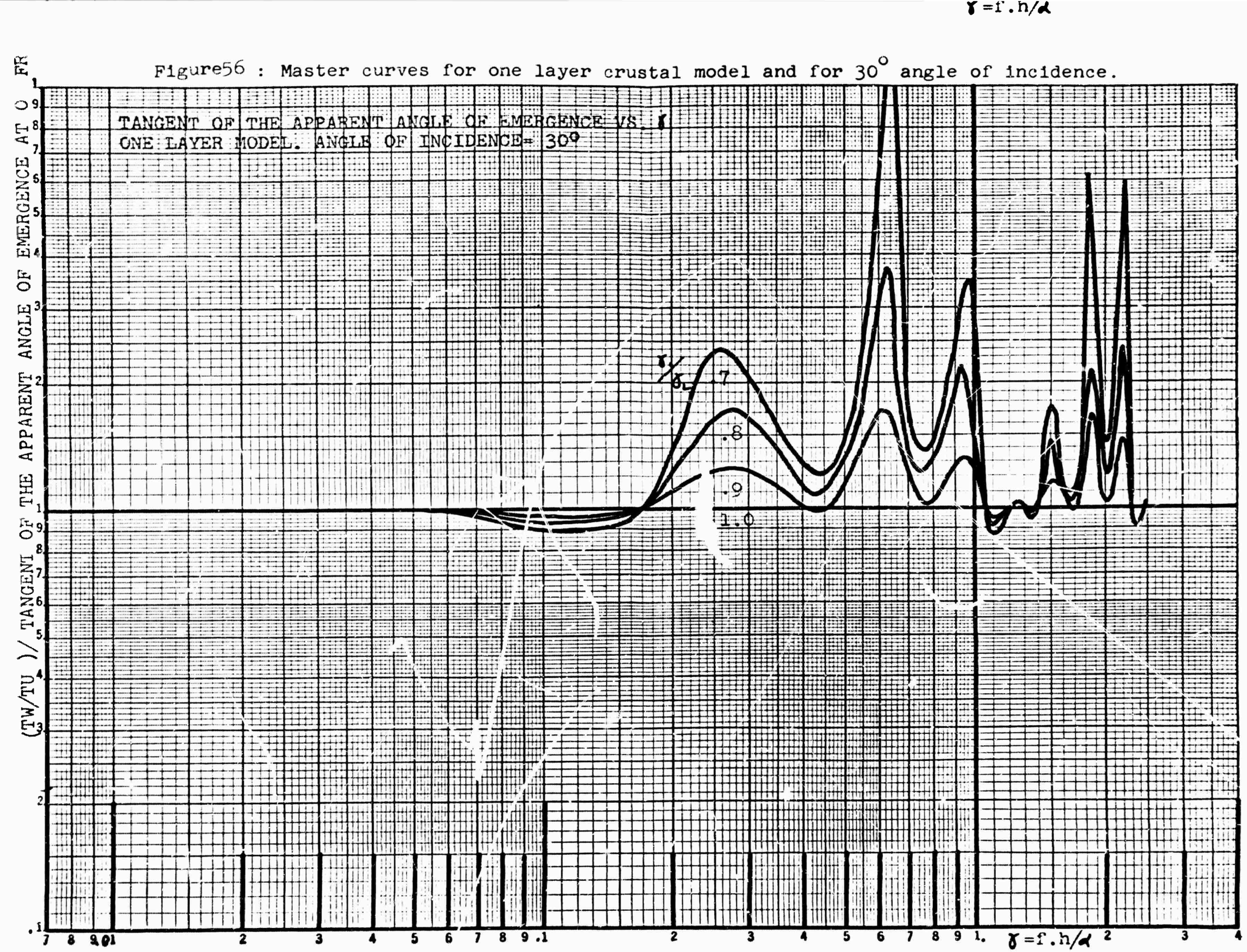

Figure 57 : Master curves for one layer crustal model and for 35° angle of incidence.

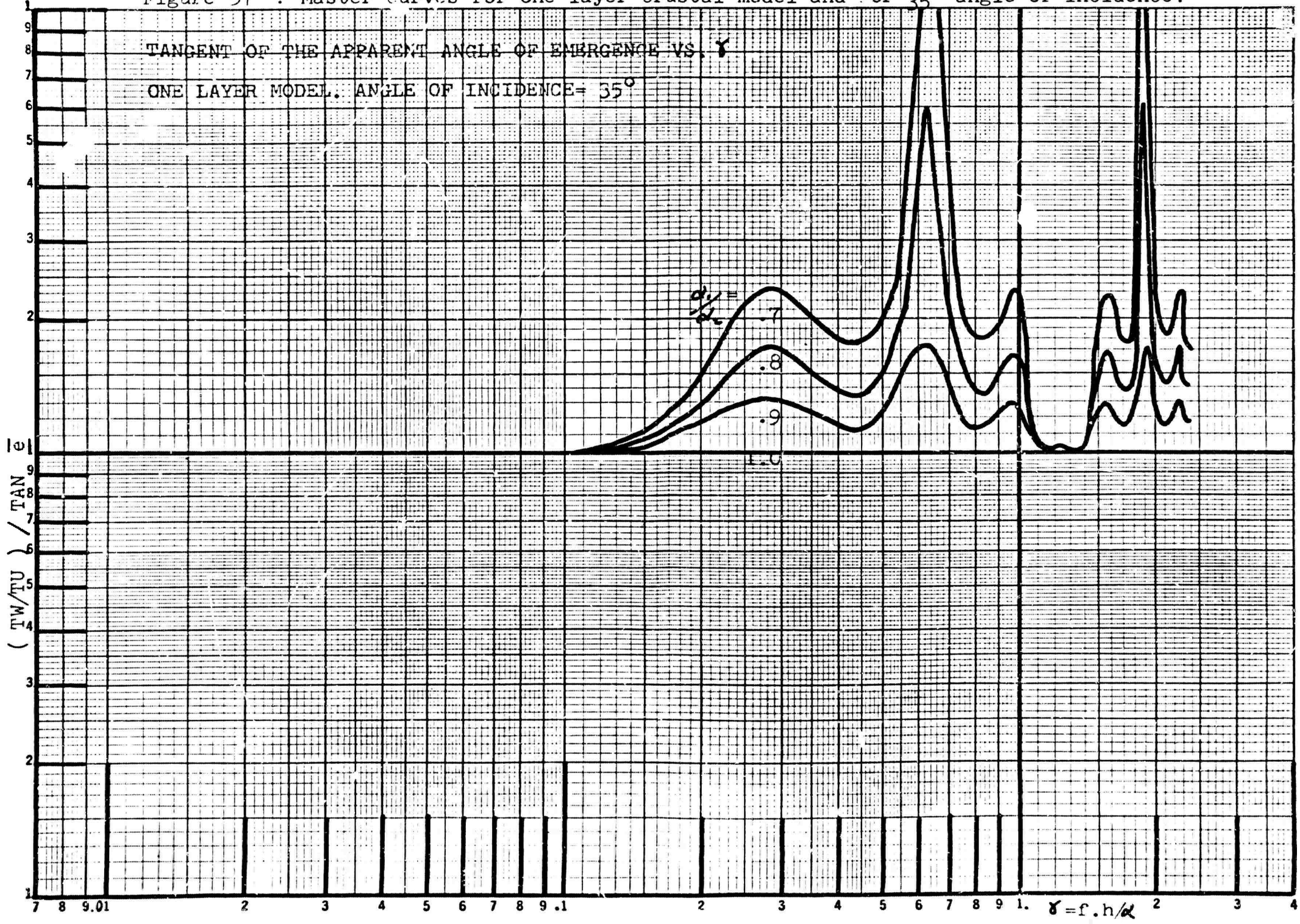

Figure 50 : Master curves for one layer crustal model and for 40° angle of incidence.

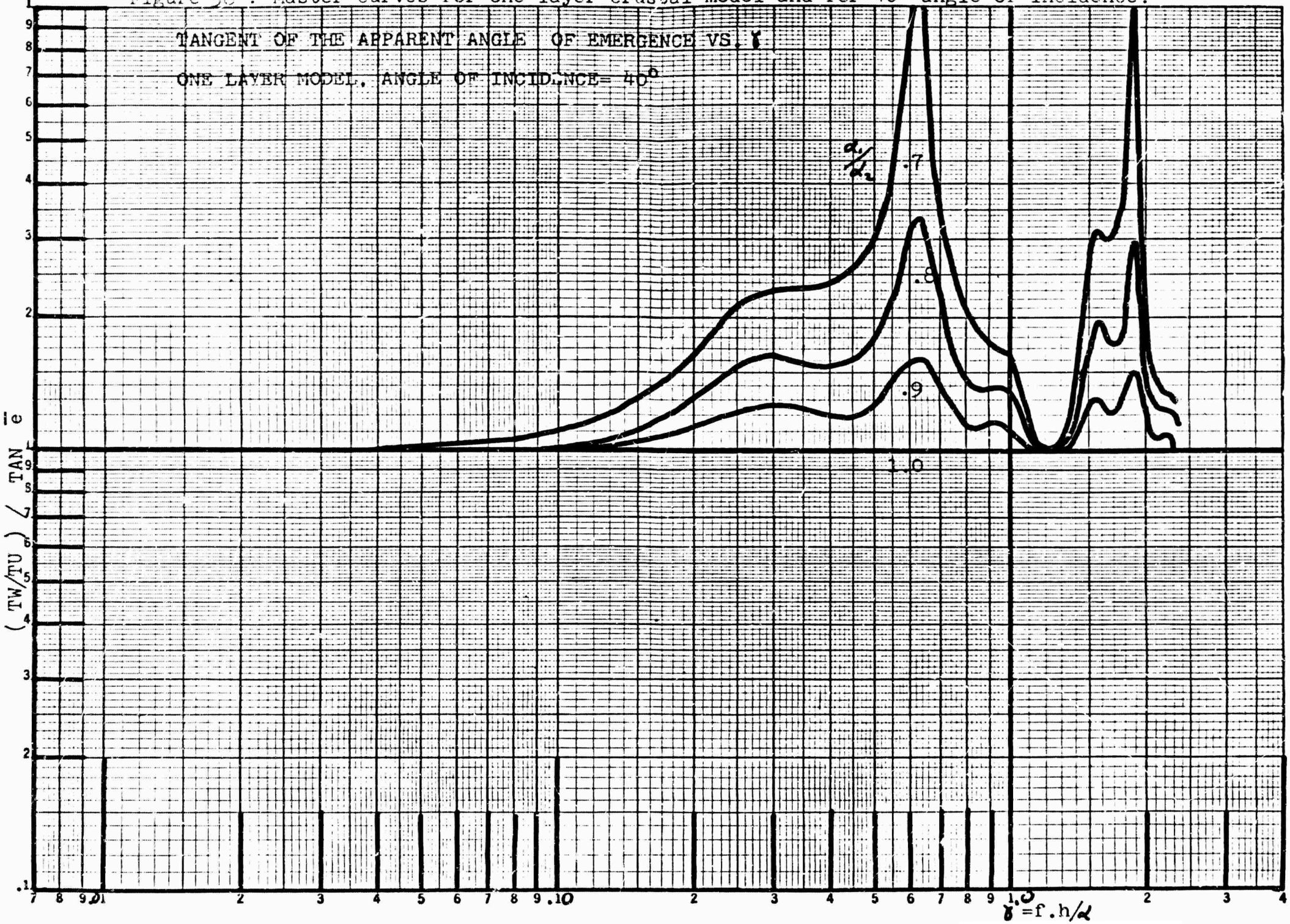

Figure 59 : Master curves for one layer crustal model and for 45° angle of incidence.

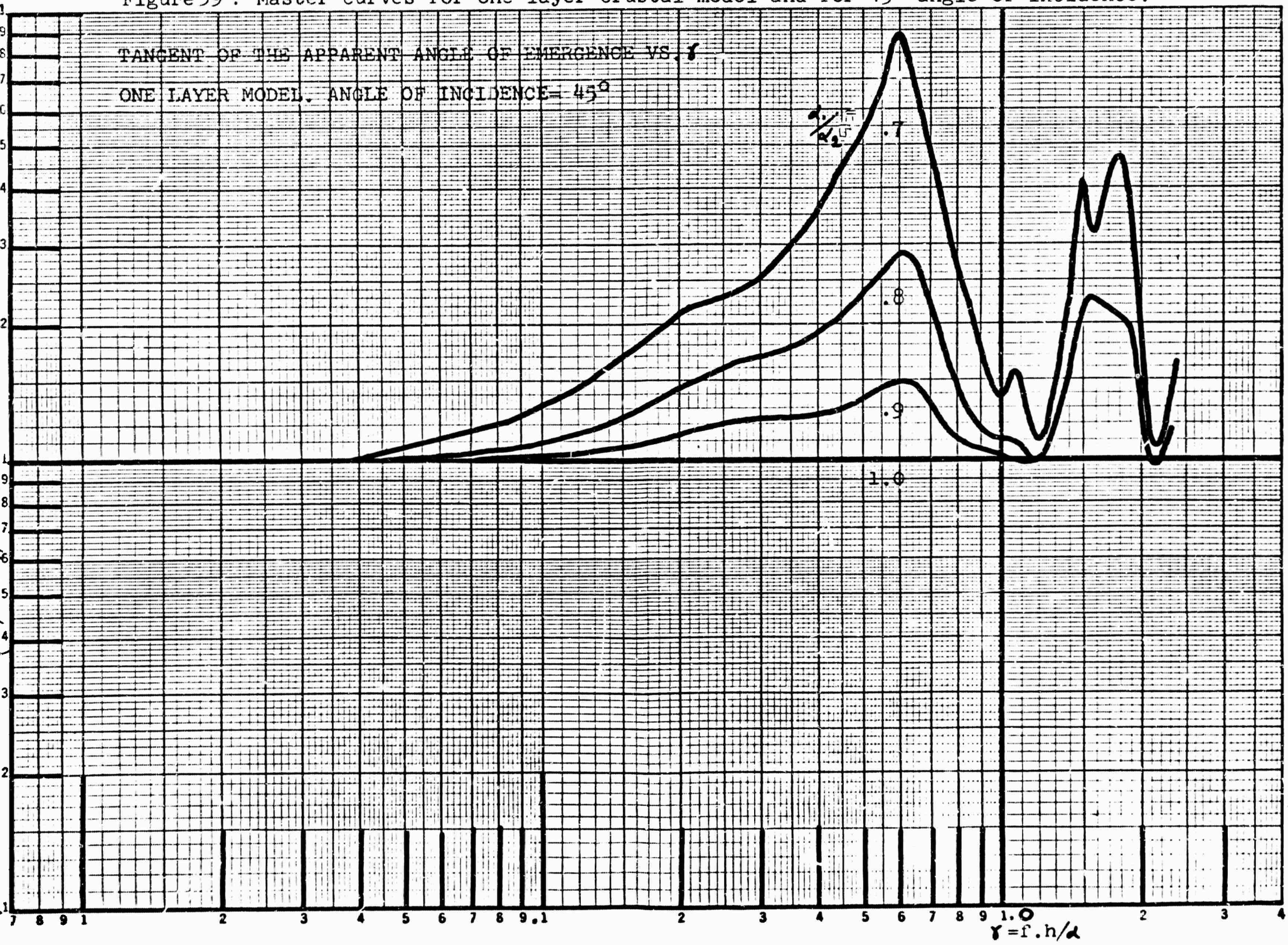

Figure 3. Master curves for one layer crustal model and 50° angle of incidence.

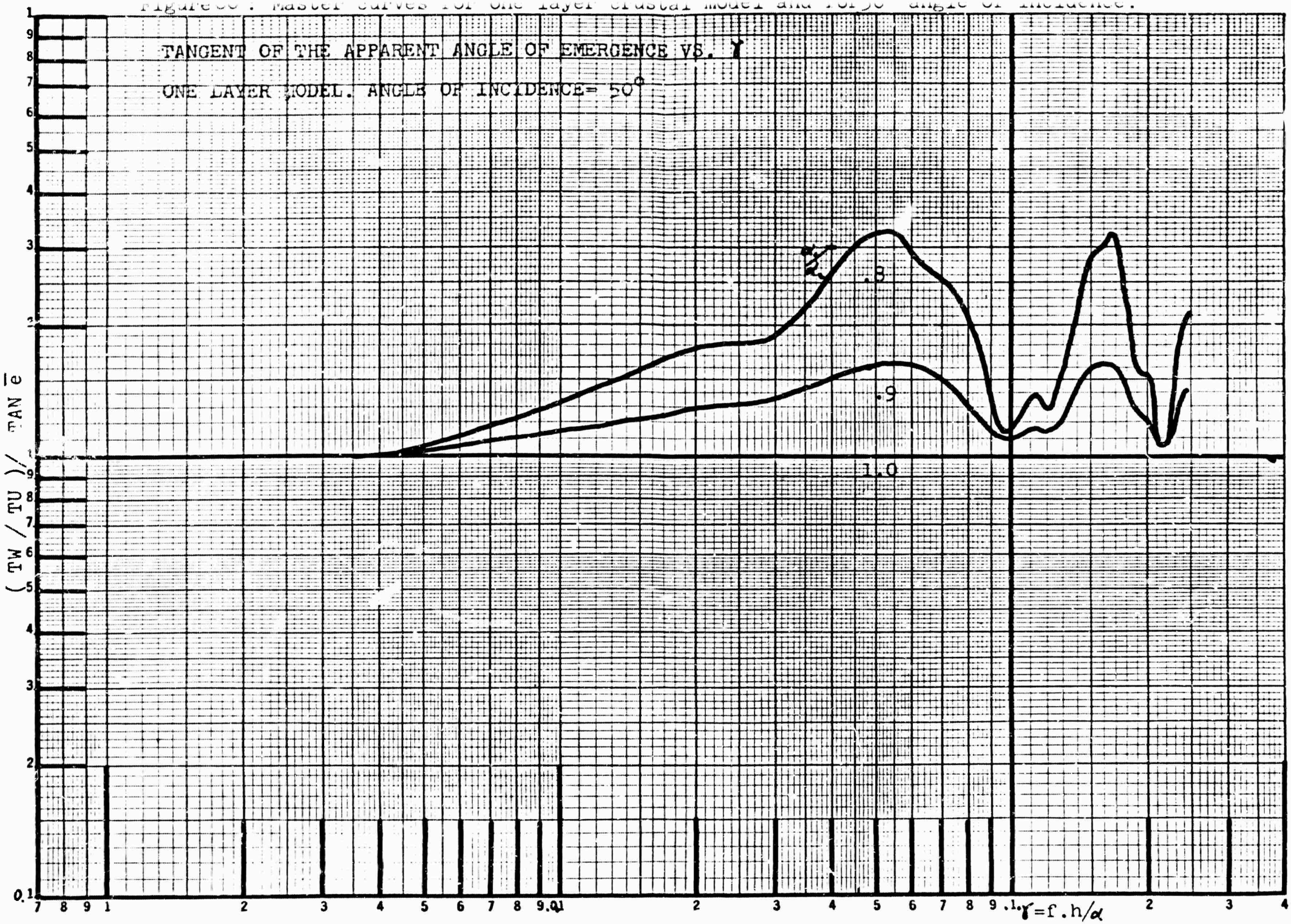

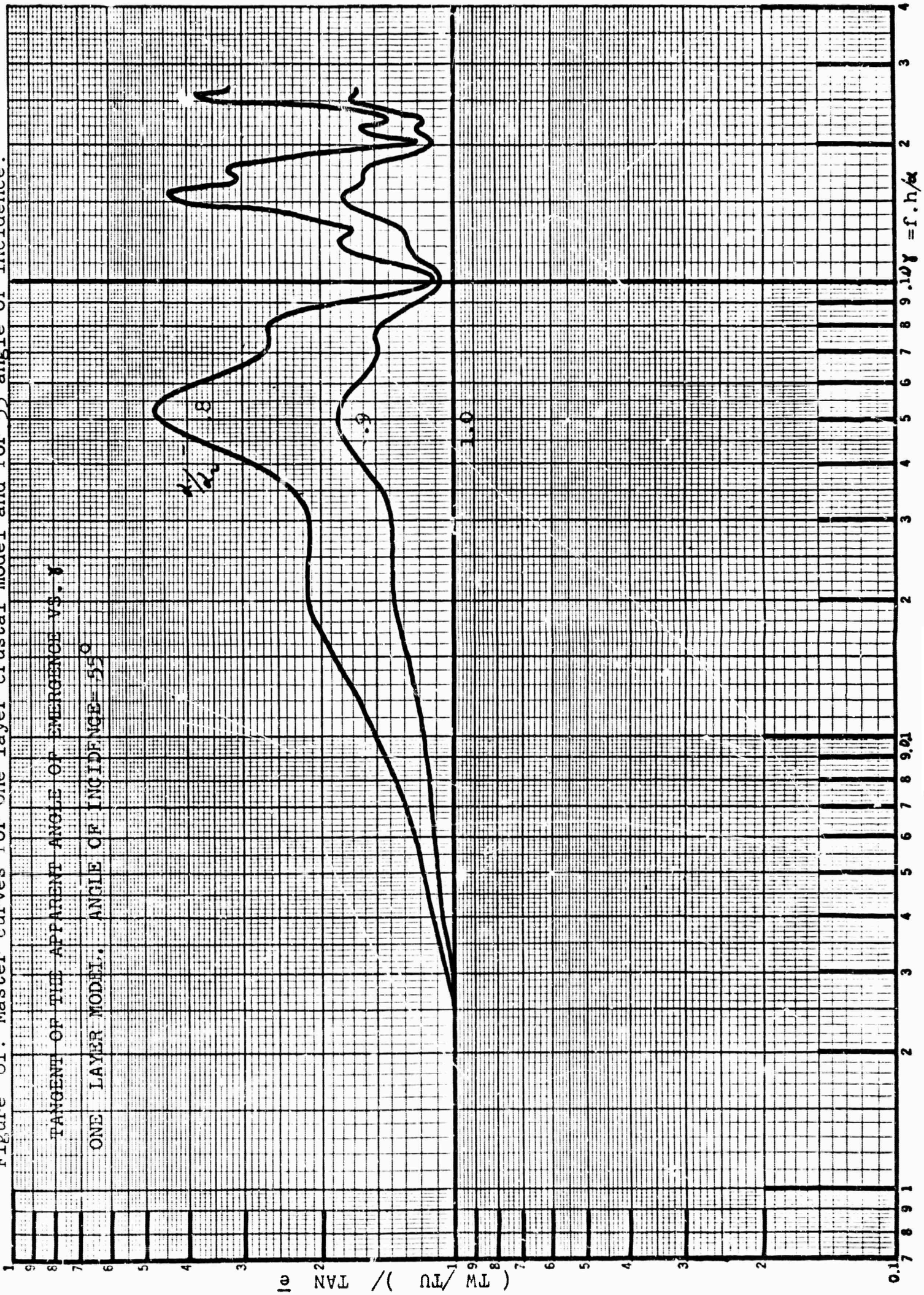

Figure 61: Master curves for one layer crustal model and for 55° angle of incidence.

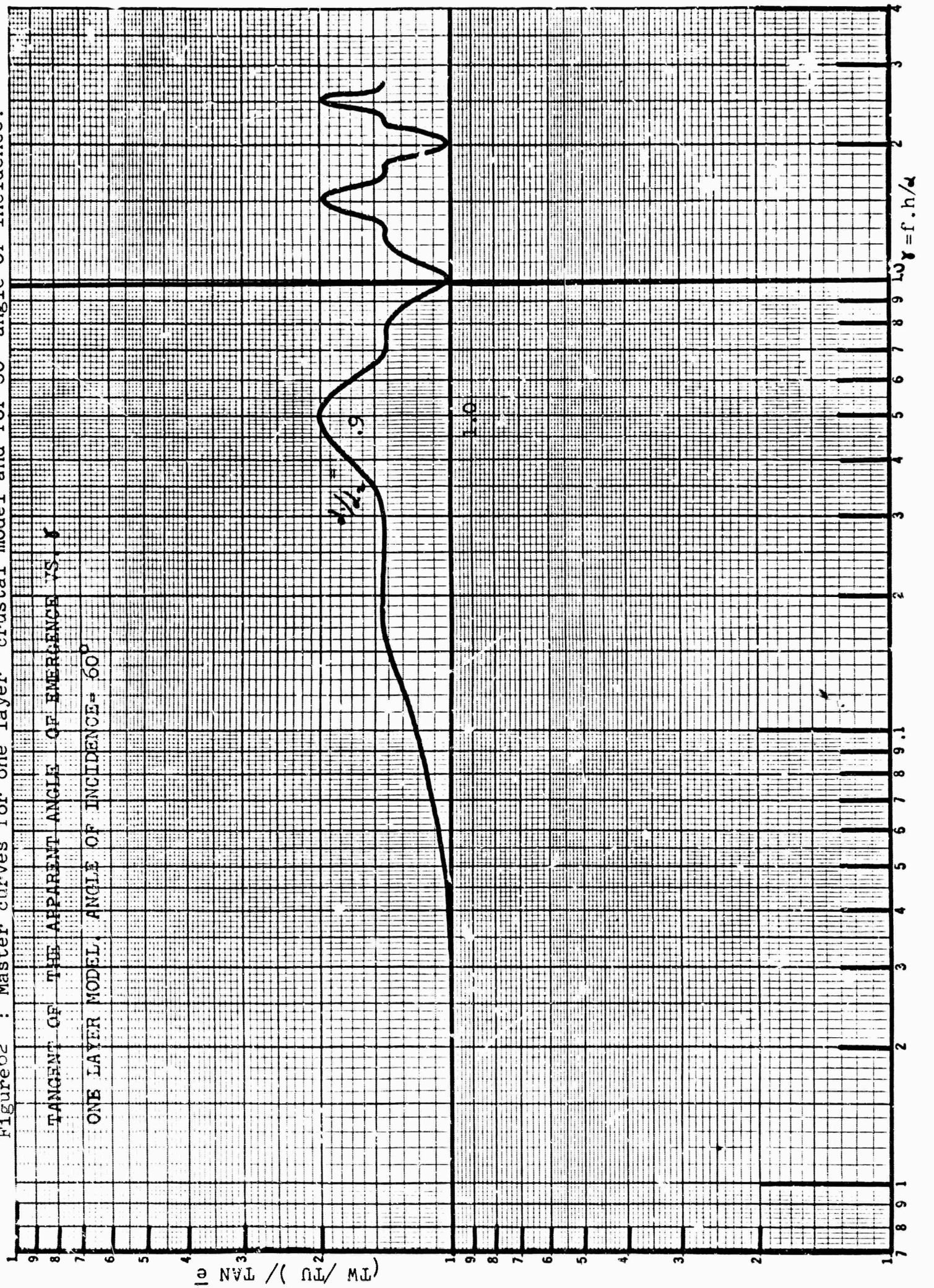

Figure62 : Master curves for one layer crustal model and for 60° angle of incidence.

Unclassified
Security Classification

DOCUMENT CONTROL DATA - R&D

(Security classification of title, body of abstract and indexing annotation must be entered when the overall report is classified)

1. ORIGINATING ACTIVITY *(Corporate author)*
Saint Louis University
St. Louis, Missouri

2a. REPORT SECURITY CLASSIFICATION
Unclassified

2b. GROUP

3. REPORT TITLE
The Determination of Crustal Thickness from the Spectrum of P Waves.

4. DESCRIPTIVE NOTES *(Type of report and inclusive dates)*
Scientific Report Interim

5. AUTHOR(S) *(Last name, first name, initial)*
Fernandez, Luis M., S.J.

6. REPORT DATE	7a. TOTAL NO. OF PAGES	7b. NO. OF REFS
September 1965	181	65

8a. CONTRACT OR GRANT NO.	9a. ORIGINATOR'S REPORT NUMBER(S)
AF 19(604)-7399	
b. PROJECT NO. 865201	
c. TASK DOD ELEMENT 62506015	9b. OTHER REPORT NO(S) *(Any other numbers that may be assigned this report)* AFCRL-65-766
d. no subelement	

10. AVAILABILITY/LIMITATION NOTICES Qualified requestors may obtain copies of this report from DDC. Other persons or organizations should apply to the Clearinghouse for Federal Scientific and Technical Information (CFSTI), Sills Building, 5285 Port Royal Road, Springfield, Virginia 22151.

11. SUPPLEMENTARY NOTES

12. SPONSORING MILITARY ACTIVITY
Hq. AFCRL, OAR (CRJ)
United States Air Force
L.G. Hanscom Field, Bedford, Mass.

13. ABSTRACT

The layers of the earth's crust act as a filter with respect to seismic energy arriving at a given station. Consequently the motion recorded at the earth's surface depends not only on the frequency content of the exciting seismic energy and on the response characteristics of the recording instrument, but also on the elastic parameters and thicknesses of the layers. This latter dependence is the basis for a method of investigating the structure of the crust.

In order to obtain information independent of the time history and spatial distribution of the source of energy the spectrum of the vertical component of motion is divided by the spectrum of the horizontal component. This ratio represents the tangent of the apparent angle of emergence as a function of frequency. It depends only on the angle of incidence of the ray and the system of layers below the recording station. The parameters of the crust may be determined by comparison of theoretical and observed spectra of this ratio. (Cont'd)

DD FORM 1 JAN 64 1473

Unclassified
Security Classification

14. KEY WORDS	LINK A		LINK B		LINK C	
	ROLE	WT	ROLE	WT	ROLE	WT
Spectra of P Waves Transfer function of crust Crustal thickness Inversion of P waves Crustal models Apparent angle of incidence Dimensionless parameter Master curves for crust models						

INSTRUCTIONS

1. ORIGINATING ACTIVITY: Enter the name and address of the contractor, subcontractor, grantee, Department of Defense activity or other organization *(corporate author)* issuing the report.

2*a*. REPORT SECURITY CLASSIFICATION: Enter the overall security classification of the report. Indicate whether "Restricted Data" is included. Marking is to be in accordance with appropriate security regulations.

2*b*. GROUP: Automatic downgrading is specified in DoD Directive 5200.10 and Armed Forces Industrial Manual. Enter the group number. Also, when applicable, show that optional markings have been used for Group 3 and Group 4 as authorized.

3. REPORT TITLE: Enter the complete report title in all capital letters. Titles in all cases should be unclassified. If a meaningful title cannot be selected without classification, show title classification in all capitals in parenthesis immediately following the title.

4. DESCRIPTIVE NOTES: If appropriate, enter the type of report, e.g., interim, progress, summary, annual, or final. Give the inclusive dates when a specific reporting period is covered.

5. AUTHOR(S): Enter the name(s) of author(s) as shown on or in the report. Enter last name, first name, middle initial. If military, show rank and branch of service. The name of the principal author is an absolute minimum requirement.

6. REPORT DATE: Enter the date of the report as day, month, year, or month, year. If more than one date appears on the report, use date of publication.

7*a*. TOTAL NUMBER OF PAGES: The total page count should follow normal pagination procedures, i.e., enter the number of pages containing information.

7*b*. NUMBER OF REFERENCES: Enter the total number of references cited in the report.

8*a*. CONTRACT OR GRANT NUMBER: If appropriate, enter the applicable number of the contract or grant under which the report was written.

8*b*, 8*c*, & 8*d*. PROJECT NUMBER: Enter the appropriate military department identification, such as project number, subproject number, system numbers, task number, etc.

9*a*. ORIGINATOR'S REPORT NUMBER(S): Enter the official report number by which the document will be identified and controlled by the originating activity. This number must be unique to this report.

9*b*. OTHER REPORT NUMBER(S): If the report has been assigned any other report numbers *(either by the originator or by the sponsor)*, also enter this number(s).

10. AVAILABILITY/LIMITATION NOTICES: Enter any limitations on further dissemination of the report, other than those imposed by security classification, using standard statements such as:

(1) "Qualified requesters may obtain copies of this report from DDC."

(2) "Foreign announcement and dissemination of this report by DDC is not authorized."

(3) "U. S. Government agencies may obtain copies of this report directly from DDC. Other qualified DDC users shall request through _____."

(4) "U. S. military agencies may obtain copies of this report directly from DDC. Other qualified users shall request through _____."

(5) "All distribution of this report is controlled. Qualified DDC users shall request through _____."

If the report has been furnished to the Office of Technical Services, Department of Commerce, for sale to the public, indicate this fact and enter the price, if known.

11. SUPPLEMENTARY NOTES: Use for additional explanatory notes.

12. SPONSORING MILITARY ACTIVITY: Enter the name of the departmental project office or laboratory sponsoring *(paying for)* the research and development. Include address.

13. ABSTRACT: Enter an abstract giving a brief and factual summary of the document indicative of the report, even though it may also appear elsewhere in the body of the technical report. If additional space is required, a continuation sheet shall be attached.

It is highly desirable that the abstract of classified reports be unclassified. Each paragraph of the abstract shall end with an indication of the military security classification of the information in the paragraph, represented as *(TS)*, *(S)*, *(C)*, or *(U)*.

There is no limitation on the length of the abstract. However, the suggested length is from 150 to 225 words.

14. KEY WORDS: Key words are technically meaningful terms or short phrases that characterize a report and may be used as index entries for cataloging the report. Key words must be selected so that no security classification is required. Identifiers, such as equipment model designation, trade name, military project code name, geographic location, may be used as key words but will be followed by an indication of technical context. The assignment of links, rules, and weights is optional.